

HARMONIC PHENOMENA ON THE D.C. SIDE OF
H.V.D.C. CONVERTER SCHEMES

A Thesis Presented to the
Faculty of Graduate Studies

The University of Manitoba

In Partial Fulfillment of the
Requirements for the Degree of

Master of Science in Electrical Engineering

Adel M. Sharaf

JUNE 1976

"HARMONIC PHENOMENA ON THE D.C. SIDE OF
H.V.D.C. CONVERTER SCHEMES

by

ADEL M. SHARAF

A dissertation submitted to the Faculty of Graduate Studies of
the University of Manitoba in partial fulfillment of the requirements
of the degree of

MASTER OF SCIENCE

© 1976

Permission has been granted to the LIBRARY OF THE UNIVERSITY OF MANITOBA to lend or sell copies of this dissertation, to the NATIONAL LIBRARY OF CANADA to microfilm this dissertation and to lend or sell copies of the film, and UNIVERSITY MICROFILMS to publish an abstract of this dissertation.

The author reserves other publication rights, and neither the dissertation nor extensive extracts from it may be printed or otherwise reproduced without the author's written permission.

ABSTRACT

Nominal operation of H.V.D.C. Converter Station produces only d.c. side harmonics of order $(p \cdot K)$ where p is the pulse number and K is an integer. In practice, converters are likely to produce all orders of harmonics.

This thesis presents a study of the harmonic phenomena on the d.c. side of a converter station. The study assumes a steady state approach even for unbalance cases that last for more than a few cycles.

The magnitudes and levels of d.c. side voltage and current harmonics are calculated for 6-pulse and 12-pulse converter operations under different combinations of unbalance parameters.

The unbalance parameters discussed are: imbalance of ignition angle (α) , commutation angle (u) , a.c. voltage depression, and the most severe case of harmonic content in the a.c. supply. Each unbalance parameter produces a certain spectrum of d.c. side voltage harmonics.

The study assumes an open loop approach, i.e., the generated harmonics on the d.c. side do not further modify the a.c. supply voltage through controllers.

An experiment had been set up to investigate the effect of inrush current of transformers during energization on the level of distortion of the a.c. voltage waveforms. It was found that severe distortions of a.c. voltages take place on account of longer duration of inrush currents.

Such studies are useful to make an assessment of the levels of the d.c. side harmonics. The data obtained are valuable in specifying and designing the filters and shielding for harmonic interference on the d.c. side.

ACKNOWLEDGEMENT

The author wishes to express his deep thanks and gratitude to his supervisor Dr. R.M. Mathur for suggesting the topic and for his valuable discussions, and to the University of Manitoba for the grant of a University Fellowship for twelve months.

TABLE OF CONTENTS

	<u>Page</u>
ABSTRACT	
ACKNOWLEDGEMENTS	ii
TABLE OF CONTENTS	iii
LIST OF FIGURES	v
LIST OF SYMBOLS	ix
LIST OF TABLES	xii
CHAPTER I INTRODUCTION	1
CHAPTER II CALCULATION OF D.C. SIDE VOLTAGE HARMONICS	6
2.1 Introduction	6
2.2 Calculation of harmonic voltages in 6-pulse operation	12
2.3 Calculation of Fourier coefficients for Δ/λ 6-pulse operation	15
2.4 Basis for computer programming	21
2.5 D.C. voltage harmonics for a general case	23
2.6 Unbalance parameters	23
CHAPTER III COMPUTATIONAL RESULTS	25
3.1 General	25
3.2 Effect of each imbalance parameter separately	27
3.3 Combinations of imbalance parameters	33
3.4 Effect of harmonic content in a.c. supply voltage	33
3.5 Conclusions	40
CHAPTER IV CALCULATION OF D.C. SIDE HARMONIC CURRENTS	45
4.1 Introduction	45
4.2 Basis for calculation	47
4.3 Analysis of the results	49
4.4 Conclusions	68

LIST OF FIGURES

- Fig. 2.1 Layout of a converter and the details of the d.c. circuit;
- Fig. 2.2 3-phase a.c. supply voltages and voltage during commutation,
- Fig. 2.3 Typical operation of a 6-pulse bridge with ignition angle (α) and commutation angle (u).
- Fig. 2.4 Relationships between angles used in the analysis
- Fig. 2.5 Star and Delta voltages with respect to the chosen fixed reference,
- Fig. 2.6 Effect of voltage depression in phase (a) on the magnitudes of conduction angles for valves in 6-pulse operation.
- Fig. 3.1 Magnitude of d.c. side mean voltage versus imbalance in a.c. supply voltages.
- Fig. 3.2 Harmonic amplitude spectra of d.c. side voltage harmonics due to voltage depression in phase (a).
- Fig. 3.3 Harmonic amplitude spectra of d.c. side voltage harmonics due to depression in phases (a), (b), (i.e., voltage rise in phase (c)).
- Fig. 3.4 Level of imbalance of u versus unbalance in inductance for different operating conditions of α , u .
- Fig. 3.5(a) Distorted a.c. supply voltage waveform (phase (a)).
- Fig. 3.5(b) Distorted a.c. supply voltage waveform (phase (c)).
- Fig. 3.6(a) A.C. supply voltage waveforms on account of balanced a.c. harmonics.

- Fig. 3.6(b) A.C. supply voltage waveform on account of unbalanced a.c. harmonics.
- Fig. 3.7(a) D.C. side harmonic generator waveform for 6-pulse operation on account of balanced a.c. harmonics.
- Fig. 3.7(b) D.C. side harmonic generator waveform for 6-pulse operation on account of unbalanced a.c. harmonics.
- Fig. 3.8(a) D.C. side harmonic generator waveform for 12-pulse operation on account of balanced a.c. harmonics.
- Fig. 3.8(b) D.C. side harmonic generator waveform for 12-pulse operation on account of unbalanced a.c. harmonics.
- Fig. 3.9 Discrete harmonic amplitude spectra of d.c. voltage harmonics for 6-pulse operation.
- Fig. 4.1 Layout of d.c. side circuit
- Fig. 4.2(a) 6th arm filter current waveform for balanced a.c. harmonics (6-pulse).
- Fig. 4.2(b) 6th arm filter current waveform for unbalanced a.c. harmonics (6-pulse).
- Fig. 4.2(c) 6th arm filter current waveform obtained by digital simulator¹⁰ on account of balanced a.c. harmonics (6-pulse).
- Fig. 4.3(a) 6th arm filter current waveform on account of balanced a.c. harmonics (12-pulse).
- Fig. 4.3(b) 6th arm filter current waveform for unbalanced a.c. harmonics (12-pulse).
- Fig. 4.4(a) 12th arm filter current waveform for unbalanced a.c. harmonics (6-pulse).
- Fig. 4.4(b) Voltage across filters for 12-pulse operation on account of unbalanced a.c. harmonics (12-pulse).

- Fig. 4.5(a) Voltage across filters for 6-pulse operation on account of unbalanced a.c. harmonics (6-pulse).
- Fig. 4.5(b) Voltage across filters for 12-pulse operation on account of unbalanced a.c. harmonics (12-pulse).
- Fig. 4.6(a) Line current waveform for unbalanced a.c. harmonics (6-pulse).
- Fig. 4.6(b) Line current waveform for unbalanced a.c. harmonics (12-pulse).
- Fig. 4.7 Amplitude spectra for 6th arm filter currents in case of 12-pulse operation on account of unbalanced a.c. supply harmonics.
- Fig. 4.8 Amplitude spectra for 12th arm filter currents in case of 12-pulse operation on account of unbalanced a.c. supply harmonics.
- Fig. 4.9 Amplitude spectra of the harmonic generator and voltage across filters in case of 12-pulse operation on account of unbalanced a.c. supply harmonics.
- Fig. 4.10 Harmonic impedance spectra of the d.c. circuit
- Fig. 4.11 Typical recorded waveforms of d.c. side currents during overloading.
- Fig. 5.1 Circuit diagram for the experimental set-up.
- Fig. 5.2 Inrush current waveform (one bank Δ/Δ).
- Fig. 5.3(a) Inrush current waveform (2-banks Δ/Δ).
- Fig. 5.3(b) Inrush current waveform (2-banks Δ/Δ).
- Fig. 5.4 Details of inrush current (one bank Δ/Δ).
- Fig. 5.5 Details of inrush current (2-banks Δ/Δ).
- Fig. 5.6 Details of inrush current (one bank Δ/Δ).

- Fig. 5.7 Details of inrush currents (2-banks Δ/Δ).
- Fig. 5.8 Phase voltage waveform without distortion.
- Fig. 5.9(a) Distorted phase voltage (one-bank Δ/Δ).
- Fig. 5.9(b) Distorted phase voltage (2-banks Δ/Δ).
- Fig. 5.10(a) Distorted phase voltage (one-bank Δ/Δ).
- Fig. 5.10(b) Distorted phase voltage (2-banks Δ/Δ).
- Fig. A2(a) Simplified half wave rectifier circuit.
- Fig. A2(b) Load voltage and current waveforms.
- Fig. A3(a) Circuit illustrating commutation between valves (1), (3).
- Fig. A4(a) Circuit configuration during conduction for 6-pulse operation.
- Fig. A4(b) Circuit configuration during commutation for 6-pulse operation.
- Fig. A4(c) Circuit configuration during commutation for 12-pulse operation.
- Fig. A4(d) Circuit configuration during conduction for 12-pulse operation.

LIST OF SYMBOLS

m	subscript distinguishing valve numbers
α_m	ignition angle of valve m
u_m	commutation angle of valve m
ϕ_m	conduction angle of valve m
θ_m	conduction delay angle of valve m measured from a fixed reference
V_{L-L}	line-to-line a.c. supply voltage
V_{dn}	nominal d.c. side voltage
I_{dn}	nominal d.c. side current
e	exponent constant
λ/λ	Star/Star connected transformer
Δ/λ	Delta/Star connected transformer
v_a, v_b, v_c	a.c. supply phase voltages on secondary of λ/λ converter transformer
v_a^i, v_b^i, v_c^i	a.c. supply phase voltages on secondary of Δ/λ converter transformer
ω	system angular frequency rad/s
C_K	Fourier complex coefficient for the <u>Kth</u> order harmonic on d.c. side
$j = 1/90^\circ$	complex operator
$f_n(\omega t)$	<u>nth</u> subfunction in the general definition of a.c. supply waveforms
K	Fourier harmonic order on d.c. side of converter
n	Fourier harmonic order on a.c. side of converter
v	instantaneous value of a voltage waveform

$\hat{v}_{an}, \hat{v}_{bn}, \hat{v}_{cn}$

Peak voltages of the nth harmonics in phases a,b,c respectively

 $\theta_{an}, \theta_{bn}, \theta_{cn}$

phase angles of the nth harmonic component in phases a,b,c respectively

 $\Delta\alpha$

incremental variation in ignition angle

 $\Delta(\alpha, u)$

incremental variation in both ignition and commutation angles

 $\Delta(\alpha, v_a)$

incremental variation in ignition angle and phase a voltage

 Δu

incremental variation in commutation angle u

 ΔL

incremental variation in leakage inductance of a converter transformer

 L_S

a.c. system inductance/phase (behind the converter transformer)

 L_T

equivalent leakage inductance/phase of converter transformers

 $L(I), L(I+1)$

general successive limits for a definite integration

 $I(I)$

value of the integral between the limits $L(I)$, $L(I+1)$

 $I_a(I), I_b(I), I_c(I)$

values of the integrals of voltage functions v_a, v_b, v_c between the limits $L(I)$, $L(I+1)$

 e_a, e_b, e_c

a.c. supply voltage sources

 $6th$

refer to 6th arm filter

 $12th$

refer to 12th arm filter

 $Z_{PI}(K), Y_{PI}(K)$

line PI - parameters for the Kth order harmonic frequency

 $Y_F(K)$

filtering branches equivalent admittance for the Kth order harmonic

$Z_L(K)$	line damping reactor impedance for the <u>Kth</u> order harmonic
$Z_{TOT}(K)$	d.c, circuit input impedance for the <u>Kth</u> order harmonic
$I_6(K)$	<u>Kth</u> order harmonic current through <u>6th</u> arm filter
$I_{12}(K)$	<u>Kth</u> order harmonic current through <u>12th</u> arm filter
$I_{Line}(K)$	<u>Kth</u> order harmonic current passing through the d.c. line
R_6, R_{12}	<u>6th</u> arm and <u>12th</u> arm resistance
L_6, L_{12}	<u>6th</u> arm and <u>12th</u> arm inductance
C_6, C_{12}	<u>6th</u> arm and <u>12th</u> arm capacitance
$V(K)$	<u>Kth</u> order harmonic voltage on d.c. side
I_K	<u>Kth</u> order harmonic in a current waveform
$I_{R.M.S.}$	effective value of a distorted current waveform
3- ϕ	3-phase system
\underline{V}	voltage phasor
\underline{I}	current phaser

LIST OF TABLES

Table 2.1	Definition and limits of subfunctions in a.c. supply waveforms for 6-pulse λ/λ rectifier operation.
Table 2.2	Definitions and limits of subfunctions in a.c. supply waveforms for 6-pulse Δ/λ rectifier operation.
Table 3.1	Characteristic harmonics for 6-pulse and 12-pulse converter operations for different operating conditions.
Table 3.2	Percentage harmonics in d.c. side voltage due to unbalance in fundamental a.c. supply
Table 3.3	Percentage d.c. side voltage harmonics under different combinations of imbalance parameters,
Table 3.4	Percentage harmonics in the chosen distorted a.c. voltage waveforms.
Table 3.5	Percentage d.c. side voltage harmonics on account of balanced and unbalanced a.c. harmonics.
Table 4.1	Percentage harmonic content in d.c. side filters and line currents for 6-pulse converter operation.
Table 4.2	Percentage harmonic content in d.c. side filters and line currents for 12-pulse operation.
Table 4.3	Percentage effective R.M.S. value of d.c. side currents during normal and abnormal operation for 6-pulse and 12-pulse converters.
Table 4.4	Percentage harmonic content in voltage across filtering branches in case of 6-pulse and 12-pulse operations.
Table 4.5	Percentage harmonic currents and voltage across the filters when <u>6th</u> arm filter is out of service (12-pulse

operation),

Table 4.6	D.C. circuit harmonic impedances in per-unit.
Table A2(a)	Calculated harmonic currents and impedances for the chosen half wave controlled rectifier.
Table A3(a)	Unbalance in commutation angle μ versus unbalance in converter transformer phase inductances.
Table A3(b)	PI - Section parameters for the transmission line.

CHAPTER I

INTRODUCTION

Nominal operation of a converter produces d.c. side harmonics of order $(K \cdot p)$ where p is the pulse number and K is an integer $K = 1, 2, 3, \dots$

The harmonics during nominal operation are called characteristic harmonics. Usually an adequate filtering is provided on the d.c. side for such harmonics. The influence of characteristic harmonics are well known^{7,8,9}.

H.V.D.C. converters generate harmonics on both d.c. and a.c. sides. Due to certain unbalance in parameters, the harmonic content on the d.c. side does not contain the characteristic harmonics only, in fact, converters produce harmonics of all orders, Reference [2,4].

The following imbalance parameters are taken into account for this investigation:

- (1) Variation in ignition angle (α) of each valve .
- (2) Variation in the a.c. supply due to:
 - (a) Imperfect transposition and regulation characteristic
 - (b) Depression of one or more phases of the a.c. supply, mainly during fault condition.
 - (c) Uncharacteristic current harmonics in the a.c. side, which in case of inadequate a.c. filtering can result in local or remote resonance, Reference [1].
 - (d) A.C. side current harmonics have a d.c. component rating which could exceed the saturation level of converter transformer.

This results in large distortion in the a.c. supply voltage due to converter transformer saturation.

- (3) Unbalance in commutation angles of some valves due to unequal converter transformer phase inductances.

It was experienced that due to energization of power transformers in the a.c./d.c. link a severe distortion of a.c. voltages takes place which causes a high content of characteristic and non-characteristic harmonics and leads to overloading of d.c. side filters.

This study handles the harmonic phenomena on the d.c. side of H.V.D.C. converter stations in a most general way.

The research was guided to cover the following aspects:

Firstly: The analysis and digital computer programs to calculate the characteristic and non-characteristic voltage and current harmonics on both 6-pulse and 12-pulse converter operations.

Secondly: It enables one to make an assessment of the level of voltage and current harmonics under any combinations of unbalance parameters.

Thirdly: The consequential d.c. line and filter branches currents that are influenced by the converter station configuration and d.c. line characteristics are considered for the unbalance case of harmonic content in the a.c. supply.

The study is performed using a steady state approach because disturbances of the a.c. supply usually last for many cycles without changing appreciably.

To account for all possible unbalance in parameters, a computer program was written in the most general form, for this reason the a.c. supply waveform was considered for a full cycle of six commutation and six non-commutation, (conduction), periods for each three phase full

wave controlled bridge.

Voltage harmonics in case of λ/λ and Δ/λ 6-pulse operations are first determined separately and then the voltage harmonics for any cascade combination of the two connected bridges are found by phasor addition of each harmonic order individually.

A.C. line-to-line voltage (v_{L-L}) is chosen as a base in the derivation of per-unit d.c. side harmonic voltages, and nominal d.c. side voltage and current (v_{dn} , I_{dn}) are used as bases for calculating per-unit harmonic voltages and currents.

A representative combination of unbalance parameters is analysed and the d.c. voltage harmonics are obtained for the following cases:

- (a) Unbalance in commutation angle (u) mainly due to unequal transformer phase inductances.
- (b) Unbalance in ignition angle (α) alone or in conjunction with other parameters.
- (c) Depression in a.c. supply phase voltages.
- (d) Imbalance of a.c. supply phase angles.
- (e) A harmonic content in the a.c. supply.

Case (e) represents the most severe source of unbalance in converter operation. A harmonic content in a.c. supply results during fault conditions, or due to initial a.c. side current harmonics entering and propagating in the a.c. system, leading to voltage unbalance particularly in the form of superimposed harmonic voltages. Moreover, high inrush currents produced in power transformers due to a state of saturation lead to a distorted a.c. supply waveform.

Chapter 5 illustrates an experimental set-up to investigate

the effect of inrush current on the level of distortion in the a.c. supply voltages.

A.C. side harmonics produced by converter operation in case of insufficient a.c. filtering can distort the a.c. supply voltages, Reference [1].

In the following analysis, case (e) was considered the most significant.

Instead of assuming arbitrary harmonic content in the a.c. supply waveform, a harmonic analysis is performed on some a.c. supply waveforms obtained from simulation studies for the case of 3-phase fault on the a.c. system.

For a better understanding of the influence of a.c. harmonics two cases of harmonic content in the a.c. supply are analysed.

(i) Balanced Case

all a.c. supply harmonics are the same for the 3 phases.

(ii) Unbalanced Case

It was considered that phase (c) has different levels of harmonics than phases (a), (b) and for simplicity the phase angles of harmonics in the 3-phases are assumed the same.

The d.c. side voltage harmonics are computed for the above cases.

Considering these d.c. side voltage harmonics as a harmonic generator, the harmonic currents through filters and line are calculated.

A special case of the 6th arm filter out of service is considered and consequential d.c. side harmonic currents are calculated.

This study indicates a very important aspect, that:

When the harmonic content in the a.c. supply is determined the d.c. side harmonic currents could be calculated using a steady state approach from the knowledge of d.c. side voltage harmonics. This procedure is computationally very efficient and shown to be quite reliable.

The results obtained from the analysis presented in this thesis are very valuable in predicting the levels of all d.c. side harmonics under different unbalance conditions. It could be used as a data in designing and setting the filter protection circuits. Moreover, the proper shielding could be arranged to limit interference with telecommunication networks, especially noise on telephone and telegraph systems.

CHAPTER II

CALCULATION OF D.C. SIDE VOLTAGE HARMONICS

2.1 Introduction

The investigation of d.c. voltage and current harmonics is based on the idea of regarding the rectifier and inverter as generators of harmonics in the d.c. circuit. The harmonics of the e.m.f. of such a generator are found from the assumption of an infinitely great inductance in the d.c. side of converter, i.e., constant d.c. current operation.

The e.m.f. harmonics are functions of the a.c. supply voltages, circuit parameters, and the angles of ignition and commutation.

To calculate the harmonic voltages on the d.c. side, each period of a.c. supply waveforms is made up of six conduction and six commutation intervals. The a.c. waveform is treated in the frequency domain and hence Fourier complex coefficients are determined for such waveforms in the most general way to allow the inclusion of different combinations of asymmetries such as imbalances in a.c. supply, ignition and commutation angles, and the most serious case of distortion of the a.c. supply voltage waveform which usually arises in the case of energization of transformers and/or during faults.

The main objective of this chapter is to calculate the levels of harmonic voltages on the d.c. side under the asymmetries outlined earlier.

D.C. side harmonics are regarded as voltage sources. Harmonic currents in filtering branches and transmission line are calculated from these with the knowledge of the transmission line equivalent impedance

at each harmonic frequency.

The procedure adopted for calculating the harmonic voltages for 12-pulse operation, is to regard the 12-pulse operation as a combination of 2 6-pulse operations with the second one having a phase lead of $(K \cdot 30^\circ)$ with respect to the Kth order harmonic. This phase lead arises from the use of a Δ/Δ converter transformer for the second bridge.

Fig. 2.1 shows the layout of a converter and the details of the d.c. circuit.

Fig. 2.2 represents 3-phase a.c. supply voltages and voltage during commutation.

The periodic waveform shown in fig. 2.3 is expanded in Fourier series by using a complex Fourier approach. This waveform is composed of six conduction and six commutation periods in the interval of $(0 - 2\pi)$.

Fig. 2.3 illustrates typical operation of a 6-pulse converter with ignition angle (α) and commutation angle (u) .

The ignition angles $(\alpha's)$ and the angles of commutation $(u's)$ for the six valves are defined individually to preserve the generality of the analysis, in an attempt to take into account all abnormal conditions arising from inequalities.

The phase angles $(\theta's)$ and conduction angles $(\phi's)$ with respect to a fixed reference are defined in terms of $\alpha_1, \dots, \alpha_6$ and u_1, \dots, u_6

Fig. 2.4 represents the relationships between the angles used in the analysis. For example

$$\theta_3 = \phi_1 + \alpha_1 + u_1 \quad (2.1)$$

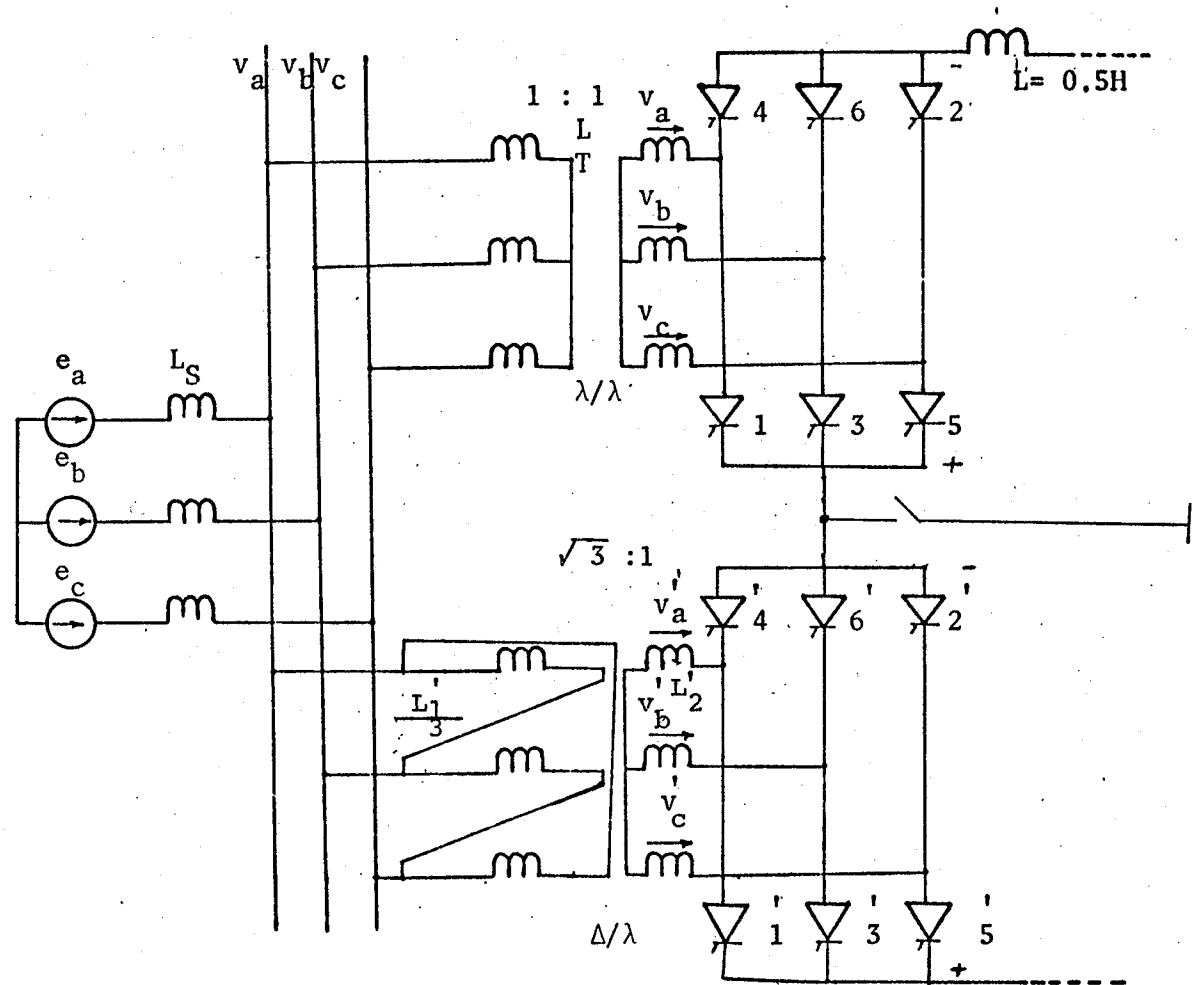
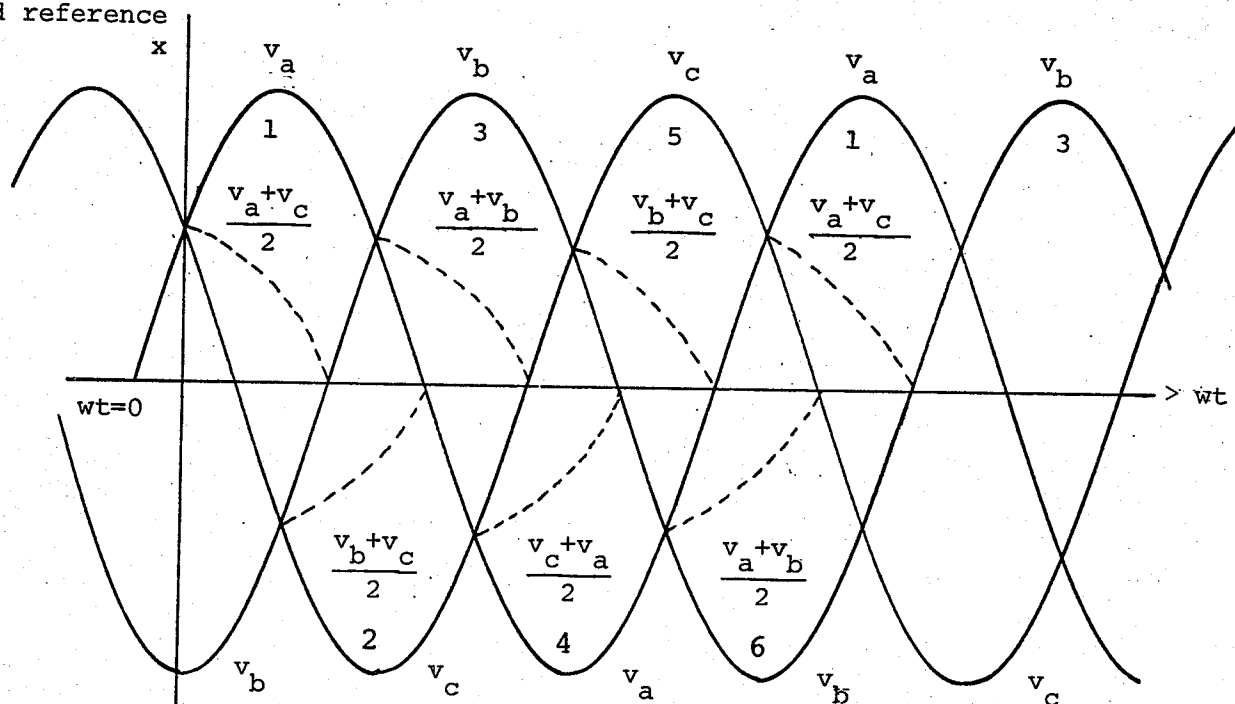


Fig. 2.1 Layout of the converter

fixed reference



x Fig. 2.2 3-phase a.c. supply voltages and voltage during commutation.

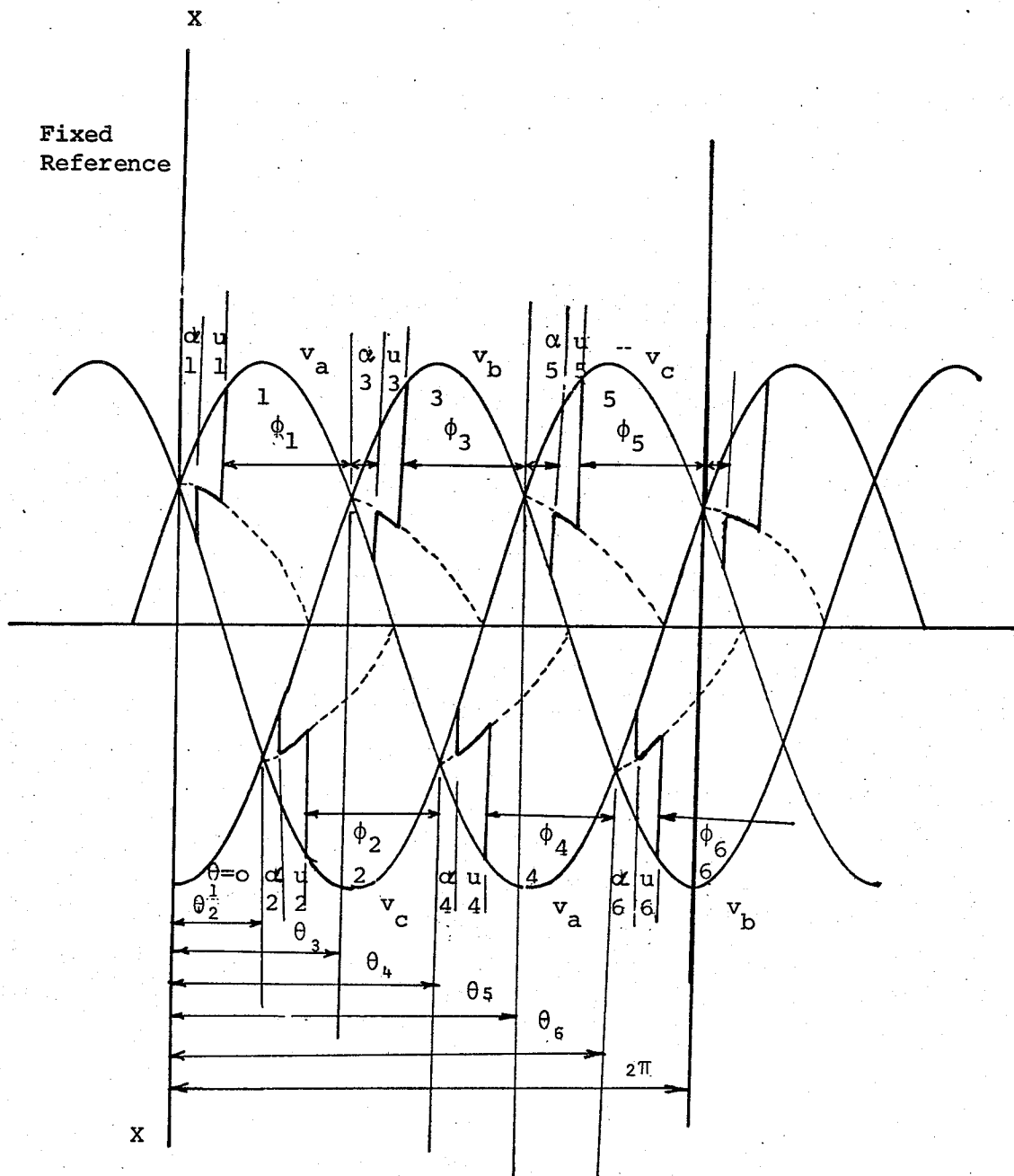


Fig. 2.3 Typical operation of a 6-pulse bridge with ignition angle (α) and commutation angle (u).

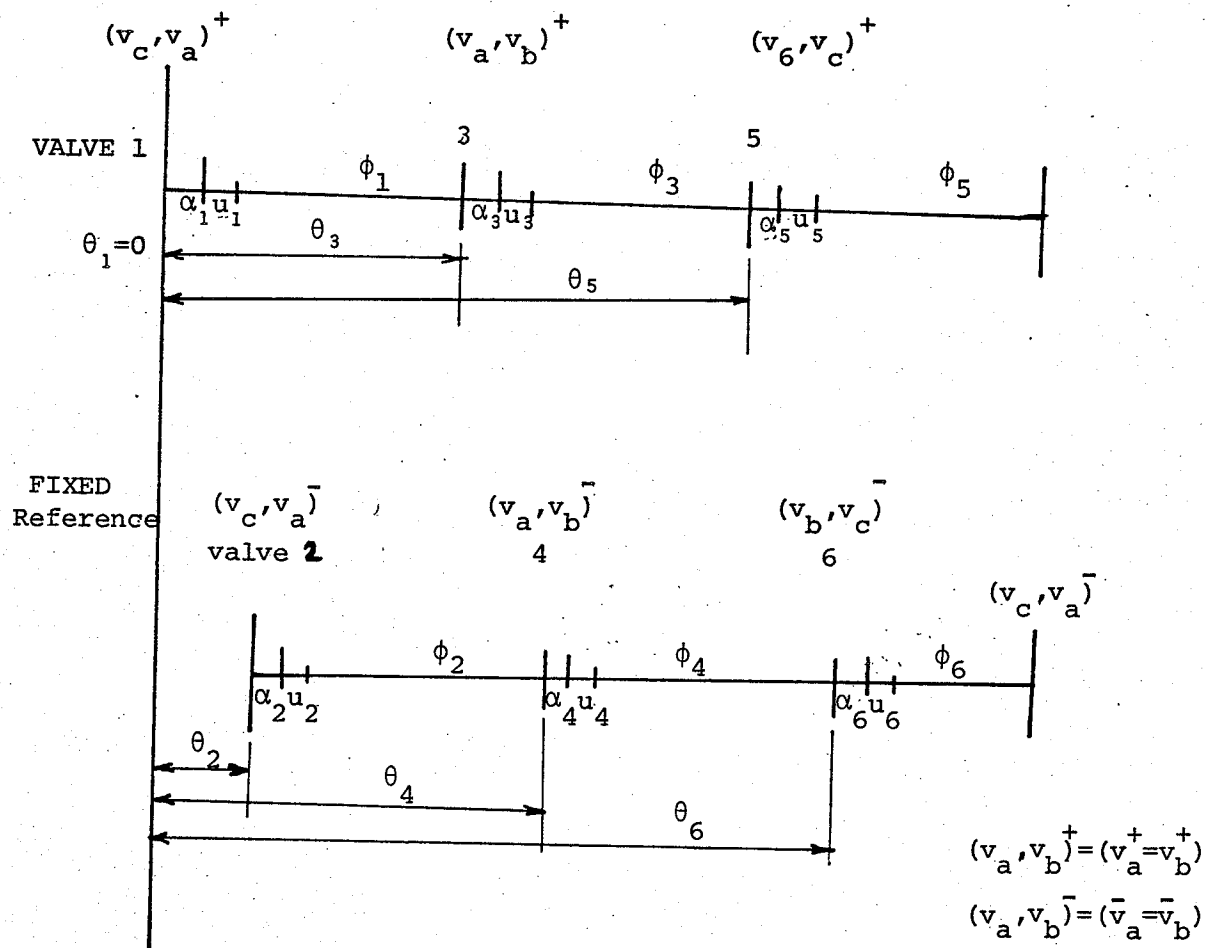


Fig. 2.4 Relationships between angles used in the analysis.

The fixed reference $(x - x)$ is taken at $\theta_1 = \omega t_1 = 0$

2.2 Calculation of harmonic voltages in 6-pulse operation

As shown in fig. 2.3 a fixed reference is taken at $\theta_1 = 0$ and hence the fundamental components of the a.c. supply are defined as

$$\begin{aligned} v_a &= \hat{V}_a \cos(\omega t - \frac{\pi}{3}) \\ v_b &= \hat{V}_b \cos(\omega t - \pi) \\ v_c &= \hat{V}_c \cos(\omega t + \frac{\pi}{3}) \end{aligned} \quad (2.2)$$

The representation of a periodic function $f(\omega t)$ by a Fourier series implies that the specification of its Fourier coefficients uniquely determines the function.

$$f(\omega t) = \sum_{K=-\infty}^{\infty} C_K e^{jK\omega t} \quad (2.3)$$

where K is the harmonic order, and C_K is the Kth complex coefficient.

By Fourier's theorem, C_K is defined as:

$$C_K = \frac{1}{2\pi} \int_0^{2\pi} f(\omega t) e^{-jK\omega t} d\omega t \quad (2.4)$$

where $K = 0, \pm 1, \pm 2, \dots$

Usually, the positive Fourier coefficients are calculated as complex numbers, then the negative coefficients are related to the positive ones by the relation

$$C_{-K} = C_K^*$$

where $(*)$ stands for the complex conjugate


The reason for using complex Fourier analysis, is that a Fourier complex coefficient C_K is equivalent to the amplitude of the Kth order harmonic phasor.

From fig. 2.3 the periodic function which is represented by a Fourier series is divided into 13 portions from $(0 - 2\pi)$.

$$f(\omega t) = f_1(\omega t) + f_2(\omega t) + f_3(\omega t) + f_4(\omega t) + f_5(\omega t) + f_6(\omega t) + f_7(\omega t) \\ + f_8(\omega t) + f_9(\omega t) + f_{10}(\omega t) + f_{11}(\omega t) + f_{12}(\omega t) + f_{13}(\omega t) \quad (2.5)$$

$$f(\omega t) = \sum_{n=1}^{13} f_n(\omega t) \quad (2.6)$$

The following table T.2.1 gives the definitions of the subfunctions $f_1(\omega t), \dots, f_{13}(\omega t)$ and the bounds of application for a 6-pulse Δ/Δ bridge rectifier.

Table 2.1Definitions and limits of subfunctions in a.c.supply waveforms for 6-pulse  rectifier operation

No	Function Definition	Limits (measured from the fixed reference)
1	$f_1(\omega t) = (v_c - v_b)$	$\theta_1 \leq \omega t \leq \theta_1 + \alpha_1$
2	$f_2(\omega t) = (\frac{v_a + v_c}{2} - v_b)$	$\theta_1 + \alpha_1 \leq \omega t \leq \theta_1 + \alpha_1 + u_1$
3	$f_3(\omega t) = (v_a - v_b)$	$\theta_1 + \alpha_1 + u_1 \leq \omega t \leq \theta_2 + \alpha_2$
4	$f_4(\omega t) = (v_a - \frac{v_b + v_c}{2})$	$\theta_2 + \alpha_2 \leq \omega t \leq \theta_2 + \alpha_2 + u_2$
5	$f_5(\omega t) = (v_a - v_c)$	$\theta_2 + \alpha_2 + u_2 \leq \omega t \leq \theta_3 + \alpha_3$
6	$f_6(\omega t) = (\frac{v_a + v_b}{2} - v_c)$	$\theta_3 + \alpha_3 \leq \omega t \leq \theta_3 + \alpha_3 + u_3$
7	$f_7(\omega t) = (v_b - v_c)$	$\theta_3 + \alpha_3 + u_3 \leq \omega t \leq \theta_4 + \alpha_4$
8	$f_8(\omega t) = (v_b - \frac{v_c + v_a}{2})$	$\theta_4 + \alpha_4 \leq \omega t \leq \theta_4 + \alpha_4 + u_4$
9	$f_9(\omega t) = (v_b - v_a)$	$\theta_4 + \alpha_4 + u_4 \leq \omega t \leq \theta_5 + \alpha_5$
10	$f_{10}(\omega t) = (\frac{v_b + v_c}{2} - v_a)$	$\theta_5 + \alpha_5 \leq \omega t \leq \theta_5 + \alpha_5 + u_5$
11	$f_{11}(\omega t) = (v_c - v_a)$	$\theta_5 + \alpha_5 + u_5 \leq \omega t \leq \theta_6 + \alpha_6$
12	$f_{12}(\omega t) = (v_c - \frac{v_a + v_b}{2})$	$\theta_6 + \alpha_6 \leq \omega t \leq \theta_6 + \alpha_6 + u_6$
13	$f_{13}(\omega t) = (v_c - v_b)$	$\theta_6 + \alpha_6 + u_6 \leq \omega t \leq 2\pi + \theta_1$

Since the Kth Fourier coefficient, by definition is

$$C_K = \frac{1}{2\pi} \int_0^{2\pi} f(\omega t) e^{-jK\omega t} d\omega t$$

So,

$$\begin{aligned} C_K = \frac{1}{2\pi} & \left\{ \int_{\theta_1 + \alpha_1}^{\theta_1 + \alpha_1 + u_1} f_1(\omega t) e^{-jK\omega t} d\omega t + \int_{\theta_1 + \alpha_2}^{\theta_1 + \alpha_1 + u_1} f_2(\omega t) e^{-jK\omega t} d\omega t \right. \\ & + \int_{\theta_1 + \alpha_1 + u_1}^{\theta_2 + \alpha_2} f_3(\omega t) e^{-jK\omega t} d\omega t + \int_{\theta_2 + \alpha_2}^{\theta_2 + \alpha_2 + u_2} f_4(\omega t) e^{-jK\omega t} d\omega t \\ & + \int_{\theta_2 + \alpha_2 + u_2}^{\theta_3 + \alpha_3} f_5(\omega t) e^{-jK\omega t} d\omega t + \int_{\theta_3 + \alpha_3}^{\theta_3 + \alpha_3 + u_3} f_6(\omega t) e^{-jK\omega t} d\omega t \\ & + \int_{\theta_3 + \alpha_3 + u_3}^{\theta_4 + \alpha_4} f_7(\omega t) e^{-jK\omega t} d\omega t + \int_{\theta_4 + \alpha_4}^{\theta_4 + \alpha_4 + u_4} f_8(\omega t) e^{-jK\omega t} d\omega t \\ & + \int_{\theta_4 + \alpha_4 + u_4}^{\theta_5 + \alpha_5} f_9(\omega t) e^{-jK\omega t} d\omega t + \int_{\theta_5 + \alpha_5}^{\theta_5 + \alpha_5 + u_5} f_{10}(\omega t) e^{-jK\omega t} d\omega t \\ & + \int_{\theta_5 + \alpha_5 + u_5}^{\theta_6 + \alpha_6} f_{11}(\omega t) e^{-jK\omega t} d\omega t + \int_{\theta_6 + \alpha_6}^{\theta_6 + \alpha_6 + u_6} f_{12}(\omega t) e^{-jK\omega t} d\omega t \\ & \left. + \int_{\theta_6 + \alpha_6 + u_6}^{2\pi + \theta_1} f_{13}(\omega t) e^{-jK\omega t} d\omega t \right\} \quad (2.7) \end{aligned}$$

2.3 Calculation of Fourier coefficients for Δ/Δ 6-pulse operation

The same procedure as used in section 2.2 is used here. Since the voltage on the a.c. bus is common to both bridges the use of Δ/Δ connection for the converter transformer for the second bridge give phase voltages on the secondary side in phase with the line voltages on the primary side and hence advanced by 30° . A choice of $\sqrt{3}:1$ turns ratio for the transformer windings however, ensures the secondary voltage for the Δ/Δ transformer to be of equal magnitude to Δ/Δ transformer.

The following table Table 2.2 illustrates the new function definitions for 6-pulse Δ/λ operation and the new limits with respect to the same fixed reference chosen before.

The definitions of line voltages with respect to a chosen fixed reference after modification by the Δ/λ transformer turns ratio are

$$\hat{v}_a = \hat{V}_a \cos(\omega t - \frac{\pi}{6}) = v_{ab}/\sqrt{3}$$

$$\hat{v}_b = \hat{V}_b \cos(\omega t - \frac{5\pi}{6}) = v_{bc}/\sqrt{3}$$

$$\hat{v}_c = \hat{V}_c \cos(\omega t + \frac{\pi}{2}) = v_{ca}/\sqrt{3}$$

Fig. 2.5 illustrates λ and Δ voltages with respect to the chosen fixed reference.

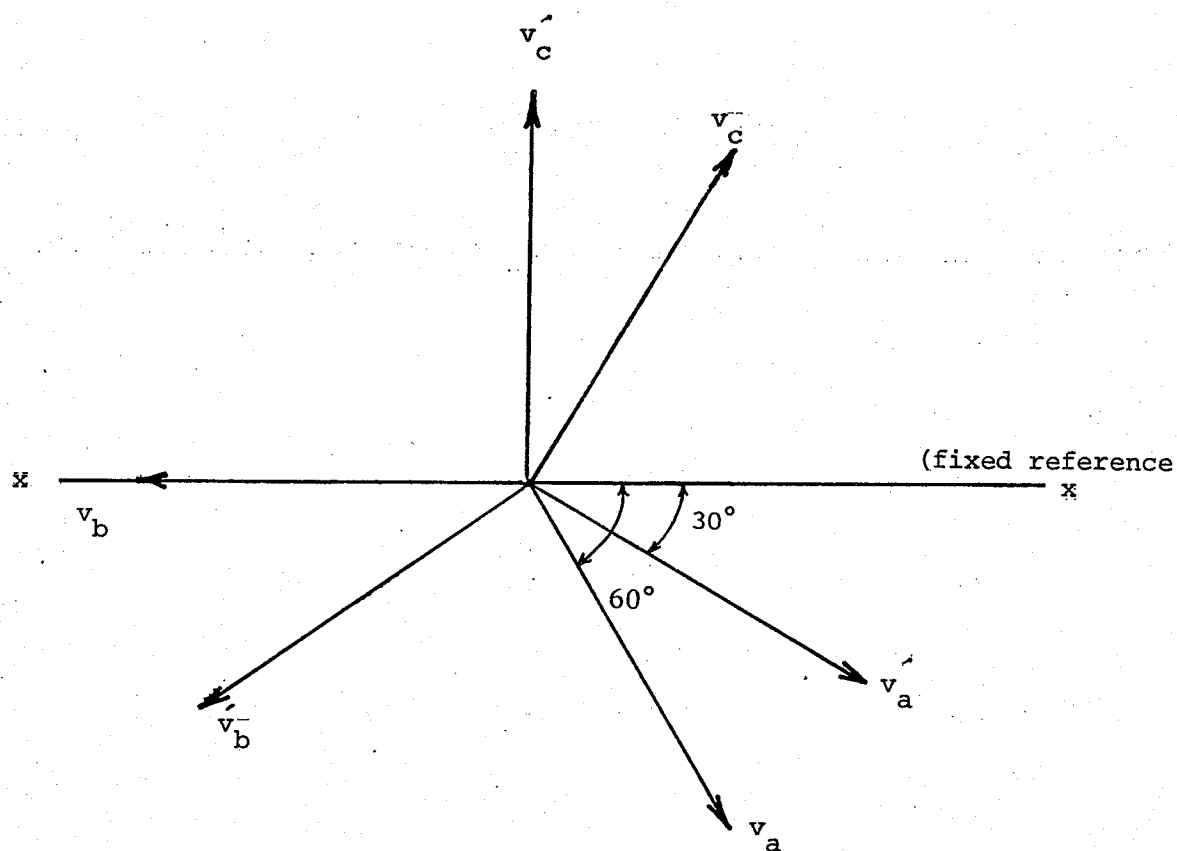


Fig. 2,5 Star and Delta voltages
with respect to the chosen fixed reference.

Table 2.2

Definitions of subfunctions and limits for
6-pulse Δ/Δ rectifier operation

Note $\theta'_n = \theta_n - \frac{\pi}{6}$

No	Function Definition	Limits (measured from the same fixed reference)
1	$f_1(\omega t) = (\dot{v}'_c - \dot{v}'_b)$	$\theta'_1 \leq \omega t \leq \theta'_1 + \alpha_1$
2	$f_2(\omega t) = (\frac{\dot{v}'_a + \dot{v}'_b}{2} - \dot{v}'_b)$	$\theta'_1 + \alpha_1 \leq \omega t \leq \theta'_1 + \alpha_1 + u_1$
3	$f_3(\omega t) = (\dot{v}'_a - \dot{v}'_b)$	$\theta'_1 + \alpha_1 + u_1 \leq \omega t \leq \theta'_2 + \alpha_2$
4	$f_4(\omega t) = (\dot{v}'_a - \frac{\dot{v}'_b + \dot{v}'_c}{2})$	$\theta'_2 + \alpha_2 \leq \omega t \leq \theta'_2 + \alpha_2 + u_2$
5	$f_5(\omega t) = (\dot{v}'_a - \dot{v}'_c)$	$\theta'_2 + \alpha_2 + u_2 \leq \omega t \leq \theta'_3 + \alpha_3$
6	$f_6(\omega t) = (\frac{\dot{v}'_a + \dot{v}'_b}{2} - \dot{v}'_c)$	$\theta'_3 + \alpha_3 \leq \omega t \leq \theta'_3 + \alpha_3 + u_3$
7	$f_7(\omega t) = (\dot{v}'_b - \dot{v}'_c)$	$\theta'_3 + \alpha_3 + u_3 \leq \omega t \leq \theta'_4 + \alpha_4$
8	$f_8(\omega t) = (\dot{v}'_b - \frac{\dot{v}'_c + \dot{v}'_a}{2})$	$\theta'_4 + \alpha_4 \leq \omega t \leq \theta'_4 + \alpha_4 + u_4$
9	$f_9(\omega t) = (\dot{v}'_b - \dot{v}'_a)$	$\theta'_4 + \alpha_4 + u_4 \leq \omega t \leq \theta'_5 + \alpha_5$
10	$f_{10}(\omega t) = (\frac{\dot{v}'_b + \dot{v}'_c}{2} - \dot{v}'_a)$	$\theta'_5 + \alpha_5 \leq \omega t \leq \theta'_5 + \alpha_5 + u_5$
11	$f_{11}(\omega t) = (\dot{v}'_c - \dot{v}'_a)$	$\theta'_5 + \alpha_5 + u_5 \leq \omega t \leq \theta'_6 + \alpha_6$
12	$f_{12}(\omega t) = (\dot{v}'_c - \frac{\dot{v}'_a + \dot{v}'_b}{2})$	$\theta'_6 + \alpha_6 \leq \omega t \leq \theta'_6 + \alpha_6 + u_6$
13	$f_{13}(\omega t) = (\dot{v}'_c - \dot{v}'_b)$	$\theta'_6 + \alpha_6 + u_6 \leq \omega t \leq 2\pi + \theta'_1$

The new limits and new definitions of subfunctions $f_1(\omega t)$,, $f_{13}(\omega t)$ are substituted in equation (2.7) to obtain the Kth Fourier coefficient for Δ/λ 6-pulse operation.

An alternative approach:

Since the Kth harmonic in a Δ/λ bridge leads that of a λ/λ bridge by $(K \cdot 30^\circ)$, to obtain the harmonics of a Δ/λ bridge the harmonic phasors in a λ/λ 6-pulse operation should be rotated through an angle of $(K \cdot 30^\circ)$.

The harmonics in a 12-pulse operation are simply obtained as the vectorial sum of the harmonics in both λ/λ and Δ/λ 6-pulse operation.

2.4 Basis for computer programming

Using the complex Fourier analysis, the integration of the functions $f_1(\omega t)$,, $f_{13}(\omega t)$ is a repetitive summation procedure. The same technique had been adopted by Reeve and Krishnayya for a.c. side current harmonics^{1,3}.

Consider the general form

$$v = \hat{V} \cos(\omega t - \theta) \quad (2.8a)$$

which is expressed in exponential form as

$$v = \frac{\hat{V}}{2} (e^{j(\omega t - \theta)} + e^{-j(\omega t - \theta)}) \quad (2.8b)$$

The definition of the integral of the function v between any two general limits $L(I)$, $L(I + 1)$ is as follows:

$$I(I) = \int_{L(I)}^{L(I+1)} v e^{-jK\omega t} d\omega t$$

$$= \int_{L(I)}^{L(I+1)} \frac{\hat{V}}{2} (e^{j(\omega t - \theta)} + e^{-j(\omega t - \theta)}) e^{-jK\omega t} d\omega t \quad (2.9)$$

$$\begin{aligned} I(I) &= \int_{L(I)}^{L(I+1)} \frac{\hat{V}}{2} [e^{-j(K-1)\omega t} e^{-j\theta} + e^{-j(K+1)\omega t} e^{j\theta}] d\omega t \\ &= 0.5 \cdot \hat{V} \cdot [e^{-j\theta} \frac{e^{-j(K-1)\omega t}}{-j(K-1)} \Big|_{L(I)}^{L(I+1)} + e^{j\theta} \frac{e^{-j(K+1)\omega t}}{-j(K+1)} \Big|_{L(I)}^{L(I+1)}] \end{aligned} \quad (2.10)$$

Put

$$\begin{aligned} Fl1(I,K) &= \frac{j}{(K-1)} e^{-j(K-1)\omega t} \Big|_{L(I)}^{L(I+1)} \\ &= \frac{j}{K-1} (e^{-j(K-1)L(I+1)} - e^{-j(K-1)L(I)}) \end{aligned} \quad (2.11)$$

and

$$Fl2(I,K) = \frac{j}{(K+1)} (e^{-j(K+1)L(I+1)} - e^{-j(K+1)L(I)}) \quad (2.12)$$

The value of the definite integral $I(I)$ tends to be equal to:

$$I(I) = 0.5 \cdot \hat{V} \cdot (e^{-j\theta} \cdot Fl1(I,K) + e^{j\theta} \cdot Fl2(I,K)) \dots \quad (2.13)$$

From (2.13) and for different voltage functions v_a, v_b, v_c

$$\begin{aligned} I_a(I) &= \int_{L(I)}^{L(I+1)} v_a e^{-jK\omega t} d\omega t = 0.5 \cdot \hat{V}_a \cdot (e^{-j\frac{\pi}{3}} \cdot Fl1(I,K) + e^{j\frac{\pi}{3}} \cdot Fl2(I,K)) \\ I_b(I) &= \int_{L(I)}^{L(I+1)} v_b e^{-jK\omega t} d\omega t = 0.5 \cdot \hat{V}_b \cdot (e^{-j\pi} \cdot Fl1(I,K) + e^{j\pi} \cdot Fl2(I,K)) \\ I_c(I) &= \int_{L(I)}^{L(I+1)} v_c e^{-jK\omega t} d\omega t = 0.5 \cdot \hat{V}_c \cdot (e^{j\frac{\pi}{3}} \cdot Fl1(I,K) + e^{-j\frac{\pi}{3}} \cdot Fl2(I,K)) \end{aligned} \quad (2.14)$$

2.5 D.C. voltage harmonics for a general case

To include the effects of harmonic content and phase imbalance of a.c. supply voltages, the phase voltages are defined as follows:

$$\begin{aligned}
 v_a &= \sum_{n=1}^N \hat{V}_{an} \cos (n\omega t - \theta_{an}) \\
 v_b &= \sum_{n=1}^N \hat{V}_{bn} \cos (n(\omega t - \frac{2\pi}{3}) - \theta_{bn}) \\
 v_c &= \sum_{n=1}^N \hat{V}_{cn} \cos (n(\omega t + \frac{2\pi}{3}) - \theta_{cn})
 \end{aligned} \tag{2.15}$$

A general digital computer program is written to calculate the Kth order harmonic on the d.c. side taking into account distortion and phase imbalance of the a.c. supply voltages defined by equation (2.15).

The procedure as explained in section 2.4 is adopted except that a summation sign in the definition of a.c. phase voltages should now be introduced.

The general integral $I(I)$ in equation (2.9) takes the form

$$I(I) = \int_{L(I)}^{L(I+1)} \sum_{n=1}^N \hat{V}_n \cos (n\omega t - \theta_n) e^{-jK\omega t} d\omega t$$

By continuity theorems, summation sign can interchange position with the integral sign, and then superposition theorem can be applied.

$$I(I) = \sum_{n=1}^N \int_{L(I)}^{L(I+1)} \hat{V}_n \cos (n\omega t - \theta_n) e^{-jK\omega t} d\omega t \tag{2.16}$$

$$\begin{aligned}
 &= \sum_{n=1}^N \frac{1}{2} \hat{V}_n \int_{L(I)}^{L(I+1)} (e^{-j\theta_n} e^{jn\omega t} + e^{j\theta_n} e^{-jn\omega t}) e^{-jK\omega t} d\omega t \\
 &\tag{2.17}
 \end{aligned}$$

$$I(I) = \sum_{\substack{n=1 \\ n \neq K}}^N \frac{1}{2} \hat{V}_n \left[e^{-j\theta_n} \frac{e^{j(n-K)\omega t}}{j(n-K)} \begin{matrix} L(I+1) \\ | \\ L(I) \end{matrix} + e^{j\theta_n} \frac{e^{-j(n+K)\omega t}}{-j(n+K)} \begin{matrix} L(I+1) \\ | \\ L(I) \end{matrix} \right] \quad (2.18)$$

$$I(I) = \sum_{\substack{n=1 \\ n=K \text{ only}}}^N \frac{1}{2} \hat{V}_n \left[e^{-j\theta_n} (L(I+1) - L(I)) + e^{j\theta_n} \frac{e^{-j(n+K)\omega t}}{-j(n+K)} \begin{matrix} L(I+1) \\ | \\ L(I) \end{matrix} \right] \quad (2.19)$$

As the functions $f_1(\omega t)$, ..., $f_{13}(\omega t)$ are formed from the combination of v_a, v_b, v_c for 6-pulse λ/λ operation, or (v'_a, v'_b, v'_c) for 6-pulse Δ/λ operation, the integral of any function of these tends to a combinations of the previously defined integrals $I_a(I), I_b(I), I_c(I)$.

The magnitudes and phase angles of complex Fourier coefficients for both 6-pulse and 12-pulse operations are obtained for harmonics up to an order of (48).

The "Complex Fourier Coefficients" program is checked using another program to calculate the "Sine and Cosine terms".

Both programs gave the same results for balanced as well as unbalanced operations.

The power frequency component and average d.c. voltage on the d.c. side are obtained by using a separate program.

A special program is written to incorporate a.c. supply harmonics.

Flow charts and computer programs are shown in Appendix (1).

2.6 Unbalance parameters

In order to gain a clear understanding of the harmonic phenomena on the d.c. side first, the influence of each asymmetry is studied individually and later combinations pertaining to any realistic cases are examined.

Cases of voltage depression in a.c. supply are likely to occur and in the following logic equations the effect of imbalance of the fundamental component of a.c. voltage on the magnitudes of conduction periods of valves is studied.

To explain the notation adopted,

$v_a \downarrow = (\phi_m, \phi_n)^+$ means, both conduction angles for values m and n increase due to a depression in phase (a) voltage.

Fig. 2.6 illustrates the effect of voltage depression on the magnitudes of conduction angles of valves in a 6-pulse operation.

a) Voltage depression in one phase

$$v_a \downarrow = (\phi_1, \phi_4)^- + (\phi_2, \phi_3, \phi_5, \phi_6)^+$$

$$v_b \downarrow = (\phi_3, \phi_6)^- + (\phi_1, \phi_2, \phi_4, \phi_5)^+$$

$$v_c \downarrow = (\phi_2, \phi_5)^- + (\phi_1, \phi_4, \phi_3, \phi_6)^+$$

b) Voltage depression in two phases

$$(v_a, v_b) \downarrow = (\phi_1, \phi_3, \phi_2, \phi_6)^- + (\phi_2, \phi_3, \phi_5, \phi_6)^+$$

$$(v_b, v_c) \downarrow = (\phi_2, \phi_3, \phi_5, \phi_6)^- + (\phi_1, \phi_2, \phi_4, \phi_5)^+$$

$$(v_c, v_a) \downarrow = (\phi_1, \phi_2, \phi_4, \phi_6)^- + (\phi_1, \phi_2, \phi_3, \phi_4)^+$$

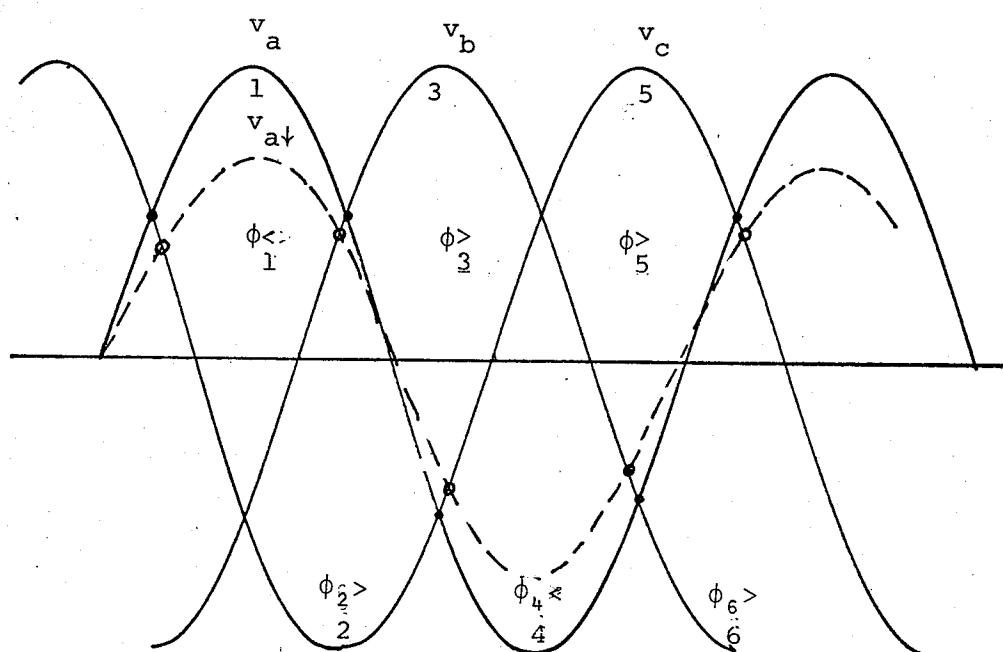


Fig. 2.6 Effect of voltage depression in phase (a) on the magnitudes of conduction angles for valves in 6-pulse operation.

CHAPTER III

COMPUTATIONAL RESULTS3.1 General

Uncharacteristic harmonics are likely to occur in a converter operation due to the following imbalance conditions:

- a) Imbalance of magnitude and phase of the a.c. supply fundamental component voltage.
- b) Imbalance in ignition angle (α) alone or in conjunction with other parameters.
- c) Imbalance in commutation angle (u) mainly due to unequal converter transformer phase inductances.
- d) Harmonic content in the a.c. supply produced either during faults or due to the energization of transformers.

3.2 Effect of each imbalance parameter separately

Table T.3.1 shows the computed results of harmonic content on the d.c. side in balanced 6-pulse and 12-pulse converter operations. These harmonics are multiples of the pulse number and are called characteristic or normal harmonics.

Table 3.1

Characteristic harmonics for 6-pulse and 12-pulse
converter operations for different operating conditions

$$V_{\text{BASE}} = \begin{matrix} (V) \\ (L-L) \end{matrix} \quad R.M.S. = 100\%$$

Harmonic order (K)	0/0 voltage harmonic							
	$\alpha_n = 0$	$\alpha_n = 0$	$\alpha_n = 15^\circ$	$u_n = 15^\circ$	$\alpha_n = 20^\circ$	$u_n = 20^\circ$	$\alpha_n = 15^\circ$	$u_n = 24^\circ$
	6-pulse	12-pulse	6-pulse	12-pulse	6-pulse	12-pulse	6-pulse	12-pulse
6	3.858	0.0	7.765	0.0	7.589	0.0	6.213	0.0
12	0.944	1.88	1.367	2.734	2.923	5.846	4.058	8.117
18	0.418	0.0	2.038	0.0	3.722	0.0	2.945	0.0
24	0.238	0.469	2.149	4.298	1.634	3.268	1.196	2.392
30	0.150	0.0	1.306	0.0	1.216	0.0	2.005	0.0
36	0.104	0.208	0.452	0.905	1.851	3.701	0.866	1.732
42	0.076	0.0	0.889	0.0	0.916	0.0	1.189	0.0
48	0.058	0.117	1.069	2.138	0.768	1.537	1.072	2.145

If imbalance takes place in phase voltages, non-characteristic harmonics are produced. It was found that imbalance in a.c. supply fundamentals or imbalance in phase angles results in only even harmonics on the d.c. side of the converter station. These results agree with Reeve and Baron⁴.

Table 3.2 shows all characteristic and non-characteristic harmonic voltages due to imbalance in a.c. supply fundamentals.

Table 3.2

Percentage harmonics in d.c. side voltage due to
unbalance in fundamental a.c. supply

Note: Only even harmonics are produced

$(\alpha_n = 15^\circ, u_n = 15^\circ), (V_{BASE} = (V) \text{ R.M.S.} = 100\%)$
 L-L

Harmonic order (K)	-5% in v_a		-5% in v_a, v_b (+5% in v_c)		-5% in phase angle θ_c
	6-pulse	12-pulse	6-pulse	12-pulse	6-pulse
2	1.115	1.032	1.116	1.932	1.15
4	0.178	0.178	0.178	0.178	0.1178
6	7.635	0.0	7.50	0.0	6.181
8	0.097	0.097	0.097	0.097	0.0175
10	0.0133	0.0231	0.0133	0.0231	0.0717
12	1.344	2.689	1.321	2.643	3.921
14	0.01133	0.01963	0.0113	0.01962	0.0828
16	0.0403	0.0403	0.0403	0.0403	0.0634
18	2.004	0.0	1.97	0.0	2.862
20	0.047	0.047	0.047	0.047	0.04148
22	0.048	0.084	0.048	0.0839	0.0054
24	2.113	4.227	2.077	4.155	1.186
26	0.044	0.077	0.0446	0.0773	0.0236
28	0.0307	0.0307	0.0307	0.0307	0.0397
30	1.284	0.0	1.262	0.0	1.9362

Figure 3.1 illustrates the magnitudes of d.c. side mean voltage versus imbalance in a.c. supply voltage

Figure 3.2 illustrates the harmonic amplitude spectra of d.c. side voltage depression in phase (a)

Figure 3.3 illustrates the harmonic amplitude spectra of d.c. side harmonic voltages due to voltage depression in phases (a), (b), i.e., voltage rise in phase (c)

Unbalance in commutation angle (u) due to unequal converter transformer phase inductances is considered in appendix 3(a) and fig. 3.4 illustrates the level of imbalance of u versus unbalance in inductance for different operating conditions of α , u .

3.3 Combinations of imbalance parameters

The effect of different combinations of imbalance parameters is also studied, and in table T. 3.3 magnitudes of d.c. side voltage harmonics for different combinations of previously mentioned unbalance parameters are illustrated. Harmonics up to 24 are included but the program is capable of calculating harmonics up to any required order.

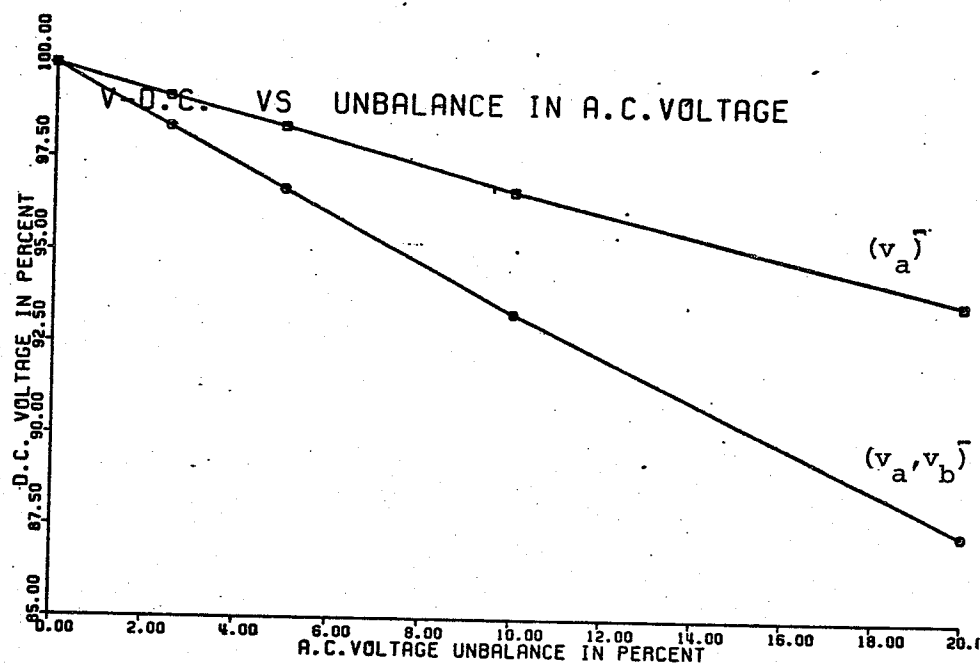


Fig. 3.1 Magnitude of d.c. side mean voltage versus imbalance in a.c. supply voltages.

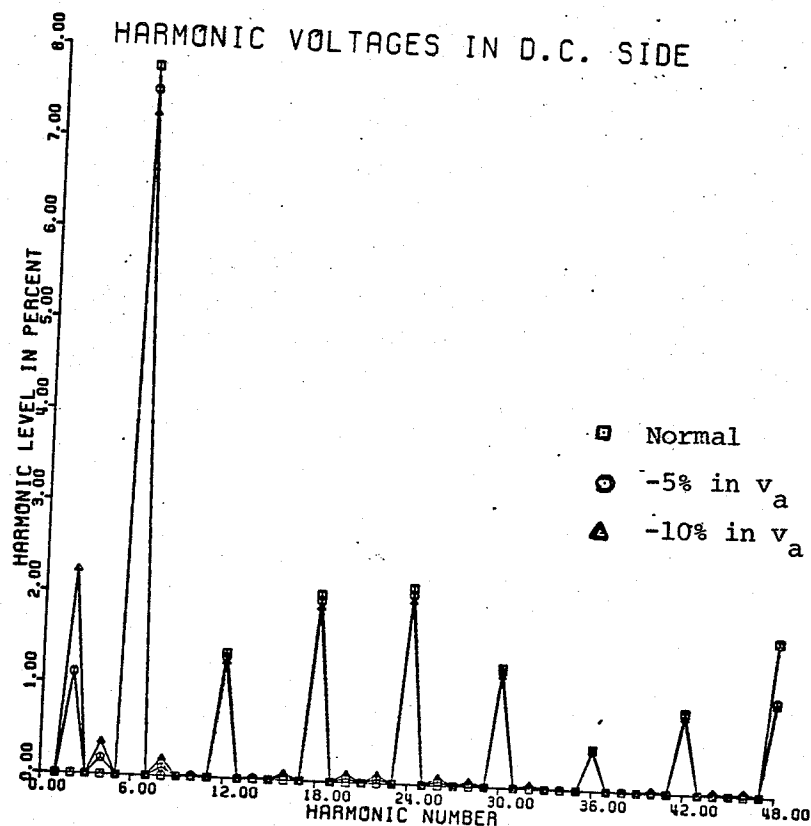


Fig. 3.2 Harmonic amplitude spectra of d.c. side voltage harmonics due to voltage depression in Phase (a)

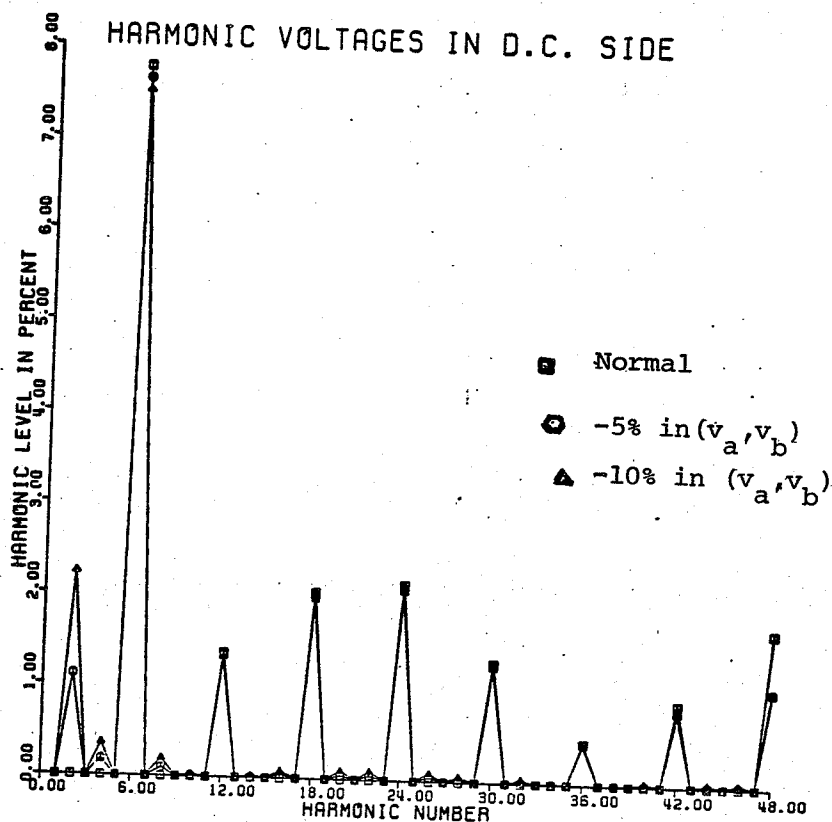


Fig. 3.3 Harmonic amplitude spectra of d.c. side voltage harmonics due to depression in phase (a), (b) (i.e. voltage rise in phase (c))

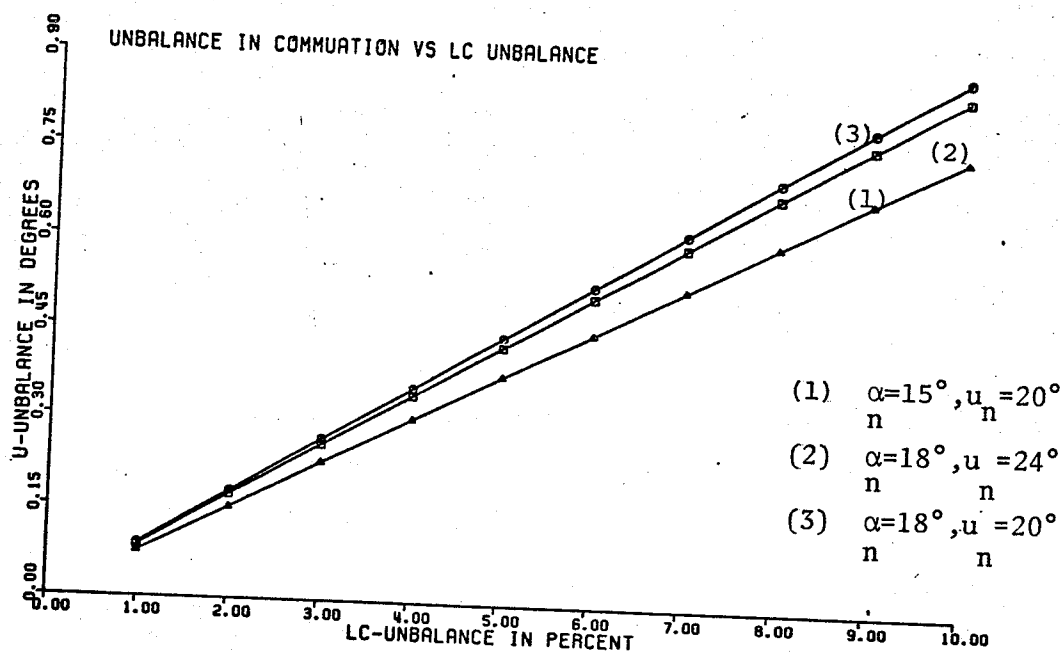


Fig. 3.4 Level of imbalance of (u) versus unbalance in inductance for different operating conditions of α, u

Table 3.3

Percentage d.c. side voltage harmonics under different combinations of unbalance parameters

$$(\alpha_n = 15^\circ, u_n = 24^\circ, V_{\text{BASE}} = (V_{L-L})_{\text{RMS}} = 100\%)$$

Harmonic order (K)	$\Delta\alpha = 0.5^\circ$		$\Delta u = 0.5^\circ$		$\Delta(\alpha, u) = 0.5^\circ$ 0.5°		$\Delta(\alpha, v_a) = 0.5^\circ$ -2%		$\Delta(\alpha, v_a, v_b) = 0.5^\circ$ -2% -2%	
	6-pulse	12-pulse	6-pulse	12-pulse	6-pulse	12-pulse	6-pulse	12-pulse	6-pulse	12-pulse
0	117.78	235.56	117.94	235.8	118.02	236.05	116.99	233.99	116.213	232.42
1	0.085	0.164	0.062	0.119	0.146	0.285	0.085	0.164	0.083	0.161
2	0.080	0.139	0.061	0.106	0.057	0.099	0.516	0.895	0.507	0.87
3	0.073	0.139	0.0	0.0	0.073	0.103	0.073	0.103	0.0717	0.101
4	0.063	0.063	0.061	0.061	0.084	0.084	0.054	0.054	0.0177	0.0177
5	0.053	0.027	0.106	0.055	0.143	0.074	0.053	0.027	0.052	0.027
6	6.21	0.0	6.28	0.0	6.27	0.0	6.168	0.0	6.127	0.0
7	0.037	0.019	0.106	0.055	0.142	0.073	0.0369	0.019	0.036	0.0189
8	0.037	0.037	0.061	0.061	0.054	0.054	0.039	0.039	0.032	0.032
9	0.043	0.061	0.0	0.0	0.041	0.058	0.043	0.0613	0.042	0.042
10	0.053	0.092	0.061	0.106	0.041	0.071	0.026	0.045	0.048	0.083
11	0.063	0.123	0.106	0.205	0.166	0.321	0.064	0.123	0.062	0.121
12	4.04	8.08	3.038	7.876	3.922	7.84	4.017	8.034	3.99	7.98
13	0.080	0.155	0.106	0.205	0.174	0.33	0.0804	0.155	0.078	0.152
14	0.084	0.14	0.061	0.106	0.076	0.132	0.1108	0.192	0.1137	0.197
15	0.086	0.122	0.0	0.0	0.085	0.121	0.086	0.122	0.084	0.119
16	0.084	0.147	0.061	0.061	0.088	0.088	0.066	0.066	0.062	0.062
17	0.08	0.0416	0.106	0.055	0.1708	0.088	0.080	0.0416	0.078	0.062
18	2.93	0.0	2.99	0.0	2.98	0.0	2.914	0.0	2.895	0.0
19	0.063	0.033	0.106	0.055	0.173	0.089	0.063	0.032	0.062	0.032
20	0.053	0.053	0.061	0.061	0.026	0.026	0.069	0.069	0.062	0.062
21	0.043	0.061	0.0	0.0	0.047	0.066	0.043	0.043	2.042	0.0605
22	0.037	0.064	0.061	0.106	0.0701	0.121	0.036	0.063	0.038	0.066
23	0.037	0.072	0.106	0.205	0.135	0.261	0.0368	0.0712	0.036	0.0706
24	1.19	2.382	1.106	2.213	1.098	2.197	1.183	2.367	1.175	2.35

* $\Delta\alpha = 0.5^\circ$ is taken as all valves except one are working at same (α) .

* $\Delta u = 0.5^\circ$ is taken as four valves are working at same (u) while the other two are working at different (u) .

3.4 Effect of harmonic content in a.c. supply voltage

The effect of harmonic content in the a.c. supply voltages is considered the most severe case that gives rise to non-characteristic harmonics of all orders and of comparatively high level.

Instead of assuming arbitrary harmonic content, two waveforms representing a.c. supply voltages during faults are obtained from results of simulation studies for the second bipole of Manitoba Hydro.

One full period of each a.c. voltage waveforms was photographically amplified to a reasonable size, and then divided into 24 ordinates to allow determination of harmonic content up to 11th order by using a numerical Fourier analysis.

Figures 3.5.a, 3.5.b illustrate these photographs of the chosen a.c. supply waveforms.

A.C. harmonics up to 9th order are considered significant for the results in this thesis.

The computer program was written to be capable to study any arbitrary combinations of harmonics in the a.c. supply voltages. In the work done by Reeve and Baron⁴, only 2nd and 3rd a.c. side harmonics were taken into account and the treatment of imbalance of a.c. supply voltage harmonics was restrictive.

Table T. 3.4 shows percentage harmonics in the chosen a.c. voltage waveforms.

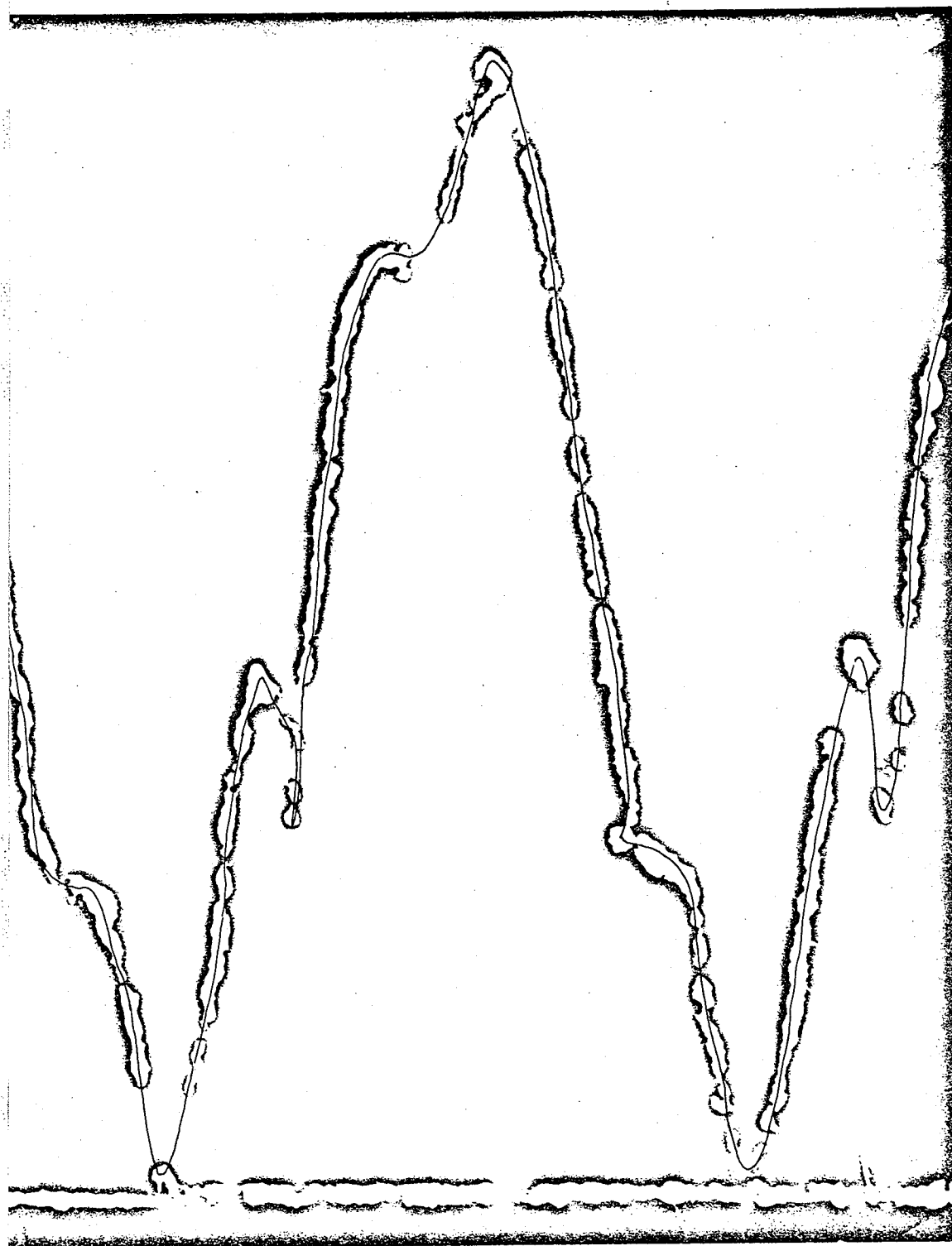


Fig. 3.5 (a) Distorted a.c. supply voltages (phase a)

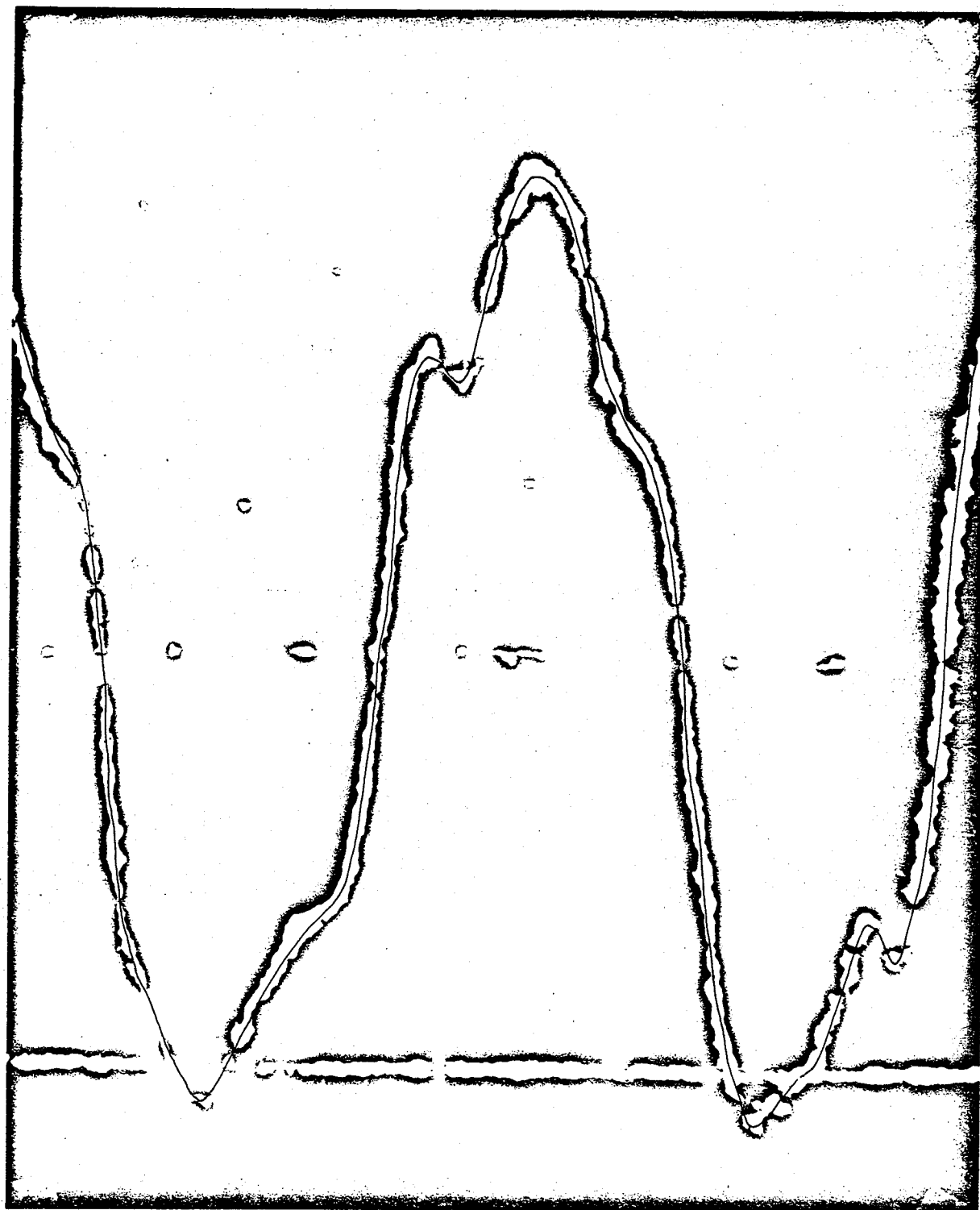


Fig. 3.5 (b) Distorted a.c. supply voltages (phase c)

Table 3.4

Harmonic content in a.c. supply voltages in
percent

($V_{ph \text{ max}} = 100\%$)

Harmonic order K	Phase (a) (V_a)	Phase (b) (V_b)	Phase (c) (V_c)
1	57.99 /60.0°	57.99 /60.0°	55.85 /60.0°
2	12.35 /57.54	12.35 /57.54	4.84 /57.54
3	1.8 /124.39	1.8 /124.39	6.18 /124.39
4	9.2 /250.7	9.2 /250.7	4.38 /250.7
5	3.66 /138.35	3.66 /138.35	4.82 /138.35
6	1.61 /76.08	1.61 /76.08	0.088 /76.35
7	1.99 /107.08	1.99 /107.08	1.69 /76.08
8	9.9 /94.73	9.9 /94.73	0.61 /107.08
9	1.6 /29.46	1.6 /29.46	1.62 /29.46

The a.c. distorted supply voltages are classified on account of harmonic content into balanced and unbalanced.

Balanced Case:

The 3-phases ~~have~~ the same harmonic content (magnitude and phase angle) as phase (a)

Unbalanced Case:

The phases (a), (b) are chosen to have the same harmonic content while phase (c) has different magnitudes of harmonics, and for simplicity the phase angles are chosen same as for phases (a), (b).

Figs. 3.6a and 3.6b illustrate a.c. supply waveforms for the two classified cases of balanced and unbalanced a.c. harmonics.

The resultant d.c. side voltage harmonics due to both cases of unbalanced and balanced harmonic contents in the a.c. supply are calculated for 6-pulse and 12-pulse converter operation.

Table 3.5 shows the levels and orders of d.c. side voltage harmonics, produced by the balanced and unbalanced a.c. supply waveforms shown in figs. 3.6a and 3.6b.

As a result of a distorted a.c. supply, the d.c. side voltage will contain harmonics of different orders and magnitudes.

It was found that the d.c. side voltage contains dominant triplen harmonics produced on account of high levels of even harmonics in a.c. supply voltages. The balanced case of harmonic content in the a.c. supply voltages leads only to triplen d.c. side harmonic voltages.

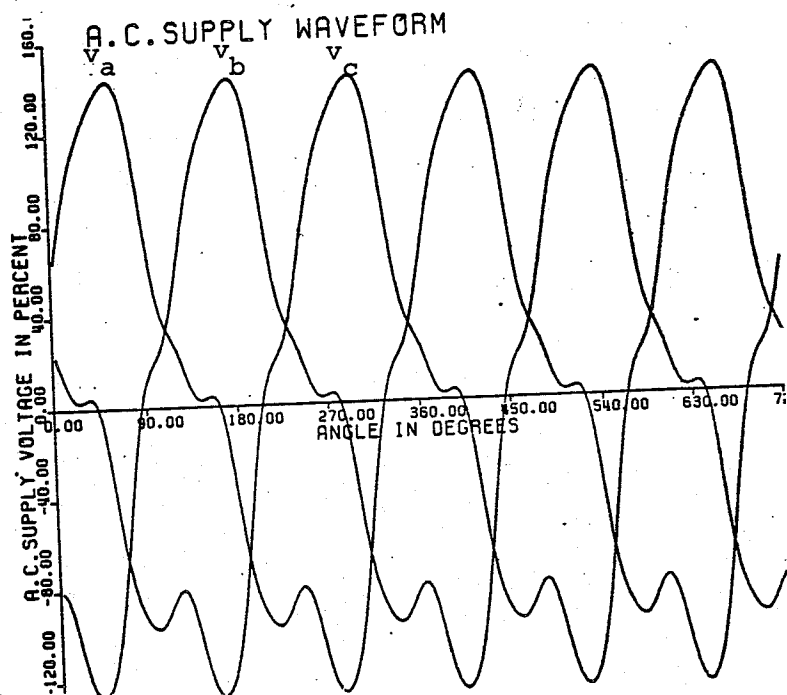


Fig. 3.6. (a) A.C. supply voltage waveform on account of balanced a.c. harmonics.

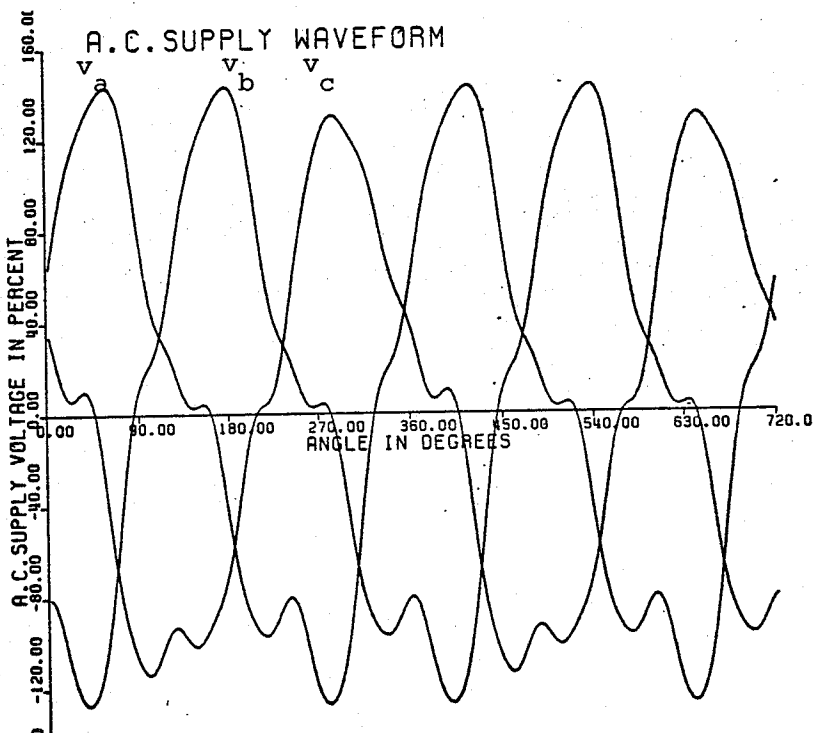


Fig. 2.6 (b) A.C. supply voltage waveform on account of unbalanced a.c. harmonics.

Table 3.5

D.C. side voltage harmonics in percent on
account of balanced and unbalanced a.c. harmonics

$$(V_{\text{BASE}} = V_{\text{dn}} = 1.35 \times (V_{\text{L-L}}) \text{R.M.S.} = 100\%)$$

Harmonic order n	v_d (Balanced a.c. harmonics)		v_d (unbalanced a.c. harmonics)	
	6-pulse	12-pulse	6-pulse	12-pulse
1	0.0	0.0	2.99	4.9
2	0.0	0.0	1.72	2.98
3	21.54	30.44	17.41	24.62
4	0.0	0.0	1.02	1.024
5	0.0	0.0	2.01	1.04
6	6.277	0.0	6.35	0.0
7	0.0	0.0	0.255	0.132
8	0.0	0.0	0.285	0.28
9	1.24	1.756	1.04	1.48
10	0.0	0.0	0.264	0.44
11	0.0	0.0	0.131	0.248
12	3.5	7.0038	3.47	6.94

The d.c. voltage harmonics will act as a harmonic generator, and the waveforms of such generator for balanced and unbalanced a.c. supply harmonics are studied for 6-pulse and 12-pulse operations. The harmonic generator waveforms are shown in figs. 3.7.a, 3.7.b, 3.8.a, 3.8.b.

For illustration, a discrete amplitude spectra of d.c. voltage harmonics is shown in fig. 3.9 for 6-pulse converter operation.

Cases of odd and even a.c. supply harmonics are considered separately and the resulting d.c. side harmonics are obtained for each case. These cases are similar to those studied by Reeve and Baron⁴, and reproduce the same results.

3.15 Conclusions

- a) Imbalance of ignition angle (α) alone or in conjunction with other parameters produce a whole spectrum of d.c. side harmonics.
- b) Imbalance of a.c. supply fundamentals produce only even harmonics on the d.c. side of converter.
- c) Odd a.c. supply harmonics, if balanced do not add any non-characteristic harmonics, if these odd harmonics are unbalanced in the 3 phases of the supply, they add to even harmonic orders on the d.c. side of converter.
- d) Imbalance in commutation angle (u) produce the whole spectrum of d.c. side voltage harmonics.
- e) Even a.c. supply harmonics produce a spectrum of odd d.c. harmonics on the d.c. side, and in case of balanced even a.c. harmonics in the 3 phases of the supply, only triplen harmonics are produced.

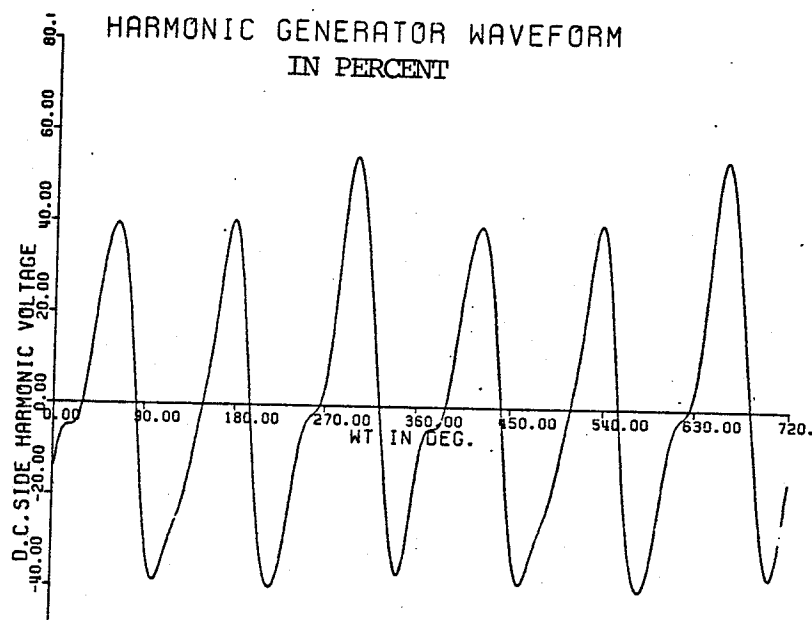


Fig. 3.7 (a) D.C. side harmonic generator waveform for 6-pulse operation on account of balanced a.c. harmonics.

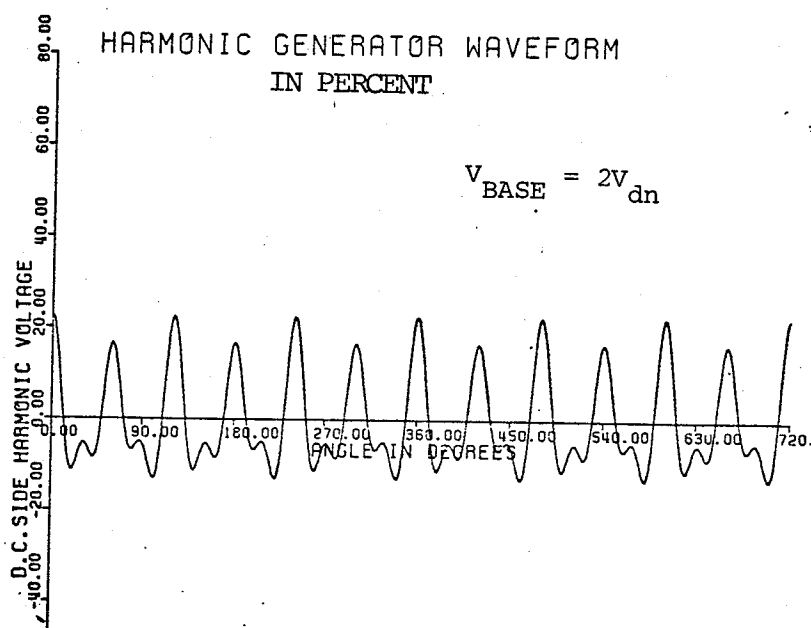


Fig. 3.7 (b) D.C. side harmonic generator waveform for 6-pulse operation on account of unbalanced a.c. harmonics.

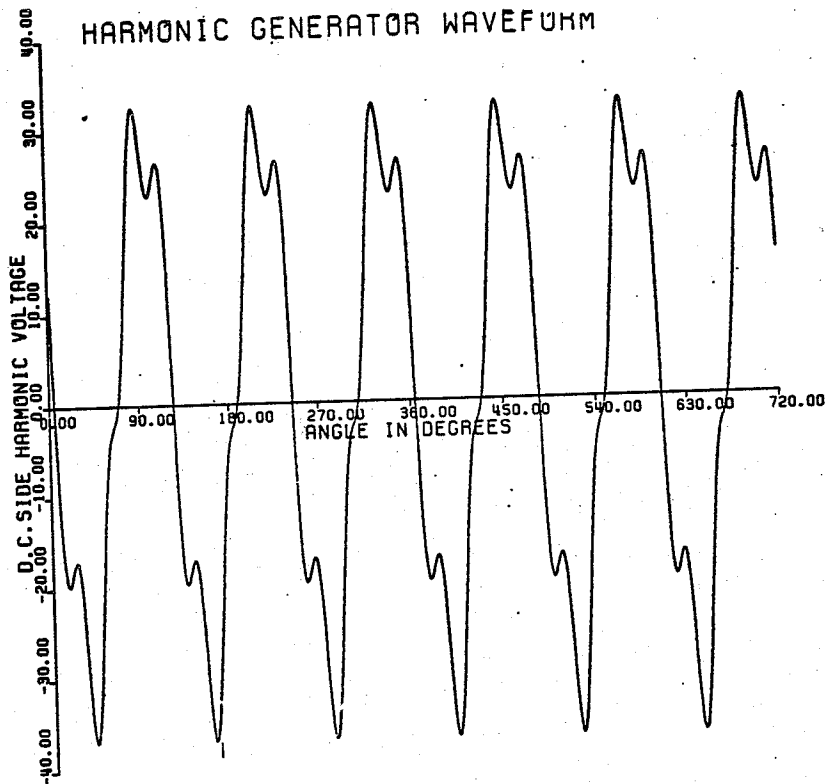


Fig. 3.8 (a) D.C. side harmonic generator waveform for 12-pulse operation on account of balanced a.c. harmonics.

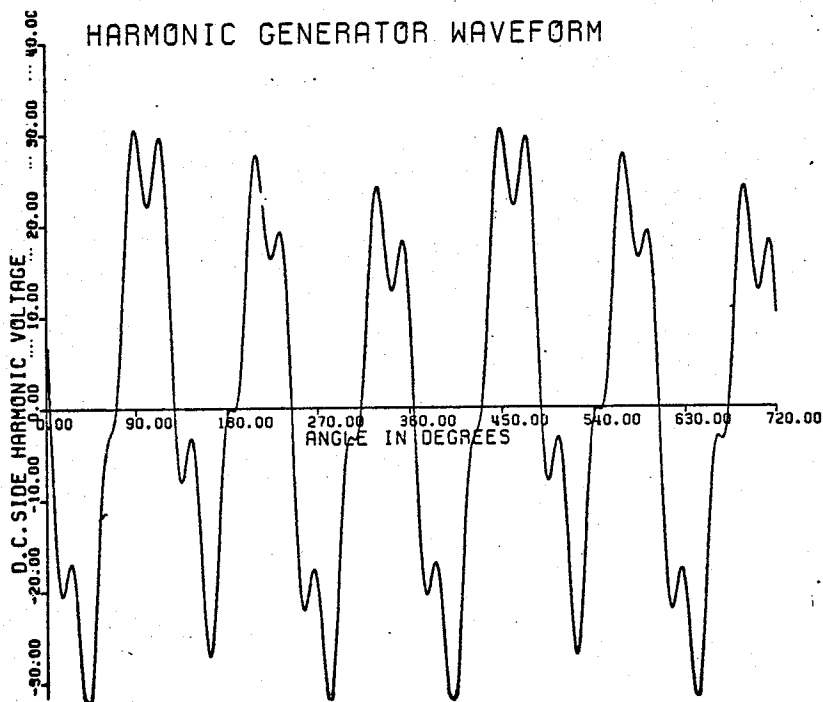


Fig. 3.8 (b) D.C. side harmonic generator waveform for 12-pulse operation on account of unbalanced a.c. harmonics.

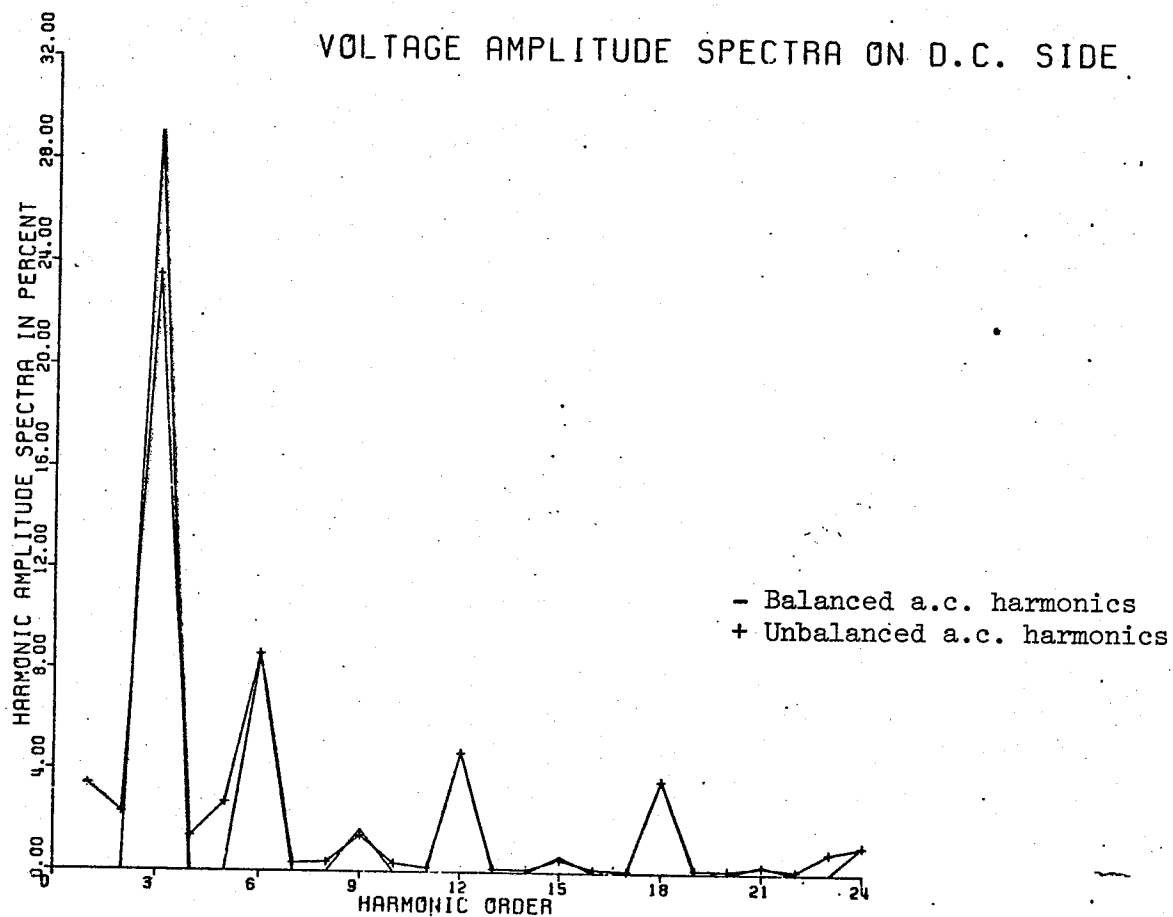


Fig. 3.9 Discrete harmonic amplitude spectra of d.c. voltage harmonics for 6-pulse operation.

- f) In all above cases, the characteristic harmonics, which already exist during normal operation are practically of the same magnitude, i.e., the asymmetries do not modify these harmonic to a large extent.

CHAPTER IV

CALCULATION OF D.C. SIDE HARMONICCURRENTS4.1 Introduction

In Chapter 3, the d.c. side voltage harmonics are calculated for various asymmetrical conditions. In the following analysis these d.c. side voltage harmonics are regarded as harmonic sources, and for both 6-pulse and 12-pulse converter operations, the current harmonics in filtering branches and transmission line and also the voltage drop across filters are calculated.

In this chapter a procedure is established for the calculation of harmonic currents in various components including line on the d.c. side of a converter. The harmonics are generated due to various asymmetries discussed in Chapter 2 and 3. The results of this chapter for the sake of compactness deal with the harmonics generated due to distortion in the a.c. waveform only, which anyhow provides the most severe case and causes system breakdown.

References [7,8] show the procedure adopted in calculating d.c. side harmonic currents; Moreover, the procedure had been elaborated in Appendix 2.(a).

There are two main reasons for calculating the harmonic currents on the d.c. side:

(a) Determining the level of harmonic currents through the 6th arm and 12th arm filters and the voltage drop across filtering branches are needed to set up the protection circuits for the filters. Manitoba

Hydro has experienced tripping of 6th arm filters sometimes due to the energization of generator transformers which lead to an interruption of power flow through the d.c. pole.

Although this occurs under certain specific conditions of system connection and system configuration, the main reason is the high levels of harmonic currents on the d.c. side produced due to extreme distortion in the a.c. supply voltage waveform. The results of this chapter provide a basis for analysing these fault conditions and others arising from various asymmetries in the system operation.

(b) Harmonic currents cause interference with the telecommunication, especially noise in the telephone lines. So, the levels of harmonic currents should be reliably predicted to provide sufficient filtering and shielding.

At high harmonic frequencies, the d.c. line is electrically long. A representation of the d.c. line as a lumped (π) section is accepted for first approximation. The (π) section parameters for different harmonic orders are shown in Appendix 3.(b).

The harmonic current corresponding to each harmonic voltage is computed and the principle of superposition is used to sum the different harmonics to a net resultant current in the filters and d.c. line.

Although the procedure adopted in calculating d.c. side harmonic currents are illustrated in different references 7,8, but the technique adopted here in regarding the problem in the steady state has never been used, to author's knowledge, to calculate filter currents and voltage across filters.

4.2 Basis for calculations

For each harmonic order, the harmonic voltage is acting as a voltage source, and the system impedance is calculated at the corresponding harmonic.

The following steps are used in the program to calculate harmonic currents through the filters and d.c. line, and the voltage drop across filtering branches:

Refer to fig. 4.1 for various impedances and admittances.

$$(1) \quad Y_{PI1}(K) = Y_{PI}(K) + 1.0/Z_{PI}(K) \quad (4.1)$$

$$(2) \quad Z_{PI1}(K) = 1.0/Y_{PI1}(K) \quad (4.2)$$

$$(3) \quad Z_{PIL}(K) = Z_{PI1}(K) + Z_L(K) \quad (4.3)$$

$$(4) \quad Y_{PIL}(K) = 1.0/Z_{PIL}(K) \quad (4.4)$$

$$(5) \quad Y_{PIL12}(K) = Y_{PIL}(K) + Y_{12}(K) \quad (4.5)$$

$$(6) \quad Y_{PILF}(K) = Y_{PIL12}(K) + Y_6(K) \quad (4.6)$$

$$(7) \quad Z_{PILF}(K) = 1.0/Y_{PILF}(K) \quad (4.7)$$

$$(8) \quad Y_F(K) = Y_6(K) + Y_{12}(K) \quad (4.8)$$

$$(9) \quad Z_{TOT}(K) = Z_{PILF}(K) + Z_L(K) \quad (4.9)$$

$$(10) \quad Y_{TOT}(K) = 1.0/Z_{TOT}(K) \quad (4.10)$$

$$(11) \quad I_{TOT}(K) = V(K) \cdot Y_{TOT}(K) \quad (4.11)$$

$$(12) \quad I_F(K) = I_{TOT}(K) \cdot Y_F(K)/Y_{PILF}(K) \quad (4.12)$$

$$(13) \quad I_6(K) = I_F(K) \cdot Y_6(K)/Y_F(K) \quad (4.13)$$

$$(14) \quad I_{12}(K) = I_F(K) \cdot Y_{12}(K)/Y_F(K) \quad (4.14)$$

$$(15) \quad I_{LINE}(K) = I_{TOT}(K) - I_F(K) \quad (4.15)$$

$$(16) \quad V_F(K) = I_F(K)/Y_F(K) \quad (4.16)$$

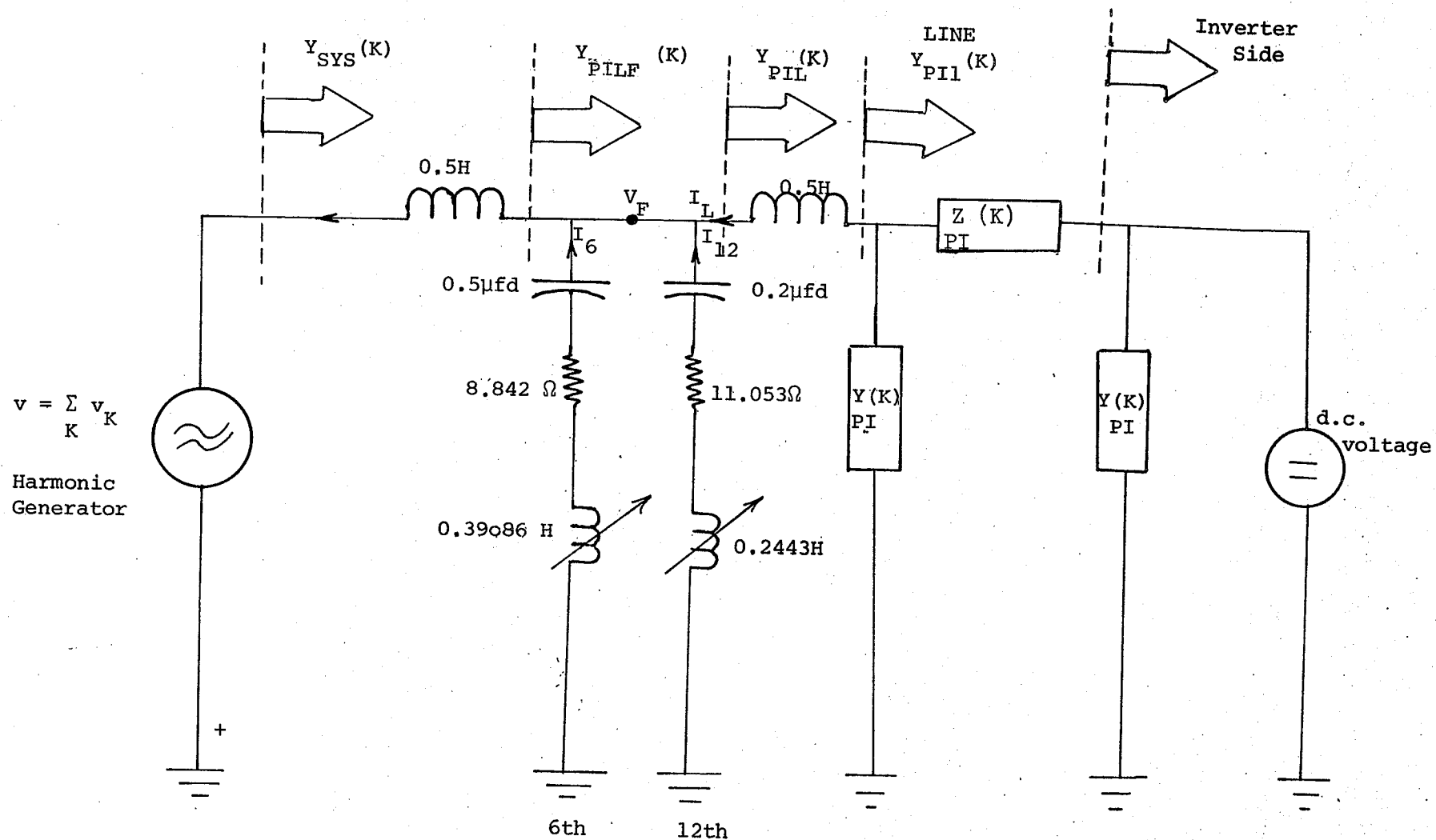


Fig. 4.1 Layout of d.c. side circuit

where

$$Z_L(K) = jK\omega L \quad (3.17)$$

$$Z_6(K) = R_6 + j \cdot K \cdot \left(\omega L_6 - \frac{1}{\omega C_6} \right) \quad (3.18)$$

$$Z_{12}(K) = R_{12} + j \cdot K \cdot \left(\omega L_{12} - \frac{1}{\omega C_{12}} \right) \quad (3.19)$$

and $V(K)$ is the Kth order harmonic voltage on the d.c. side.

4.3 Analysis of the results

On account of balanced and imbalanced harmonic contents in the a.c. supply, harmonics are generated in the d.c. side voltage. These harmonic voltages are calculated in the case of 6-pulse and 12-pulse operations (refer to table 3.5 in Chapter 3). By considering these harmonics as voltage sources, filter currents, voltage drop and line currents are calculated in case of 6-pulse and 12-pulse converter operations.

Table 4.1 illustrates the percentage harmonic content in d.c. side filters and line currents for 6-pulse operation

Table 4.1 Percentage harmonic content in d.c. side
filters and line currents for 6-pulse converter operation

$$\left(\frac{I}{I_{\text{Base}}}\right) = 1800 = 100\%$$

Harmonic order K	6th arm filter current (I_6)		12th arm filter current (I_{12})		Line Current (I_L)		Filters Current (I_F)	
	Balanced	Unbalanced	Balanced	Unbalanced	Balanced	Unbalanced	Balanced	Unbalanced
1	0.0/0°	0.105/43.4°	0.0/0°	0.04/43.4	0.0/0°	0.12/-42.2	0.0/0	0.145/43.4
2	0.0/0°	0.072/-63.1	0.0/0°	0.26/-62.1	0.0/0	0.44/138.7	0.0/0	0.332/62.1
3	1.338/-69.4	1.08/-69.2	0.428/20.7	0.34/-69.0	5.20/115.8	4.20/115.8	1.338/-69.4	1.419/-69.15
4	0.0/0	0.299/-9.8	0.0/0	0.074/-9.36	0.31/-178.2	0.31/-178.2	0.0/0	0.372/-9.712
5	0.0/0	0.567/0.16	0.0/0	0.083/1.42	0.11/-145.8	0.11/-145.8	0.0/0	0.649/0.32
6	0.955/-22.26	0.967/-18.2	0.005/-21.37	0.005/-71.37	0.008/-100.9	0.008/-96.6	0.95/-22.25	0.970/-18.43
7	0.0/0	0.028/97.8	0.0/0	0.006/134.6	0.0/0	0.005/34.4	0.0/0	0.033/103.958
8	0.0/0	0.0307/136.8	0.0/0	0.017/-5.78	0.0/0	0.008/139.12	0.0/0	0.020/105.80
9	0.193/50.27	0.162/84.02	0.22/-66.03	0.18/133.67	0.07/41.2	0.059/39.12	0.219/-13.88	0.310/110.239
10	0.0/0	0.069/154.9	0.0/0	0.16/-26.05	0.0/0	0.038/168.6	0.0/0	0.091/-26.77
11	0.0/0	0.0028/40.2	0.0/0	0.016/-143.7	0.0/0	0.0014/130.4	0.0/0	0.0132/-144.52
12	0.0022/-50.52	0.0022/50.01	0.26/38.74	0.269/39.67	0.001/-36	0.0014/-36.8	0.266/38.25	0.271/39.75

Figures 4.2.(a), 4.2.(b) illustrate the 6th arm filter current waveforms for balanced and unbalanced a.c. supply harmonics for 6-pulse operation.

The d.c. side harmonic currents had been determined using a point-by-point digital simulator by Dr. K.S. Rao, Dr. R.M. Mathur¹⁰. For illustration the 6th arm filter current waveform obtained by the simulator is shown in fig. 4.2.(c) for the same case of balanced a.c. supply harmonics.

Figures 4.3.(a), (b) represent the 6th arm filter current waveforms for balanced and unbalanced a.c. supply harmonics in case of 12-pulse operation.

Figures 4.4.(a), (b) illustrate the 12th arm filter current waveforms for 6-pulse and 12-pulse operations, on account of unbalanced a.c. supply harmonics.

In table T.4.2 the d.c. side currents are calculated for 12-pulse operation.

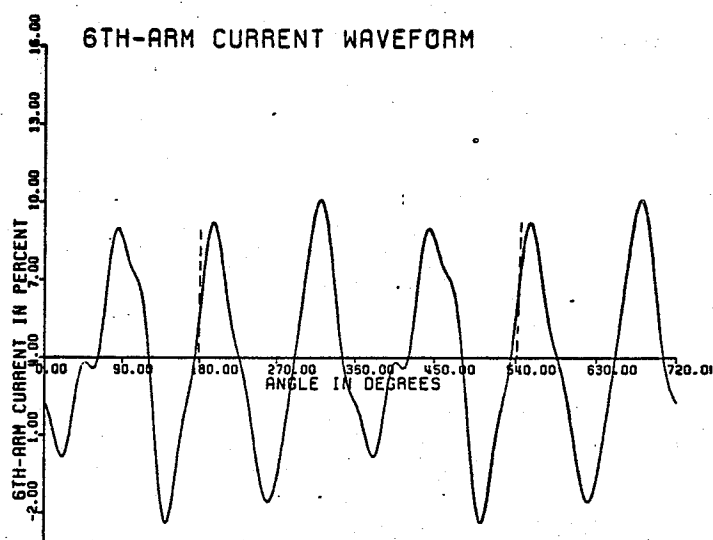


Fig. 4.2(a) 6th arm filter current for balanced a.c. harmonics (6-pulse)

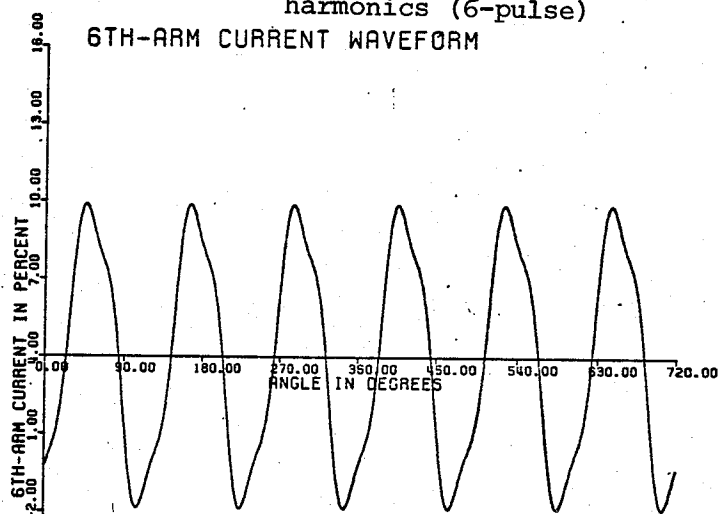


Fig. 4.2(b) 6th arm filter current for unbalanced a.c. harmonics (6-pulse)

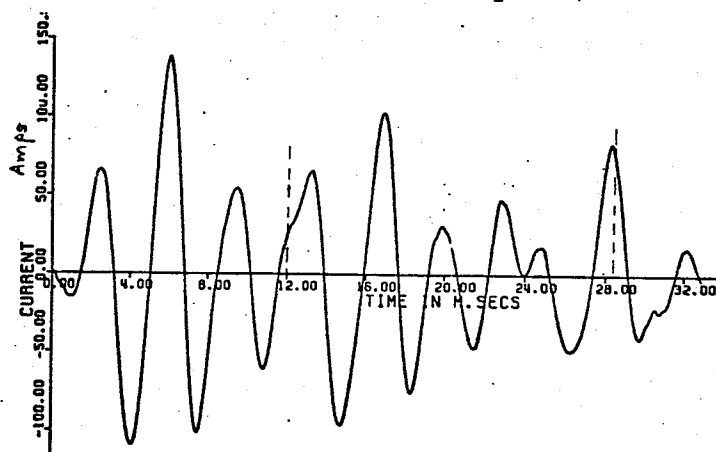


Fig. 4.2(c) 6th arm filter current waveform obtained using the digital simulator for balanced a.c. harmonics (6-pulse).

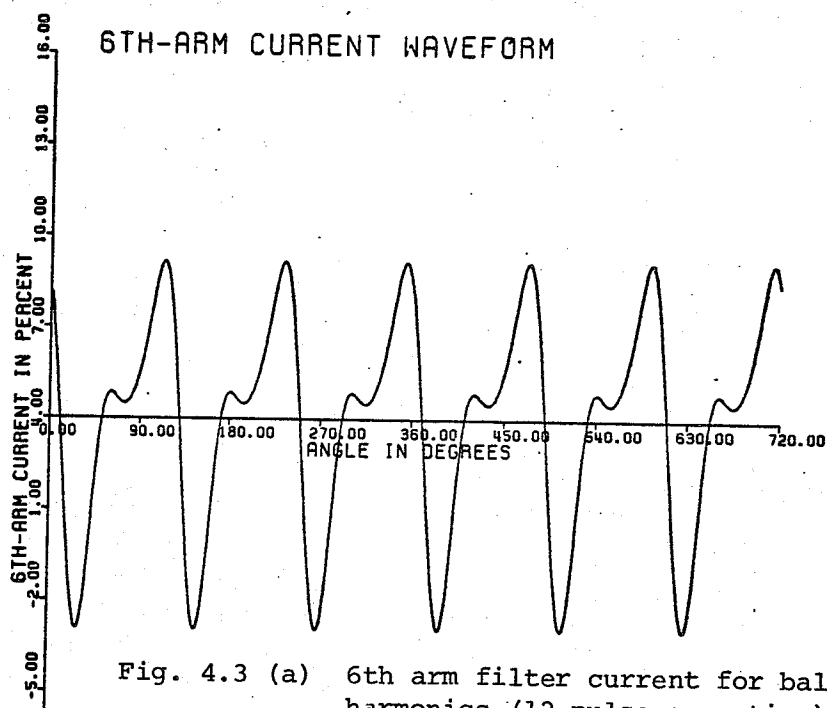


Fig. 4.3 (a) 6th arm filter current for balanced a.c. harmonics (12-pulse operation).

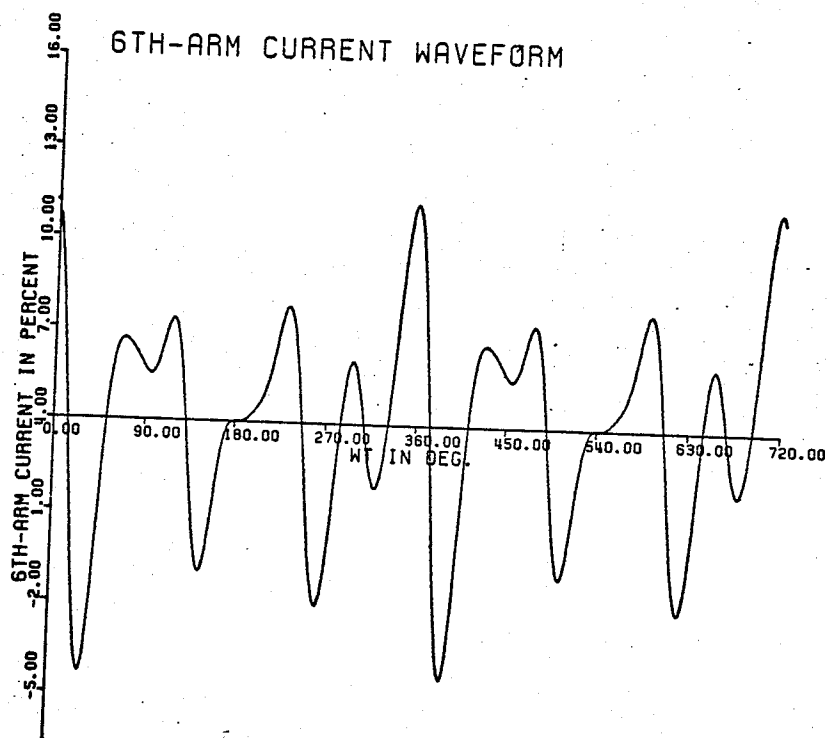


Fig. 4.3 (b) 6th arm filter current for unbalanced a.c. harmonics (12-pulse operation)

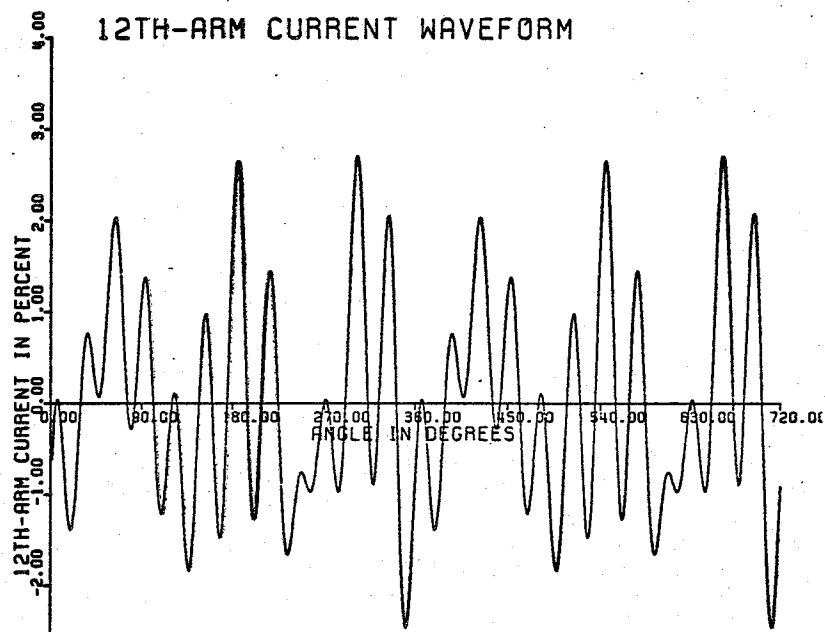


Fig. 4.4 (a) 12th arm filter current for balanced
a.c. harmonics
(6-pulse operation)

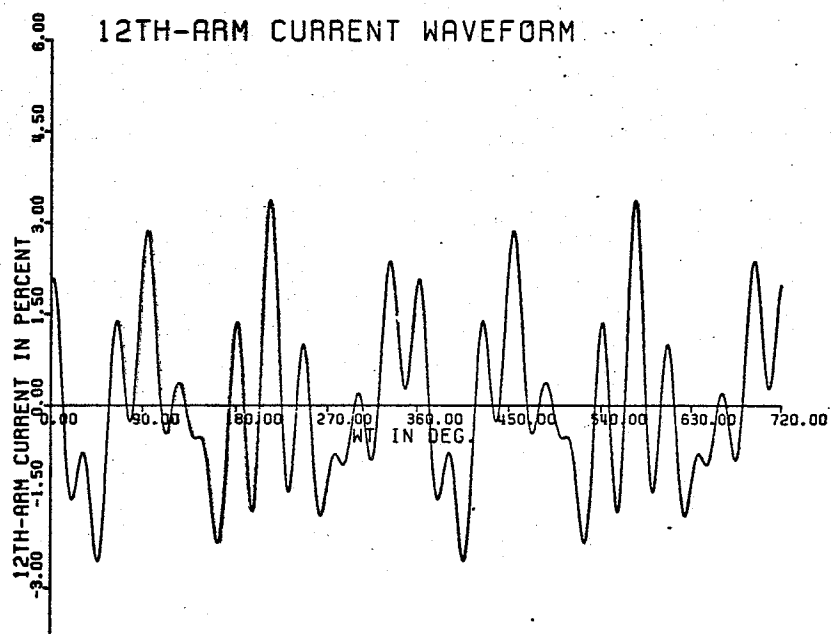


Fig. 4.4 (b) 12th arm filter current for unbalanced
a.c. harmonics (12-pulse operation)

Table 4.2 Percentage harmonic content in d.c. side
filters and line currents for 12-pulse operation

$(I_{BASE} = 1800 \text{ Amperes})$

Harmonic order	6th arm filter current (I_6)		12th arm filter current (I_{12})		Line Current (I_L)		Filters Current (I_F)	
	Balanced	Unbalanced	Balanced	Unbalanced	Balanced	Unbalanced	Balanced	Unbalanced
1	0.0/0°	0.17/40.5	0.0/0°	0.067/49.5	0.0/0	0.198/135°.16	0.0/0°	0.236/43.04
2	0.0/0	0.126/-92.27	0.0/0	0.046/177.7	0.0/0	0.772/-18.7	0.0/0	0.134/-112.7
3	1.893/-154.6	1.528/-114.18	0.604/-156.2	0.488/-156	7.34/18.8	5.94/19.12	2.496/154.98	1.919/-123.94
4	0.0/0	0.299/91.55	0.0/0	0.074/159.3	0.0/0	0.312/-31.8	0.0/0	0.334/103.37
5	0.0/0	0.293/164.8	0.0/0	0.042/170	0.0/0	0.058/-49.14	0.0/0	0.335/165.45
6	0.0/0	0.0/0.0	0.0/0	0.0/0	0.0/0	0.0/0.0	0.0/0	0.0/0
7	0.0/0	0.014/33.25	0.0/0	0.003/150.25	0.0/0	0.003/-19.65	0.0/0	0.0129/45.192
8	0.0/0	0.03/106.6	0.0/0	0.0168/74.8	0.0/0	0.008/-109.3	0.0/0	0.045/95.2
9	0.272/-5.13	0.228/-2.94	0.31/176.54	0.262/178.7	0.10/3.78	0.084/5.99	0.0389/171.7	0.0347/-170.4
10	0.0/0	0.118/-95.92	0.0/0	0.279/88.17	0.0/0	0.066/-108.6	0.0/0	0.1615/91.15
11	0.0/0	0.005/100.88	0.0/0	0.03/-74.64	0.0/0	0.0022/90.4	0.0/0	0.025/-73.7
12	0.0044/140.3	0.0044/140.5	0.532/50.26	0.528/50.41	0.0028/-36	0.0022/94.16	0.00379/140.4	0.528/50.88

Figures 4.5.(a), (b) show the voltage waveforms across the filtering branches for 6-pulse and 12-pulse operations on account of unbalanced a.c. supply harmonics.

A comparison is made between the effective R.M.S. values of filters and line currents during normal and abnormal operations. The effective R.M.S. value is calculated as

$$I_{\text{R.M.S.}} = \sqrt{\sum_K I_K^2}$$

Table T.4.3. shows the calculated values of 6th arm and 12th arm filters and line currents for both normal and abnormal 6-pulse and 12-pulse converter operations.

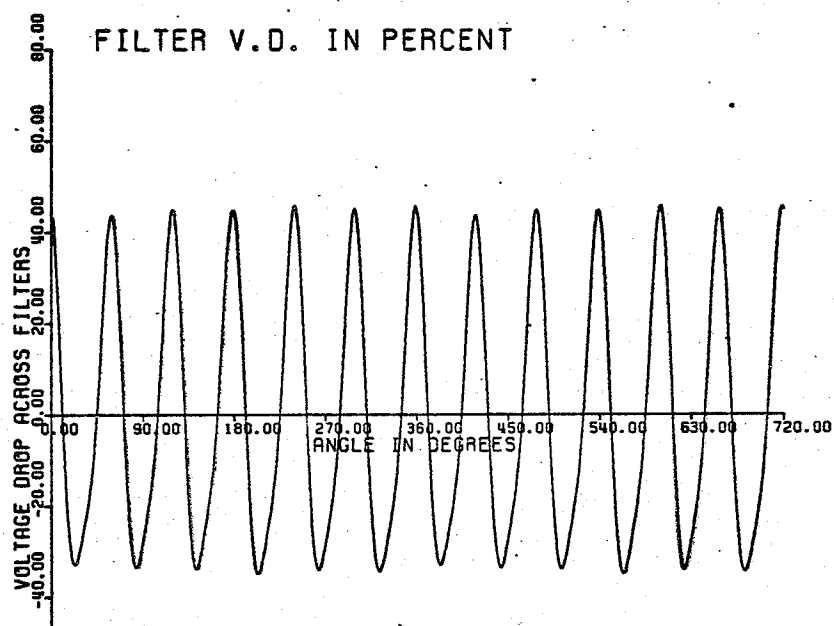


Fig. 4.5 (a) Voltage across filters on account of unbalanced a.c. harmonics (6-pulse operation)

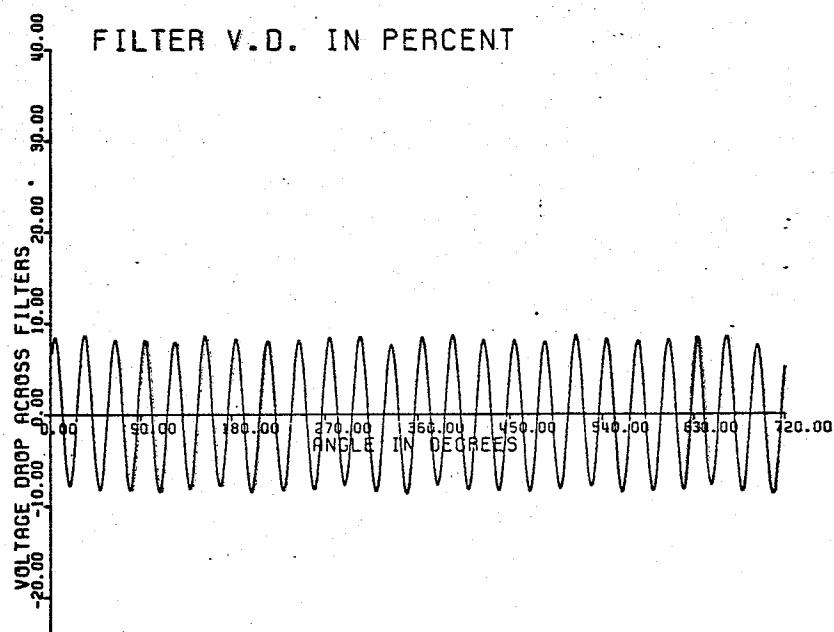


Fig. 4.5 (b) voltage across filters on account of unbalanced a.c. harmonics (12-pulse operation)

Table 4.3

Percentage effective R.M.S. value of d.c. side filters and line currents during normal and abnormal operations for 6-pulse and 12-pulse converters

($I_{\text{BASE}} = 1800 \text{ Amps}$)

Case	6th arm Current (I_6)		12th arm Current (I_{12})		Line Current (I_L)	
	6-pulse	12-pulse	6-pulse	12-pulse	6-pulse	12-pulse
Normal operation (only characteristic harmonics)	0.8125	0.0013	0.2652	0.1562	0.00733	0.00081
Abnormal operation (on account of unbalanced a.c. harmonics)	1.6004	1.619	0.5084	0.8236	4.238	6.002

Table T.4.4 shows the magnitudes of harmonics in the voltage across filtering branches for 6-pulse and 12-pulse operations in both balanced and unbalanced cases of harmonic content in the a.c. supply.

Table 4.4

Percentage harmonic content in voltage
across filtering branches in case of 6-pulse
and 12-pulse operations

$$(V_{\text{BASE}} = V_{\text{dn}} = 100\%)$$

$$(I_{\text{BASE}} = I_{\text{dn}} = 1800 \text{ Amperes})$$

Harmonic Order (K)	6-pulse (V_F)		12-pulse (V_F)	
	Balanced	Unbalanced	Balanced	Unbalanced
1	0.0	0.0068	0.0	0.0112
2	0.0	0.0099	0.0	0.0172
3	0.303	0.245	0.428	0.34
4	0.0	0.109	0.0	0.108
5	0.0	0.397	0.0	0.024
6	18.64	18.87	0.0	0.0
7	0.0	0.0108	0.0	0.0054
8	0.0	0.002	0.0	0.00196
9	0.221	0.0008	0.013	0.00114
10	0.0	0.022	0.0	0.0386
11	0.0	0.0102	0.0	0.0196
12	4.168	4.134	8.33	8.27

Figures 4.6.(a), (b) represent the d.c. line current waveforms in case of 6-pulse and 12-pulse operations on account of unbalanced harmonic content in the a.c. supply voltages.

Figures 4.7, 4.8 represent the amplitude spectra of 6th arm and 12th arm filter currents for 12-pulse operation on account of unbalanced harmonics in the a.c. supply voltages.

Figure 4.9 represents the amplitude spectra of the harmonic generator and voltage across filters in case of 12-pulse operation on account of unbalanced harmonics in the a.c. supply voltages.

A special case, when the 6th arm filter is out of service in a 12-pulse operation was studied. In table T.4.5 the harmonic currents and voltage across the 12th arm filter are calculated for 12-pulse operation.

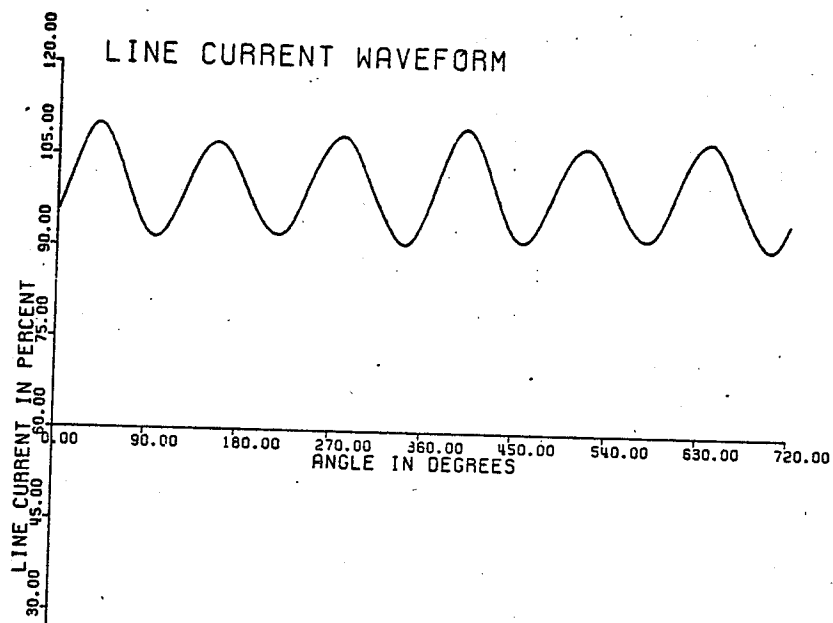


Fig. 4.6 (a) Line current waveform on account of balanced a.c. harmonics

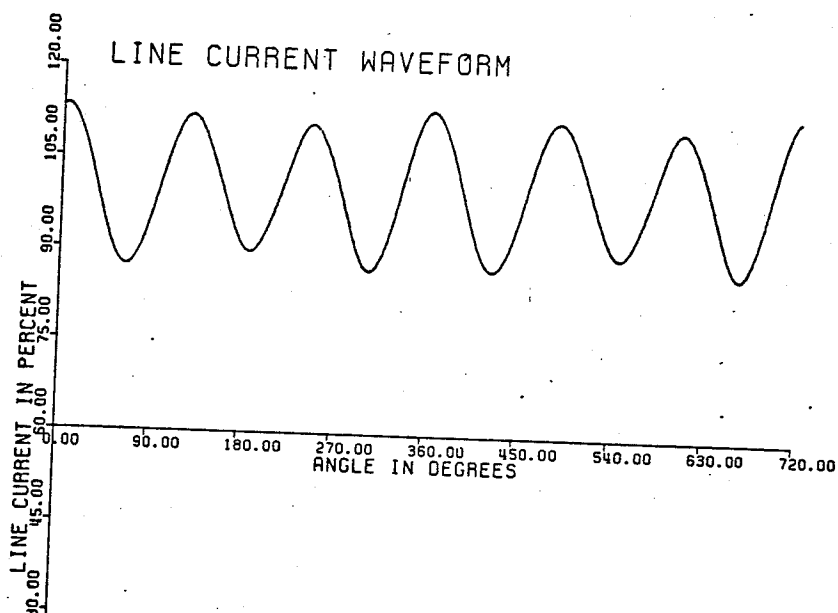


Fig 4.6 (b) Line current waveform on account of unbalanced a.c. harmonics (12-pulse operation)

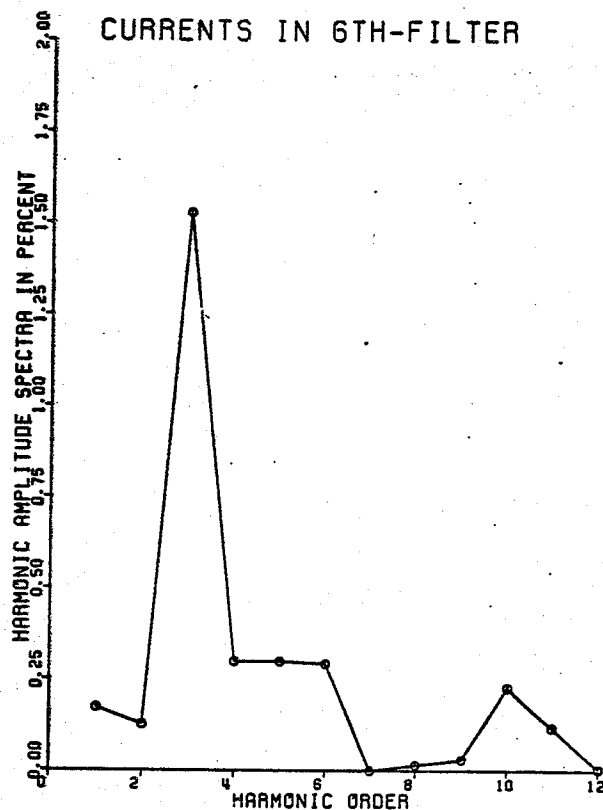


Fig. 4.7 Amplitude spectra for 6th arm filter currents
on account of unbalanced a.c. harmonics
(12-pulse operation)

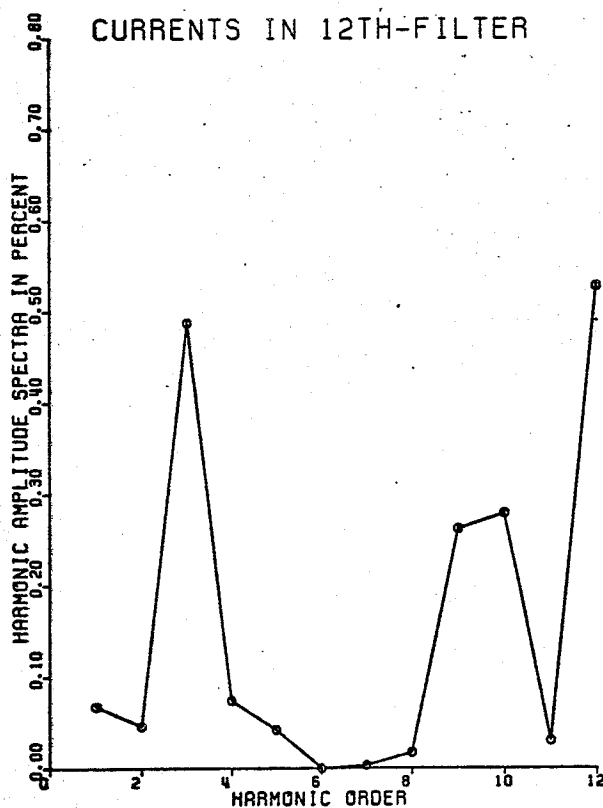


Fig. 4.8 Amplitude spectra for 12th arm filter
currents on account of unbalanced a.c.
supply harmonics (12-pulse operation)

Table 4.5

Percentage harmonic currents and
voltage across filters when 6th arm
filter is out of service, in 12-pulse
converter operation

$$\left\{ \begin{array}{l} V_{\text{BASE}} = V_{\text{dn}} = 100\% \\ I_{\text{BASE}} = I_{\text{dn}} = 100\% = 1800 \text{ A} \end{array} \right\}$$

Harmonic order	12th arm current (I_{12})		12th arm voltage (V.D.)	
	Balanced	Unbalanced	Balanced	Unbalanced
1	0.0	0.0326	0.0	0.0
2	0.0	0.0211	0.0	0.0
3	0.2517	0.203	0.02096	0.0169
4	0.0	0.0165	0.0	0.002
5	0.0	0.037	0.0	0.0058
6	0.0	0.0	0.0	0.0
7	0.0	0.0098	0.0	0.0052
8	0.0	0.1306	0.0	0.0026
9	0.2944	0.248	0.1575	0.0488
10	0.0	0.037	0.0	0.132
11	0.0	0.0126	0.0	0.0076
12	0.2667	0.26477	8.376	8.265

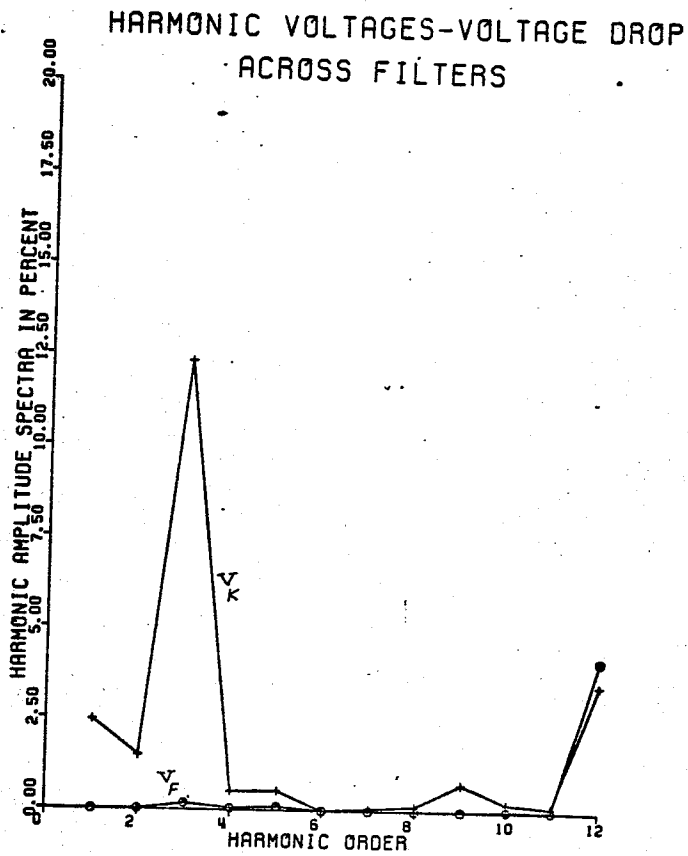


Fig. 4.9 Amplitude spectra of the harmonic generator and the voltage drop across filters (12-pulse operation)

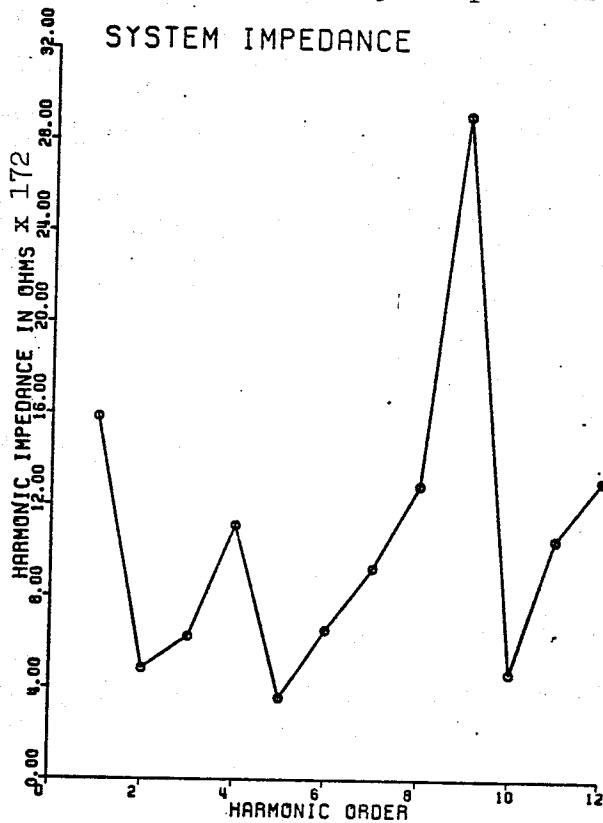


Fig. 4.10 Harmonic impedance spectra of the d.c. circuit

Figure 4.10 and table T.4.6 illustrate the d.c. circuit harmonic

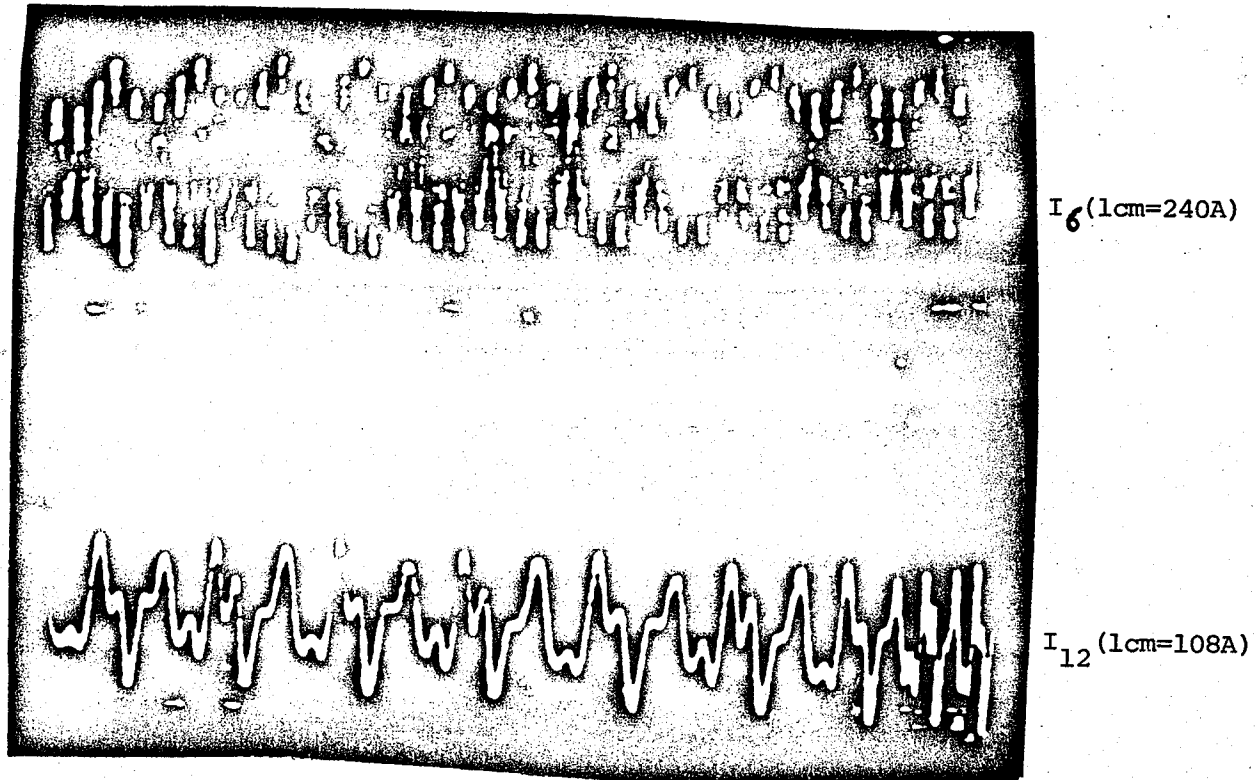
Table 4.6

D.C. circuit harmonic impedance

$$1 \text{ p.u.} = 172 \text{ ohms} = \left(\frac{V_{dn}}{I_{dn}} \right)$$

Harmonic order (K)	1	2	3	4	5	6	7	8	9	10	11	12
Z system (p.u.)	15.85	4.85	6.25	11.10	3.58	6.55	9.26	12.87	29.69	4.69	10.53	13.11
*Z loop (p.u.)	20.4	7.82	2.54	0.954	3.82	6.55	9.67	15.52	19.76	6.81	10.67	13.11

* Z_{Loop} represents the impedance of the loop formed by 6th arm, 12th arm filters plus the damping reactor (0.5H)



SCALE 2:1

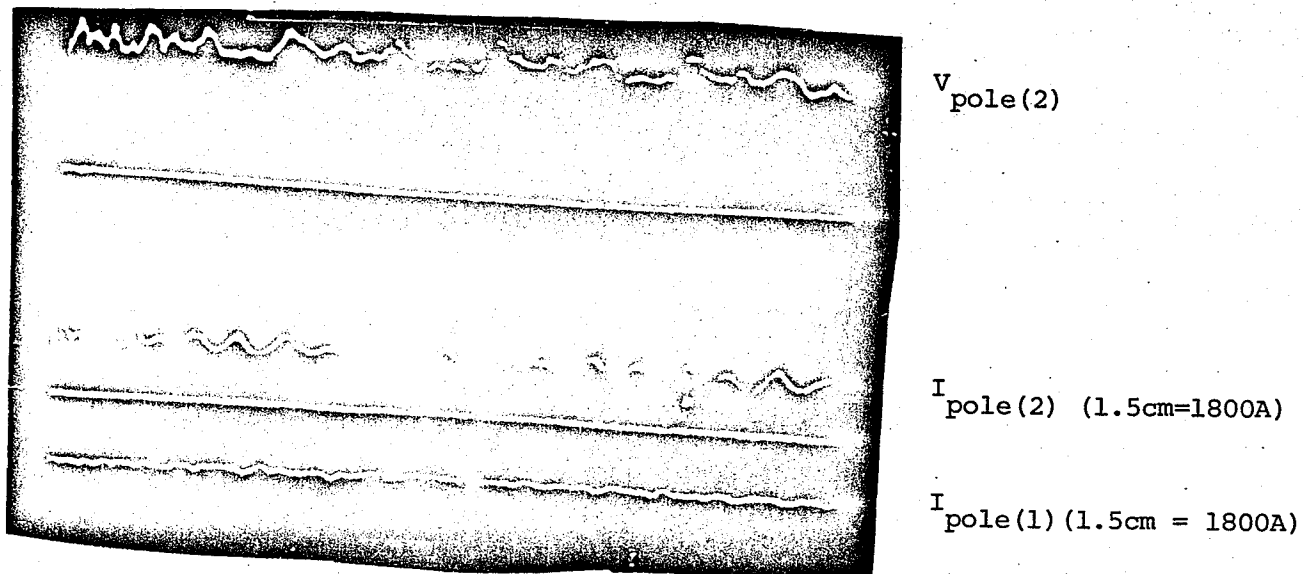


Fig. 4.11 Typical recorded waveforms of 6th arm, 12th arm, and d.c. pole voltage and current waveforms (Manitoba Hydro-Nelson River Scheme).

4.4 Conclusions

The distorted a.c. supply waveforms considered in Chapter 3, have dominant even harmonics which produce high levels of odd harmonics on the d.c. side voltage.

The d.c. circuit impedances have low values for some of these harmonic orders (2, 3, 5, 10), which cause high magnitudes of harmonic currents to flow through the 6th arm and 12th arm filters. In turn the voltage drop across filtering branches could exceed the threshold of protection circuits for filters, which causes the tripping of filters, hence blocking of the whole d.c. pole.

Fig. 4.11 illustrates typical recorded waveforms of 6th arm, 12th arm and line currents during overloading, for Manitoba Hydro Nelson River D.C. Scheme.

In this chapter it is shown that for a given a.c. supply waveform, harmonic currents on the d.c. side could be calculated.

CHAPTER V

EXPERIMENTAL INVESTIGATION OF THE HARMONIC PHENOMENA5.1 Introduction

In Chapter 3, 4 it has been shown clearly that a.c. supply voltage distortion is the major cause for the generation of harmonics on the d.c. side of HVDC converters.

Imbalance and distortion in the a.c. supply voltages occur mainly during transients and fault conditions which usually last for many cycles.

It was experienced that under certain configurations of the interconnected a.c. system, cases of highly distorted a.c. voltages take place subsequent to the energization of power transformers due to their inrush currents.

The voltage distortion is accelerated if the transformers to be energized are located at the far end of a transmission line as in Kettle Rapids of Nelson River Scheme. The distortion depends on the instants when the transformers are energized and re-energized, since the magnitudes of the inrush currents are dependent on the magnetic state of the transformer magnetic core and instant of energization, the inrush current effects are, therefore, not repeatable but we must concern ourselves with the worst situation.

In connection with transformer energization it was anticipated that simultaneous energization of two parallel connected transformer banks present an added complexity in that if the magnetic states of two banks are different, an oscillatory interchange of inrush currents takes place which tends to sustain the a.c. voltage waveform distortion for very

much longer time and that the total current in the collector line is not the simple phasor addition of the currents in the banks.

The investigation taken up in this chapter is to verify the above by conducting simple tests in the laboratory to simulate the field conditions as best as possible.

5.2 Experimental set-up

Fig. 5.1 illustrates the circuit diagram, where the a.c. supply is replaced by a synchronous generator driven by a d.c. motor. A synchronous generator was chosen to simulate the limited power source behind the a.c. bus. Use of normal a.c. 3- ϕ supply generates an infinite bus condition.

The generator is fed through a set of inductors. A 3- ϕ variac was employed for adjustable values of inductors.

The experiment is performed in two cases, first: transformer banks are connected in Δ/Δ , second: they are connected in Δ/Y . The transformers secondaries are open circuited.

The neutrals of the banks are connected through a variable resistance to the neutral of the supply to simulate earth resistance.

The inrush current waveform was displayed using the first channel of a 2-channel storage oscilloscope and a resistive shunt of 4 ohms.

The phase voltage waveform is displayed using the other channel of the storage oscilloscope with 1:10 resistive voltage divider.

As shown in fig. 5.1 3-pole switch (S_1) is provided to allow isolation between the two transformer banks, another single pole switch (S_2) is provided to disconnect the neutral wire.

The ratings of the circuit elements are shown in fig. 5.1.

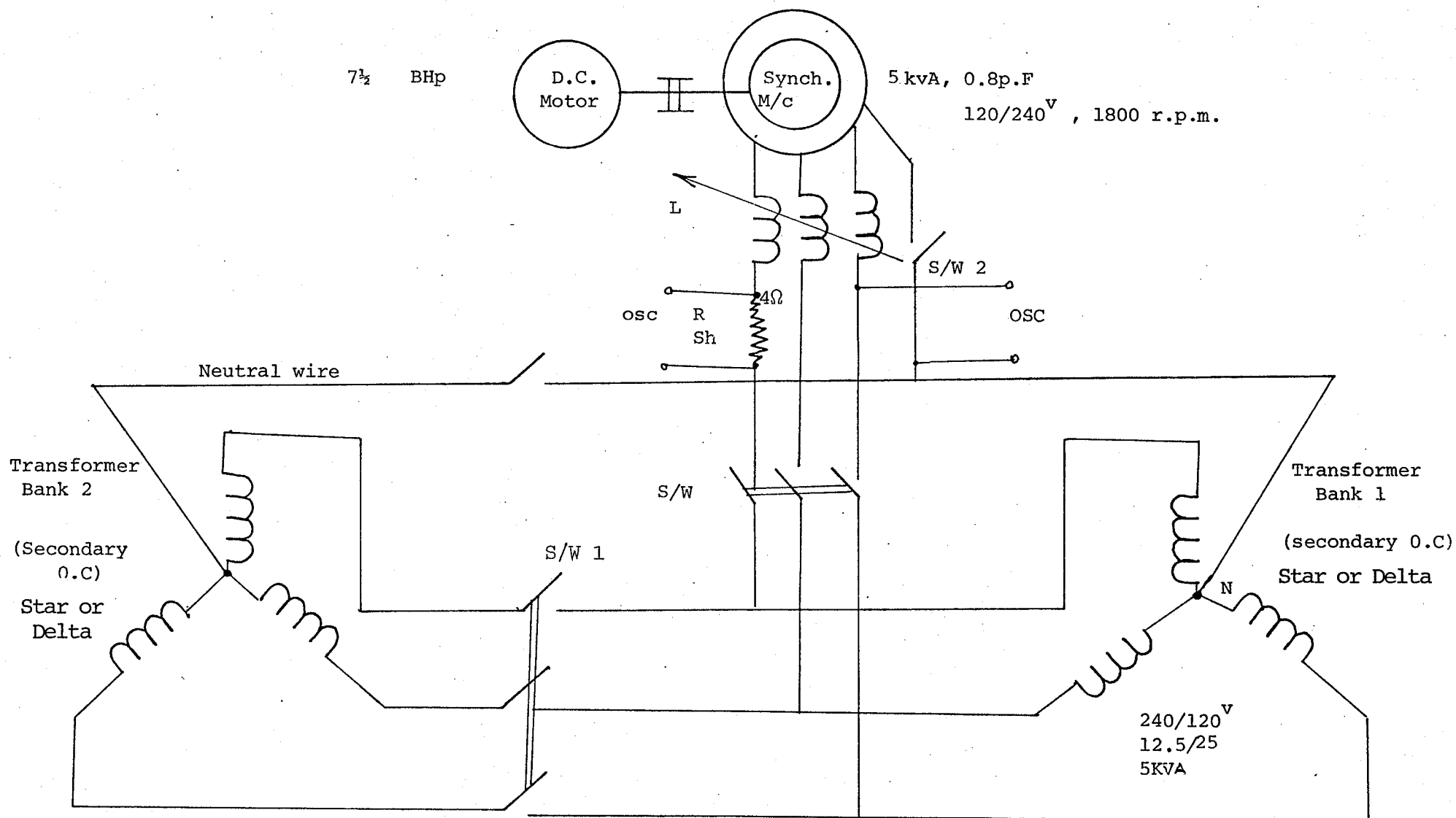


Fig. 5 1 Circuit diagram of the experimental set-up

5.3 Analysis of the results

A number of tests were performed using the set-up of fig. 5.1. In the following paragraphs some of the results are presented and discussed which lead to interesting conclusions.

a) The inrush current waveforms last for a comparatively much longer time in case of parallel connection of transformers, in our experiment for more than 9 times as compared to energization of a single bank.

Figures 5.2, 5.3(a) show the currents in case of one bank and two banks of transformers during energization (transformer banks are connected in Δ/Δ).

Fig. 5.3(b) shows the current in case of 2-bank energization (transformer banks are connected in Δ/Δ).

Figures 5.4, 5.5 show the details of inrush current in case of energization of one bank and 2 banks (transformer are connected in Δ/Δ).

Figures 5.6, 5.7 show the details of inrush current in case of energization of one bank and 2 banks (banks are connected in Δ/Δ).

b) A high distortion in the a.c. voltages was found especially in case of the neutral connection of the two banks while the generator neutral is isolated.

The voltage distortion in case of 2-parallel banks was found to be higher than in case of one bank alone, figs. 5.9, 5.10.

Figure 5.8 shows the phase voltage waveform without distortion.

Figures 5.9(a), 5.9(b) show the distorted phase voltage in case of one bank and two banks (banks are connected in Δ/Δ).

Figures 5.10(a), 5.10(b) show the distorted phase voltage waveforms in case of one bank and two banks (banks are connected in Δ/Δ).

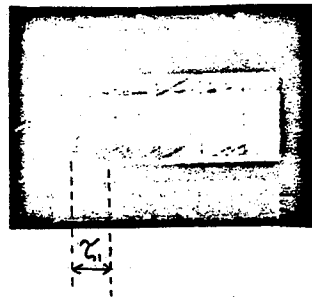


Fig. 5.2 Inrush current waveform
(one-bank Δ/Δ)

$2^V/\text{Div}$

$0.5 \text{ Sec}/\text{Div}$ (one division = 7.5 mm)

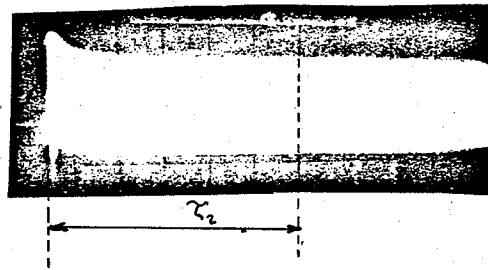
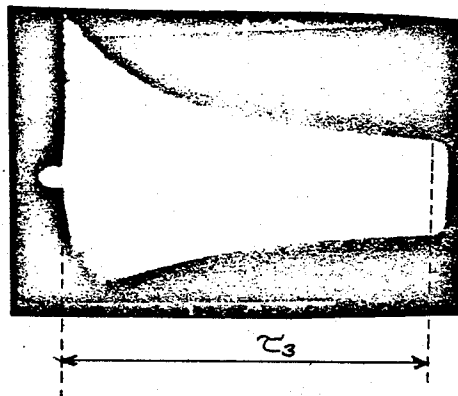


Fig. 5.3(a) Inrush current waveform
(2-banks Δ/Δ)

$5^V/\text{Div}$

$0.5 \text{ Sec}/\text{Div}$



$$\tau_3 = 9\tau_1$$

Fig. 5.3(b) Inrush current waveform
(2-banks Δ/Δ)

$5^V/\text{Div}$

$0.5 \text{ Sec}/\text{Div}$

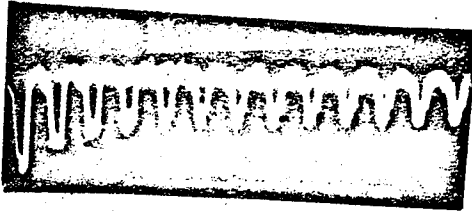


Fig. 5.4 Details of inrush current
(one-bank Δ/Δ)

5^V/Div
20 mS/Div

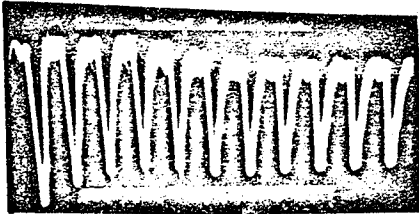


Fig. 5.5 Details of inrush current
(2-banks Δ/Δ)

5^V/Div
20 mS/Div

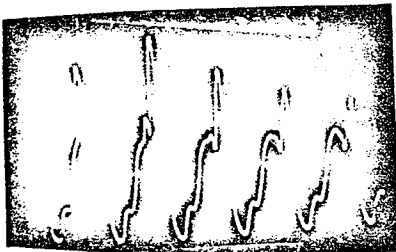


Fig. 5.6 Details of inrush current
(one-bank Δ/Δ)

10^V/Div
10 mS/Div

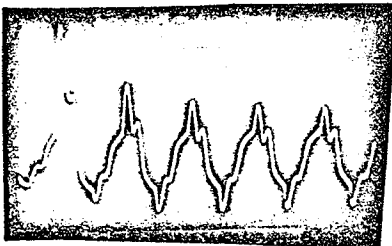


Fig. 5.7 Details of inrush current
(2-banks Δ/Δ)

10^V/Div
10 mS/Div

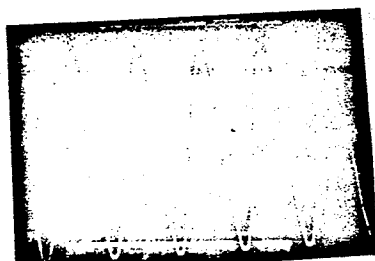


Fig. 5.8 Phase voltage waveform
(no distortion)

5^V/Div
20 mS/Div

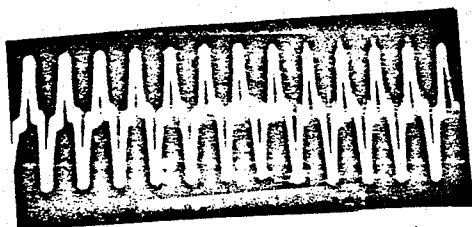


Fig. 5.9(a) Distorted phase voltage
(one-bank π/Δ)

10^V/Div
20 mS/Div

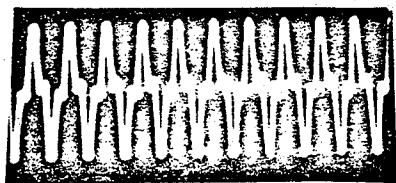


Fig. 5.9(b) Distorted phase voltage
(2-banks π/Δ)

10^V/Div
20 mS/Div

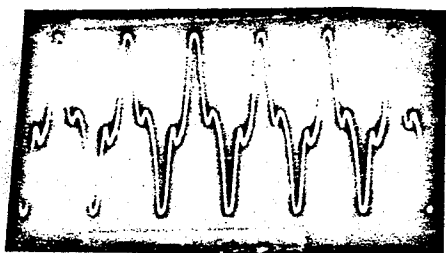


Fig. 5.10(a) Distorted phase voltage
(one-bank λ/λ)

$10^V/\text{Div}$
 $10 \text{ mS}/\text{Div}$

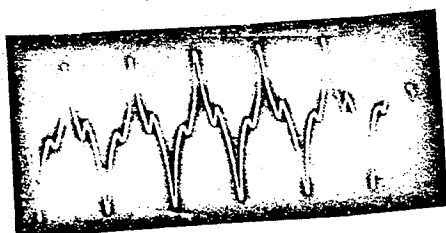


Fig. 5.10(b) Distorted phase voltage
(2-banks λ/λ)

$10^V/\text{Div}$
 $10 \text{ mS}/\text{Div}$

- c) From figures 5.6 - 5.7 it appears that the harmonic content in the inrush current waveforms are mainly triplen harmonics.
- d) If the neutral wire is connected to the generator neutral through a resistance, a.c. supply voltages are also distorted.
- e) The inductance, in the a.c. circuit plays a major role on the level of distortions on the a.c. supply, and hence a higher distortion of the transformers are located at a distance from the a.c. bus.
- f) In case of absence of a neutral wire between the transformer banks and generator neutral, highly distorted voltage waveforms are obtained.

5.4 Conclusions

Although the experiment was limited and in the absence of a point on wave switch, all results corresponding to a known instant of switching could not be obtained, it is nevertheless shown clearly that the inrush current during energization of interconnected a.c. side transformers can cause a severe distortion in the a.c. supply waveforms, which in turn produce high magnitudes of harmonics on the d.c. side of a converter station.

The results obtained from the experimental investigation highly recommend that the generators and the neutrals of transformer banks be solidly grounded to minimize the distortion in the supply voltages due to inrush currents.

It is noteworthy to mention that the distorted a.c. supply waveforms which had been analyzed in Chapter 3 look to some extent similar to the voltage waveforms obtained from experimental analysis.

CHAPTER VI

SUMMARY AND CONCLUSIONS

6.1 General

The main objective of an assessment of the level of d.c. side voltage and current harmonics under any combinations of imbalance parameters has been successfully achieved.

Normal imbalance of converter is a steady-state problem and as such the threatment of this thesis is fully justified. The imbalance and distortions of the a.c. bus voltages which arise on account of a.c. system disturbances, such as three - phase faults and inrush current caused effects due to the energization of generator transformers, are found from field records and experimentally on a reduced scale model in the laboratory, to last for a significant duration of time. The steady-state approach is considered quite satisfactory for all these cases.

The results of this thesis are computed very economically as compared to the investigation of the same problem on an analog or digital d.c. simulator and yet the reliability of the results is not significantly influenced.

For the analysis of this thesis the converter valves were represented as ideal switches and the a.c. supply waveform was analyzed to obtain the harmonics using a complex Fourier analysis in the frequency domain.

The analysis covers both the 6 and 12 pulse operation of converters,

6.2 D.C. Side Harmonics

It was found that different unbalance parameters give rise to different harmonic spectra on the d.c. side

The following cases were studied;

a) Unbalance in ignition angle (α)

Unbalance in ignition angle separately or in conjunction with other disturbances, produce a complete spectrum of d.c. side harmonics.

b) Unbalance in commutation angle (u)

This unbalance arises due to unbalance in the leakage reactance of transformers. This type of unbalance results in a spectrum of all harmonics on the d.c. side.

c) Unbalance in the a.c. supply

(i) Voltage imbalance in any one phase of the a.c. supply result- in a spectrum of all even harmonics.

(ii) Phase angle imbalance in a.c. supply produces a spectrum of even harmonics on the d.c. side.

(iii) Even harmonics in a.c. supply produce only odd harmonics on the d.c. side, and if the even a.c. supply harmonics are balanced in the three phases they result in triplen harmonics on the d.c. side.

(iv) Balanced odd a.c. supply harmonics do not contribute to any uncharacteristic d.c. side harmonics.

d) Modification in characteristic harmonics

Most unbalance parameters practically do not modify the magnitudes of the characteristic harmonics.

6.3 General Conclusions

It is found that the non-characteristic harmonics are generally small in relation to the lower orders of characteristic harmonics, but they cannot be ignored,

Upon calculation of the d.c. side harmonic currents, it was found that the aggregate effect of the whole spectrum of non-characteristic harmonics is most pronounced, due a low impedance of the d.c. circuit at certain frequencies,

These non-characteristic harmonics exceed the normal tolerance in the ratings of the filters and also the noise and interference levels for communication lines.

The cases studied for a.c. voltage distortions showed worst overloadings of 10,000 % for 6th arm filter and 500% for 12th arm filter.

Such studies of problems involving computation of the levels of d.c. side harmonic voltages and currents are regarded extremely useful as a starting point in the specification and design of adequate filtering and shielding on the d.c. side of converter stations.

The d.c. side harmonic currents into any d.c. filter or the d.c. line will depend on the impedance of the d.c. side seen from the converter station d.c. terminals.

The representation of the d.c. line for different harmonic orders is difficult, and only lumped parameters could be specified to transmission line impedance and admittance, usually these parameters are obtained from experimental analysis.

The assumption of an open loop analysis as used in this thesis may need modification to include the secondary feedback and control circuit

effects,

This work could be considered as a first approximation of the problem of computing the harmonics on the d.c. side of converter station, also in explaining the theoretical aspects about generation of non-characteristic d.c. side harmonics.

REFERENCES

1. J. Reeve and P.C.S. Krishnayya, "Unusual current harmonics arising from HVDC transmission", I.E.E.E. Trans. Power Apparatus and Systems, Vol. PAS-87, pp. 883-893, March, 1968.
2. A.G. Phadke and J.H. Harlow, "Generation of abnormal harmonics in high voltage ac/dc power systems", I.E.E.E. Trans. Power Apparatus and Systems, Vol. PAS-87, pp. 873-883, March, 1968.
3. J. Reeve, J.A. Baron, and P.C.S. Krishnayya, "A general approach to harmonic current generation by HVDC converters", I.E.E.E. Trans. Power Apparatus and Systems, Vol. PAS-88, pp. 989-995, July, 1969.
4. J. Reeve and J.A. Baron, "Harmonic D.C. line voltages arising from HVDC power conversion", I.E.E.E. Trans. Power Apparatus and Systems, Vol. PAS-89, pp. 1619-1623, Sept./Oct., 1970.
5. J. Reeve and S.C. Kapoor, "Analysis of transient short circuit currents in HVDC power systems", I.E.E.E. Trans. Power Apparatus and Systems, Vol. PAS-89, pp. 1174-1181, April, 1970.
6. N.G. Hingorani, R.H. Kitchen, and J.L. Hay, "Dynamic simulation of HVDC power transmission systems on digital computers - generalized mesh analysis approach", I.E.E.E. Trans. Power Apparatus and Systems, Vol. 87, No. 4, pp. 989-996, April, 1968.
7. High Voltage Direct Current Converters and Systems, Book, by B.J. Cory, MacDonald, London, 1965.
8. High Voltage Direct Current Power Transmission, Book, by C. Adamson, and N.G. Hingorani
9. Direct Current Transmission, Book
Volume I

By Edward W. Kimbark, Wiley-Interscience.

10. K.S. Rao et. al., "An Improved Digital Transient Simulator for Systems Including Controlled Switches", International Symposium on Large Engineering Systems, Winnipeg, Manitoba 1976.
11. U.S.S.R., Direct Current Research, book, Pergamon Press, London, 1964, "Calculation of the Harmonics of Audio Frequency Currents in D.C. Power Lines", A.M. Pintsov, pp. 221-235.

APPENDIX I

Flowchart and computational programs for d.c. side voltage harmonics

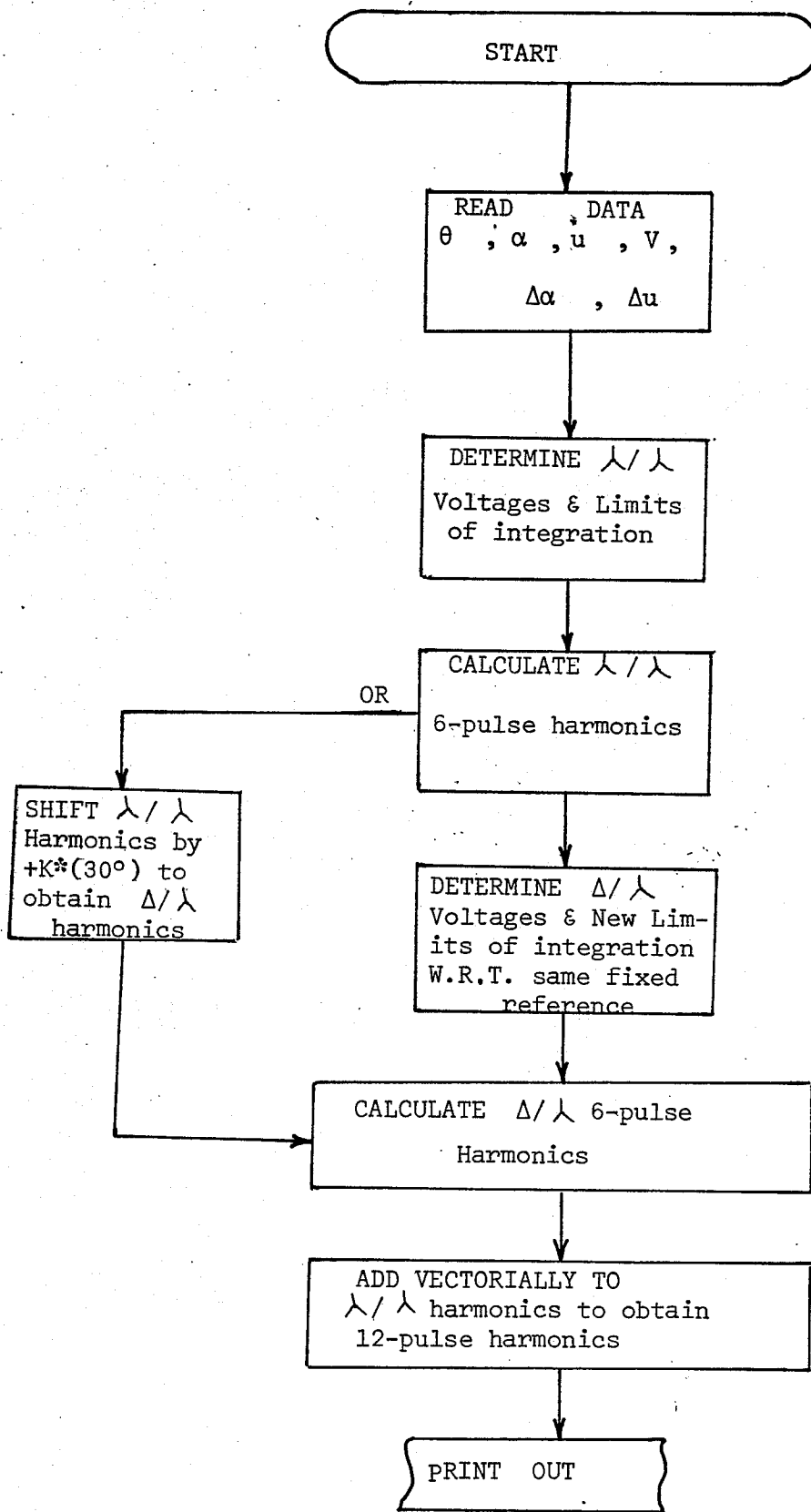
The calculation of the converter d.c. voltage harmonics is done using the complex Fourier coefficients approach. There are two reasons for working the problem in the frequency domain instead of the time domain:

- (1) The magnitudes of Fourier complex coefficients represent directly the amplitudes of the harmonic voltages.
- (2) The simplicity of transferring integrals in a closed form to a repetitive procedure of summations.

The program is checked for the balanced operation of the converter bridge where only characteristic harmonics are produced. A special program is written to calculate the mean d.c. voltage and the fundamental harmonic component which was found to be practically negligible.

To include harmonic content in the a.c. supply waveform, another program is written to accomodate the extra a.c. supply harmonics besides the fundamentals. This program is also checked for the balanced operation when only the characteristic harmonics are produced.

In the following, a simplified flowchart is shown. Later copies of the three programs used for calculating the d.c. side voltage harmonics are appended.



FLOWCHART OF D.C. SIDE VOLTAGE HARMONICS

```

1  *ATTN V SHARAF
2  COMPLEX CEXP
3  COMPLEX V(50)
4  COMPLEX CC(50),DCC(50)
5  REAL W
6  COMPLEX Z
7  COMPLEX F11(15,50),F12(15,50)
8  COMPLEX I1(50),I2(50),I3(50)
9  COMPLEX CVPLX,Z1,Z2,Z3,Z4,Z5,Z6,Z7
10 COMPLEX C12(50)
11 COMPLEX Z75,Z76,Z77
12 REAL Y(50),DY(50),Y12(50)
13 REAL N(50),N(50),DM(50),DN(50),M12(50),N12(50)
14 REAL X(10),U(10),BR(10),L(15)
15 REAL V1M,V2M,V3M
16 REAL W1,W2,W3,W4,W5,W6,W7,W8
17 REAL XX,UU,LL
18 XIS ALPHA,U IS GAMMA,BR IS THETA
19 LIS LIMIT OF INTEGRATION
20 CC,DCC,C12 ARE COMPLEX FOURIER COEFFICIENTS
21 COMM. AND COND. OF EACH VALVE IS CALCULATED.
22 FOR STAR,DELTA,12-PULSE OPERATION
23 DELTA/STAR HARMONICS ARE CAL. USING REFERRED VOLTAGES
24 OF A.C. SUPPLY W.R.T. FIXED REFERENCE
25 DELTA/STAR...AND 12-PULSE...HARMONICS ARE REFERRED TO DATA
26 READ,(BR(I)),I=1,6)
27 READ,(X(I)),I=1,6)
28 READ,(U(I)),I=1,6)
29 READ,V1M,V2M,V3M
30 READ,XX,UU
31 PI=4.0*ATAN(1.0)
32 H=2.0*PI/360.0
33 WC=377.0
34 W=1.0
35 Z=CMPLX(0.0,W)
36 W5=PI/3.0
37 Z5=CMPLX(0.0,W5)
38 Z75=-75
39 W6=PI
40 Z6=CMPLX(0.0,W6)
41 Z76=-76
42 W7=-PI/3.0
43 Z7=CMPLX(0.0,W7)
44 Z77=-77
45 L(1)=H*(BR(1)+X(1))
46 L(2)=H*(BR(1)+X(1)+U(1))
47 L(3)=H*(BR(2)+X(2))
48 L(4)=H*(BR(2)+X(2)+U(2))
49 L(5)=H*(BR(3)+X(3))
50 L(6)=H*(BR(3)+X(3)+U(3))
51 L(7)=H*(BR(4)+X(4))
52 L(8)=H*(BR(4)+X(4)+U(4))
53 L(9)=H*(BR(5)+X(5))
54 L(10)=H*(BR(5)+X(5)+U(5))
55 L(11)=H*(BR(6)+X(6))
56 L(12)=H*(BR(6)+X(6)+U(6))
57 L(13)=H*X(1)+2.0*PI
DO 1 K=2,48
DO 2 I=1,12
W1=-(K-1)*L(I+1)
Z1=CMPLX(0.0,W1)
W2=-(K-1)*L(I)
Z2=CMPLX(0.0,W2)
W3=-(K+1)*L(I+1)
Z3=CMPLX(0.0,W3)
W4=-(K+1)*L(I)

```

Program (1)

Calculation of d.c. side voltage harmonics
(only a.c. supply fundamentals considered)

```

58      Z4=CMPLX(0.0,W4)
59      F11(I,K)=(Z/(K-1))*(CEXP(Z1)-CEXP(Z2))
60      F12(I,K)=(Z/(K+1))*(CEXP(Z3)-CEXP(Z4))
61      I1(I)=0.5*V1M*(CEXP(Z25)*F11(I,K)+CEXP(Z5)*F12(I,K))
62      I2(I)=0.5*V2M*(CEXP(Z26)*F11(I,K)+CEXP(Z6)*F12(I,K))
63      I3(I)=0.5*V3M*(CEXP(Z27)*F11(I,K)+CEXP(Z7)*F12(I,K))
64      CONTINUE
65      C
        STAR/STAR DATA
        CC(K)=(1.0/(2.0*PI))*((I1(1)+I3(1))*0.5-I2(1)+I1(2)-I2(2)+
X11(3)-(I2(3)+I3(3))*0.5+I1(4)-I3(4)+(I1(5)+I2(5))*0.5-I3(5)+
X12(6)-I3(6)+I2(7)-(I1(7)+I3(7))*0.5+I2(8)-I1(8)+(I2(9)+I3(9))*
X0.5-I1(9)+I3(10)-I1(10)+I3(11)-(I1(11)+I2(11))*0.5+I3(12)-I2(1
66      Y(K)=CABS(CC(K))
67      M(K)=AIMAG(CC(K))
68      N(K)=REAL(CC(K))
69      C
        1
        DELTA /STAR DATA
70      DO 9 I=1,6
71      LL=30.0
72      RE(I)=RR(I)-LL
73      X(I)=X(I)-XX
74      U(I)=U(I)-UU
75      9
        CONTINUE
76      DO 8 K=2,48
77      DO 3 I=1,12
78      L(1)=H*(RR(1)+X(1))
79      L(2)=H*(RR(1)+X(1)+U(1))
80      L(3)=H*(RR(2)+X(2))
81      L(4)=H*(RR(2)+X(2)+U(2))
82      L(5)=H*(RR(3)+X(3))
83      L(6)=H*(RR(3)+X(3)+U(3))
84      L(7)=H*(RR(4)+X(4))
85      L(8)=H*(RR(4)+X(4)+U(4))
86      L(9)=H*(RR(5)+X(5))
87      L(10)=H*(RR(5)+X(5)+U(5))
88      L(11)=H*(RR(6)+X(6))
89      L(12)=H*(RR(6)+X(6)+U(6))
90      L(13)=H*X(1)+11.0*PI/6.0
91      W5=PI/6.0
92      Z5=CMPLX(0.0,W5)
93      Z25=-Z5
94      W6=5.0*PI/6.0
95      Z6=CMPLX(0.0,W6)
96      Z26=-Z6
97      W7=-PI/2.0
98      Z7=CMPLX(0.0,W7)
99      Z27=-Z7
100     W1=-(K-1)*L(I+1)
101     Z1=CMPLX(0.0,W1)
102     W2=-(K-1)*L(I)
103     Z2=CMPLX(0.0,W2)
104     W3=-(K+1)*L(I+1)
105     Z3=CMPLX(0.0,W3)
106     W4=-(K+1)*L(I)
107     Z4=CMPLX(0.0,W4)
108     F11(I,K)=(Z/(K-1))*(CEXP(Z1)-CEXP(Z2))
109     F12(I,K)=(Z/(K+1))*(CEXP(Z3)-CEXP(Z4))
110     I1(I)=0.5*V1M*(CEXP(Z25)*F11(I,K)+CEXP(Z5)*F12(I,K))
111     I2(I)=0.5*V2M*(CEXP(Z26)*F11(I,K)+CEXP(Z6)*F12(I,K))
112     I3(I)=0.5*V3M*(CEXP(Z27)*F11(I,K)+CEXP(Z7)*F12(I,K))
113     CONTINUE
114     3
        V(K)=(1.0/(2.0*PI))*((I1(1)+I3(1))*0.5-I2(1)+I1(2)-I2(2)+
X11(3)-(I2(3)+I3(3))*0.5+I1(4)-I3(4)+(I1(5)+I2(5))*0.5-I3(5)+
X12(6)-I3(6)+I2(7)-(I1(7)+I3(7))*0.5+I2(8)-I1(8)+(I2(9)+I3(9))*
X0.5-I1(9)+I3(10)-I1(10)+I3(11)-(I1(11)+I2(11))*0.5+I3(12)-I2(1
115     DCC(K)=V(K)

```

```

116      DY(K)=CABS(DCC(K))
117      DV(K)=AIMAG(DCC(K))
118      DN(K)=REAL(DCC(K))
119      C      CONTINUE
120      C      12 PULSE OPERATION
121      DO 11 K=2,48
122      C12(K)=CC(K)+DCC(K)
123      Y12(K)=CABS(C12(K))
124      M12(K)=AIMAG(C12(K))
125      N12(K)=REAL(C12(K))
126      11 CONTINUE
127      DO 100 K=2,48
128      PRINT 55
129      55 FORMAT(' ', 'STAR/STAR 6-PULSE')
130      PRINT 20, K, V(K), N(K)
131      20 FORMAT(' ', 'ORDER=', I5, 3X, 'IMAG=', F10.7, 3X, 'REAL=', F10.7)
132      100 CONTINUE
133      DO 200 K=2,48
134      PRINT 65
135      65 FORMAT(' ', 'DELTA/STAR 6-PULSE')
136      PRINT 30, K, DV(K), DN(K)
137      30 FORMAT(' ', 'ORDER=', I5, 3X, 'IMAG=', F10.7, 3X, 'REAL=', F10.7)
138      200 CONTINUE
139      DO 300 K=2,48
140      PRINT 75
141      75 FORMAT(' ', '12-PULSE OPERATION')
142      PRINT 40, K, V12(K), N12(K)
143      40 FORMAT(' ', 'ORDER=', I5, 3X, 'IMAG=', F10.7, 3X, 'REAL=', F10.7)
144      300 CONTINUE
145      DO 400 K=2,48
146      PRINT 85
147      85 FORMAT(' ', '12-PULSE OPERATION')
148      PRINT 50, K, Y(K), DY(K), Y12(K)
149      50 FORMAT(' ', 'ORDER=', I3, 3X, 'STAR=', F10.7, 3X, 'DELTA=', F10.7, 3X
150      X' 12-PULSE ', F10.7)
151      400 CONTINUE
152      STOP
153      END

```

```

1  $JOB  WATFIV  SHARAF
2  INTEGER  K,I,M
3  REAL  VA,VB,VC
4  REAL  VNA(15),VNB(15),VNC(15)
5  REAL  NA(15),NB(15),NC(15)
6  REAL  WK,W1,W2,W3,W4,W5,W6
7  REAL  XXA(15),XXB(15),XXC(15)
8  REAL  XA(15),XB(15),XC(15)
9  REAL  X(15),U(15),PB(15)
10 REAL  YS(52),YD(52),Y12(52)
11 REAL  L(15)
12 COMPLEX  SUM1,SUM2,SUM3
13 COMPLEX  CMPLX,CEXP
14 COMPLEX  ZM1,ZM2,ZM3,ZM4,ZM5,ZM6
15 COMPLEX  FAM(15,15),FHM(15,15),FCM(15,15)
16 COMPLEX  S1(15,15),S2(15,15)
17 COMPLEX  AI(15),BI(15),CI(15)
18 COMPLEX  ZXA(15),ZXP(15),ZXC(15)
19 COMPLEX  CS(52),CD(52),C12(52)
20 COMPLEX  ZDS(52)
21 READ,(BB(I),I=1,6)
22 READ,(X(I),I=1,6)
23 READ,(U(I),I=1,6)
24 READ,VA,VB,VC
25 READ,(XXA(I),I=1,9)
26 READ,(NA(I),I=1,9)
27 READ,(NB(I),I=1,9)
28 READ,(NC(I),I=1,9)
29 PI=4.0*ATAN(1.0)
30 H=2.0*PI/360.0
31 DO 1  K=1,9
32  XA(K)=XXA(K)*H
33  XB(K)=XA(K)+K*(2.0*PI/3.0)
34  XC(K)=XA(K)-K*(2.0*PI/3.0)
35  VNA(K)=0.5*(2.0)*NA(K)*VA
36  VNB(K)=0.5*(2.0)*NB(K)*VB
37  VNC(K)=0.5*(2.0)*NC(K)*VC
38  ZXA(K)=CMPLX(0.0,XA(K))
39  ZXP(K)=CMPLX(0.0,XB(K))
40  ZXC(K)=CMPLX(0.0,XC(K))
41 1  CONTINUE
42  L(1)=H*(PB(1)+X(1))
43  L(2)=H*(PB(1)+X(1)+U(1))
44  L(3)=H*(PB(2)+X(2))
45  L(4)=H*(PB(2)+X(2)+U(2))
46  L(5)=H*(PB(3)+X(3))
47  L(6)=H*(PB(3)+X(3)+U(3))
48  L(7)=H*(PB(4)+X(4))
49  L(8)=H*(PB(4)+X(4)+U(4))
50  L(9)=H*(PB(5)+X(5))
51  L(10)=H*(PB(5)+X(5)+U(5))
52  L(11)=H*(PB(6)+X(6))
53  L(12)=H*(PB(6)+X(6)+U(6))
54  L(13)=H*X(1)+2.0*PI
55  M=1
56 2  CONTINUE
57  DO 4  I=1,12
58  DO 3  K=1,9
59  W5=-(K+M)*L(I+1)
60  ZM5=CMPLX(0.0,W5)
61  W6=-(K+M)*L(I)
62  ZM6=CMPLX(0.0,W6)
63  W2=1.0/(K+M)
64  ZM2=CMPLX(0.0,W2)
65  W3=(K-M)*L(I+1)
66  ZM3=CMPLX(0.0,W3)

```

Program (2)

Calculation of d.c. side voltage harmonics
(a.c. harmonics included)


```

66      W4=(K-M)*L(I)
67      ZM4=CMPLX(0.0,W4)
68      IF(K.EQ.N) GO TO 5
69      W1=-1.0/(K-M)
70      ZM1=CMPLX(0.0,W1)
71      S1(I,K)=ZM1*(CEXP(ZM3)-CEXP(ZM4))
72      IF(K.NE.M) GO TO 55
73      S1(I,K)=L(I+1)-L(I)
74      S2(I,K)=ZM2*(CEXP(ZM5)-CEXP(ZM6))
75      FAM(I,K)=VNA(K)*(CEXP(-7XA(K))*S1(I,K)+CEXP(7XA(K))*S2(I,K))
76      FBM(I,K)=VNB(K)*(CEXP(-7XB(K))*S1(I,K)+CEXP(7XB(K))*S2(I,K))
77      FCM(I,K)=VNC(K)*(CEXP(-7XC(K))*S1(I,K)+CEXP(7XC(K))*S2(I,K))
78      3  CCNTINUE
79      4  CCNTINUE
80      DO 6 I=1,12
81      SUM1=(0.0,0.0)
82      SUM2=(0.0,0.0)
83      SUM3=(0.0,0.0)
84      DC 7 K=1,9
85      SUM1=SUM1+FAM(I,K)
86      SUM2=SUM2+FBM(I,K)
87      SUM3=SUM3+FCM(I,K)
88      7  CCNTINUE
89      AI(I)=SUM1
90      BI(I)=SUM2
91      CI(I)=SUM3
92      6  CCNTINUE
93      CS(M)=(1.0/(2.0*PI))*((AI(1)+CI(1))*0.5-BI(1)+AI(2)-BI(2)+
XAI(3)-BI(3)+CI(3))*0.5+AI(4)-CI(4)+(AI(5)+BI(5))*0.5-CI(5)+
XBI(6)-CI(6)+BI(7)-(AI(7)+CI(7))*0.5+BI(8)-AI(8)+(BI(9)+CI(9))*
X0.5-AI(9)+CI(10)-AI(10)+CI(11)-(AI(11)+BI(11))*0.5+CI(12)-BI(12)
94      YS(M)=CABS(CS(M))
95      M=M+1
96      IF(M.LE.24) GO TO 2
97      IF(M.EQ.25) CCNTINUE
98      DO 11 K=1,24
99      WK=+K*(PI/6.0)
100     ZDS(K)=CMPLX(0.0,WK)
101     11  CCNTINUE
102     PRINT 100
103     100  FORMAT(' ',' HARM. VOLTAGES IN STAR/STAR 6-PULSE OPERATION')
104     DO 101 K=1,24
105     CD(K)=CS(K)*CEXP(7ZDS(K))
106     C12(K)=CS(K)+CD(K)
107     YD(K)=CABS(CD(K))
108     Y12(K)=CABS(C12(K))
109     PRINT102,K,YD(K),C12(K)
110     102  FORMAT(' ',3X,I4,'STAR-V=',F12.6,3X,'V-REAL=',F12.6,3X,'V-IMAG='
XF12.6)
111     101  CCNTINUE
112     PRINT 200
113     200  FORMAT(' ',' HARM. VOLTAGES IN DELTA/STAR 6- PULSE OPERATION')
114     DO 201 K=1,24
115     PRINT202,K,YD(K),CD(K)
116     202  FORMAT(' ',3X,I4,'DELTA/STAR VOLTAGES=',F12.6,3X,'V-REAL=',
XF12.6,3X,'V-IMAG=',F12.6)
117     201  CCNTINUE
118     PRINT 300
119     300  FORMAT(' ',' HAR.VOLTAGES IN 12- PULSE OPERATION')
120     DO 301 K=1,24
121     PRINT302,K,Y12(K),C12(K)
122     302  FORMAT(' ',5X,I4,'12-PULSE V=',F12.6,3X,'V-REAL=',F12.6,3X,
X'V-IMAG=',F12.6)
123     301  CCNTINUE
124     STOP
125     END

```

\$JOB

WATFIV

SHATAF

91

```

1 REAL X(10),U(10),L(15),XX,UU
2 REAL BX(10)
3 REAL V1M,V2M,V3M
4 REAL W,V,Y,W1,V1,Y1
5 REAL SAN,SNB,SNB1
6 REAL DAN,DBN,DBN1
7 REAL MS,NS,SCN
8 REAL MD,ND,DCN
9 REAL M12,N12,C12
10 COMPLEX ZS,ZD,Z12,Z,Z1,Z2,CMPLX,CEXP,ZDD
11 REAL I1(15),I2(15),I3(15)
12 REAL J1(15),J2(15),J3(15)
13 REAL S,S1,S,31,T,T1
14 REAL A(15),AA(15),B(15),BB(15)
15 REAL C(15)
16 REAL PI,H
17 REAL VD,VD1,VD2
18 REAL DC1(15),DC2(15)
19 COMPLEX F1(15),F2(15),F3(15)
20 REAL SV,DV,V12
C X(I),U(I),BX(I)...ARE IGNITION,COMM...AND DELAY ANGLES F/R VALVES
C L(I)...ARE LIMITS OF INTEGRATION FOR FOURIER COEFFICIENTS
C V1,V2,V3...ARE...COSINE WAVEFORMS W.R.T. DATUM X_X
C SCN,DCN,C12...ARE MAN
C SCN,DCN,C12...ARE MAGNITUDES OF FOURIER COEFF. FOR S/S,D/S,12-
C PULSE OPERATIONS
C 1ST HARMONIC IN D/S BRIDGE IS SHIFTED (30) DEG.
C XX,UU...ARE DEVIATIONS BETWEEN S/S,D/S BRIDGES,IGNITION,COMM.
C SV...DV...V12 ARE RECTIFIED VOLTAGES FOR STAR/STAR,...
C ...DELTA/STAR...AND 12-PULSE OPERATIONS
C OBJECTIVE...IS 1ST...AND...AVERAGE VOLTAGES UNDER IMBALANCE
C CONDITIONS IN 1 BRIDGE AND COMBINED 12-PULSE OPERATIONS
21 READ,(BX(I),I=1,6)
22 READ,W,V,Y
23 READ,XX,UU
24 50. CONTINUE
25 READ,(X(I),I=1,6)
26 READ,(U(I),I=1,6)
27 READ,V1M,V2M,V3M
28 IF(X(1).EQ.0.0) STOP
29 PI=4.0*ATAN(1.0)
30 H=2.0*PI/360.0
31 L(1)=H*(BX(1)+X(1))
32 L(2)=H*(BX(1)+X(1)+U(1))
33 L(3)=H*(BX(2)+X(2))
34 L(4)=H*(BX(2)+X(2)+U(2))
35 L(5)=H*(BX(3)+X(3))
36 L(6)=H*(BX(3)+X(3)+U(3))
37 L(7)=H*(BX(4)+X(4))
38 L(8)=H*(BX(4)+X(4)+U(4))
39 L(9)=H*(BX(5)+X(5))
40 L(10)=H*(BX(5)+X(5)+U(5))
41 L(11)=H*(BX(6)+X(6))
42 L(12)=H*(BX(6)+X(6)+U(6))
43 L(13)=H*X(1)+2.0*PI
44 W1=H*W
45 V1=H*V
46 Y1=H*Y
47 S1=SIN(W1)
48 S=COS(W1)
49 R1=SIN(V1)
50 R=COS(V1)
51 T1=SIN(Y1)
52 T=COS(Y1)
53 DO 1 I=1,12

```

Program (3)

Calculation of mean d.c. voltage and 1st harmonic voltage on the d.c. side

```

54 A(I)=SIN(2.0*L(I+1))
55 AA(I)=SIN(2.0*L(I))
56 S(I)=COS(2.0*L(I+1))
57 BB(I)=COS(2.0*L(I))
58 C(I)=L(I+1)-L(I)
59 I1(I)=0.25*V1M*(S*(A(I)-AA(I)+2.0*C(I))-S1*(B(I)-BB(I)))
60 I2(I)=0.25*V2M*(R*(A(I)-AA(I)+2.0*C(I))-R1*(B(I)-BB(I)))
61 I3(I)=0.25*V3M*(T*(A(I)-AA(I)+2.0*C(I))-T1*(B(I)-BB(I)))
62 J1(I)=-0.25*V1M*(S*(B(I)-BB(I))+S1*(A(I)-AA(I)-2.0*C(I)))
63 J2(I)=-0.25*V2M*(R*(B(I)-BB(I))+R1*(A(I)-AA(I)-2.0*C(I)))
64 J3(I)=-0.25*V3M*(T*(B(I)-BB(I))+T1*(A(I)-AA(I)-2.0*C(I)))
65 CONTINUE
66 SAN=(1.0/PI)*((I1(1)+I3(1))*0.5-I2(1)+I1(2)-I2(2)+
X11(3)-(I2(3)+I3(3))*0.5+ I1(4)-I3(4)+(I1(5)+I2(5))*0.5-I3(5)+
X12(6)-I3(6)+I2(7)-(I1(7)+I3(7))*0.5+I2(8)-I1(8)+(I2(9)+I3(9))*
X0.5-I1(9)+I3(10)-I1(10)+I3(11)-(I1(11)+I2(11))*0.5+I3(12)-I2(12)
SBN=(1.0/PI)*((J1(1)+J3(1))*0.5-J2(1)+J1(2)-J2(2)+
XJ1(3)-(J2(3)+J3(3))*0.5+J1(4)-J3(4)+(J1(5)+J2(5))*0.5-J3(5)+
XJ2(6)-J3(6)+J2(7)-J3(7)+J1(7)+J3(7)+J2(8)-J1(8)+(J2(9)+J3(9))*
X0.5-J1(9)+J3(10)-J1(10)+J3(11)-0.5*(J1(11)+J2(11))+J3(12)-J2(12)
67 SBN1=-SBN
Z1=CMPLX(SAN,SBN1)
70 ZS=(0.5)*Z1
71 MS=AIMAG(ZS)
72 NS=REAL(ZS)
73 SCN=CABS(ZS)
74 DO 4 I=1,12
75 DC1(I)=SIN(L(I+1))-SIN(L(I))
76 DC2(I)=COS(L(I+1))-COS(L(I))
77 F1(I)=V1M*(S*DC1(I)-S1*DC2(I))
78 F2(I)=V2M*(R*DC1(I)-R1*DC2(I))
79 F3(I)=V3M*(T*DC1(I)-T1*DC2(I))
80 CONTINUE
81 VD1=((F1(1)+F3(1))*0.5-F2(1)+F1(2)-F2(2)+
XF1(3)-(F2(3)+F3(3))*0.5+F1(4)-F3(4)+(F1(5)+F2(5))*0.5-F3(5)+
XF2(6)-F3(6)+F2(7)-(F1(7)+F3(7))*0.5+F2(8)-F1(8)+(F2(9)+F3(9))*
X0.5-F1(9)+F3(10)-F1(10)+F3(11)-(F1(11)+F2(11))*0.5+F3(12)-F2(12)
DO 2 I=1,6
82 X(I)=X(I)-XX
83 U(I)=U(I)-UU
84 L(1)=H*(RX(1)+X(1))
85 L(2)=H*(RX(1)+X(1)+U(1))
86 L(3)=H*(RX(2)+X(2))
87 L(4)=H*(RX(2)+X(2)+U(2))
88 L(5)=H*(RX(3)+X(3))
89 L(6)=H*(RX(3)+X(3)+U(3))
90 L(7)=H*(RX(4)+X(4))
91 L(8)=H*(RX(4)+X(4)+U(4))
92 L(9)=H*(RX(5)+X(5))
93 L(10)=H*(RX(5)+X(5)+U(5))
94 L(11)=H*(RX(6)+X(6))
95 L(12)=H*(RX(6)+X(6)+U(6))
96 L(13)=H*X(1)+2.0*PI
97 CONTINUE
98 DO 3 I=1,12
99 A(I)=SIN(2.0*L(I+1))
100 AA(I)=SIN(2.0*L(I))
101 S(I)=COS(2.0*L(I+1))
102 BB(I)=COS(2.0*L(I))
103 C(I)=L(I+1)-L(I)
104 I1(I)=0.25*V1M*(S*(A(I)-AA(I)+2.0*C(I))-S1*(B(I)-BB(I)))
105 I2(I)=0.25*V2M*(R*(A(I)-AA(I)+2.0*C(I))-R1*(B(I)-BB(I)))
106 I3(I)=0.25*V3M*(T*(A(I)-AA(I)+2.0*C(I))-T1*(B(I)-BB(I)))
107 J1(I)=-0.25*V1M*(S*(B(I)-BB(I))+S1*(A(I)-AA(I)-2.0*C(I)))
108 J2(I)=-0.25*V2M*(R*(B(I)-BB(I))+R1*(A(I)-AA(I)-2.0*C(I)))
109 J3(I)=-0.25*V3M*(T*(B(I)-BB(I))+T1*(A(I)-AA(I)-2.0*C(I)))
110

```

```

111 3 CONTINUE
112 DAN=(1.0/PI)*((I1(1)+I3(1))*0.5-I2(1)+I1(2)-I2(2)+
XI1(3)-(I2(3)+I3(3))*0.5+I1(4)-I3(4)+(I1(5)+I2(5))*0.5-I3(5)+
XI2(6)-I3(6)+I2(7)-(I1(7)+I3(7))*0.5+I2(8)-I1(8)+(I2(9)+I3(9))*
X0.5-I1(9)+I3(10)-I1(10)+I3(11)-(I1(11)+I2(11))*0.5+I3(12)-I2(12)
113 DBN=(1.0/PI)*((J1(1)+J3(1))*0.5-J2(1)+J1(2)-J2(2)+
XJ1(3)-(J2(3)+J3(3))*0.5+J1(4)-J3(4)+(J1(5)+J2(5))*0.5-J3(5)+
XJ2(6)-J3(6)+J2(7)-0.5*(J1(7)+J3(7))+J2(8)-J1(8)+(J2(9)+J3(9))*
X0.5-J1(9)+J3(10)-J1(10)+J3(11)-0.5*(J1(11)+J2(11))+J3(12)-J2(12)
114 DBN1=-DBN
115 Z2=CMPLX(DAN,DBN1)
116 ZD=0.5*Z2
117 WW=-PI/6.0
118 Z=CMPLX(0.0,WW)
119 ZDD=ZD*EXP(Z)
120 MD=AIMAG(ZDD)
121 ND=REAL(ZDD)
122 DCN=CABS(ZDD)
123 Z12=ZS+ZDD
124 M12=AIMAG(Z12)
125 N12=REAL(Z12)
126 C12=CABS(Z12)
127 DO 6 I=1,12
128 DC1(I)=SIN(L(I+1))-SIN(L(I))
129 DC2(I)=COS(L(I+1))-COS(L(I))
130 F1(I)=V1M*(S*DC1(I)-S1*DC2(I))
131 F2(I)=V2M*(R*DC1(I)-R1*DC2(I))
132 F3(I)=V3M*(T*DC1(I)-T1*DC2(I))
133 6 CONTINUE
134 VD2=((F1(1)+F3(1))*0.5-F2(1)+F1(2)-F2(2)+
XF1(3)-(F2(3)+F3(3))*0.5+F1(4)-F3(4)+(F1(5)+F2(5))*0.5-F3(5)+
XF2(6)-F3(6)+F2(7)-(F1(7)+F3(7))*0.5+F2(8)-F1(8)+(F2(9)+F3(9))*
X0.5-F1(9)+F3(10)-F1(10)+F3(11)-(F1(11)+F2(11))*0.5+F3(12)-F2(12)
135 VD=VD1+VD2
136 SV=VD1/(2.0*PI)
137 DV=VD2/(2.0*PI)
138 V12=VD/(2.0*PI)
139 PRINTF,SV,DV,V12
140 5 FORMAT(' ',3X,'STAR DC VOLT.=',F10.7,3X,'DELTA DC VOLT.=',F10.7
X3X,'12-PULSE DC VOLT.=',F10.7)
141 PRINT10,MS,NS,SCN
142 10 FORMAT(' ',3X,'STAR IMAG=',F10.5,3X,'STAR REAL=',F10.5,3X,
X'STAR/STAR FUNDAMENTAL=',F10.5)
143 PRINT20,MD,ND,DCN
144 20 FORMAT(' ',3X,'DELTA IMAG=',F10.5,3X,'DELTA REAL=',F10.5,3X,
X'DELTA/STAR FUNDAMENTAL=',F10.5)
145 PRINT30,SCN,DCN,C12
146 30 FORMAT(' ',3X,'STAR/STAR=',F10.5,3X,'DELTA/STAR=',F10.5,3X,
X'12-PULSE OPERATION=',F10.5)
147 GO TO 50
148 END

```

APPENDIX II

(a) Justification of the procedure adopted in calculating d.c. side harmonic currents

To justify the determination of harmonic currents from the harmonic voltages by determining the quotient of the K th harmonic voltage by the K th harmonic impedance of the system first a simple circuit was studied.

The circuit consists of a simple half wave controlled rectifier Fig. A2(a) with an (R-L) load. The current through the circuit is determined by solving a first order differential equation, then, the complex Fourier approach is applied to both voltage and current waveforms. The thyristor starts conducting after a delay angle (α) and stops conduction at an angle (θ) when $i = 0$ and the rectifier is reverse biased. This angle (θ) depends on the ratio ($\frac{L}{R}$) of the circuit load.

The current differential equation is

$$L \frac{di}{dt} + Ri = E_o \sin \omega t \quad (A2-1)$$

after transforming equ. (A2-1) into an exact ordinary differential equation by multiplying both sides by

$$e^{\beta t} \quad \text{where} \quad \beta = \frac{L}{R}$$

The current waveform is defined as

$$i = I_m \sin(\omega t - \phi) - I_m \sin(\alpha - \phi) e^{-\frac{R}{L}(\omega t - \alpha)}$$

$$\text{in the range} \quad \alpha \leq \omega t \leq \theta \quad (A2-2)$$

where

$$I_m = \frac{E_o}{\sqrt{R^2 + \omega^2 L^2}}, \quad \phi = \text{ATAN} \frac{\omega L}{R} \quad (A2-3)$$

The angle θ at which conduction stops is determined graphically.

The voltage waveform across the load terminals is defined as

$$v = E_o \sin \omega t \quad \alpha \leq \omega t \leq \theta \quad (A2-4)$$

The harmonic contents in both v , i are calculated and the ratio of $\left(\frac{V_K}{I_K}\right)$ is determined for each harmonic order (K) .

This ratio is found to be exactly equal to the load harmonic impedance (Z_K) where,

$$Z_K = R + j K \omega L \quad (A2-5)$$

fig. A2(a) is a simplified half wave rectifier circuit

fig. A2(b) illustrates the resultant load voltage and current waveforms.

Table T,A2(a) illustrates the harmonic contents and the ratio of

$\left(\frac{V_K}{I_K}\right)$ compared with the system harmonic impedance.

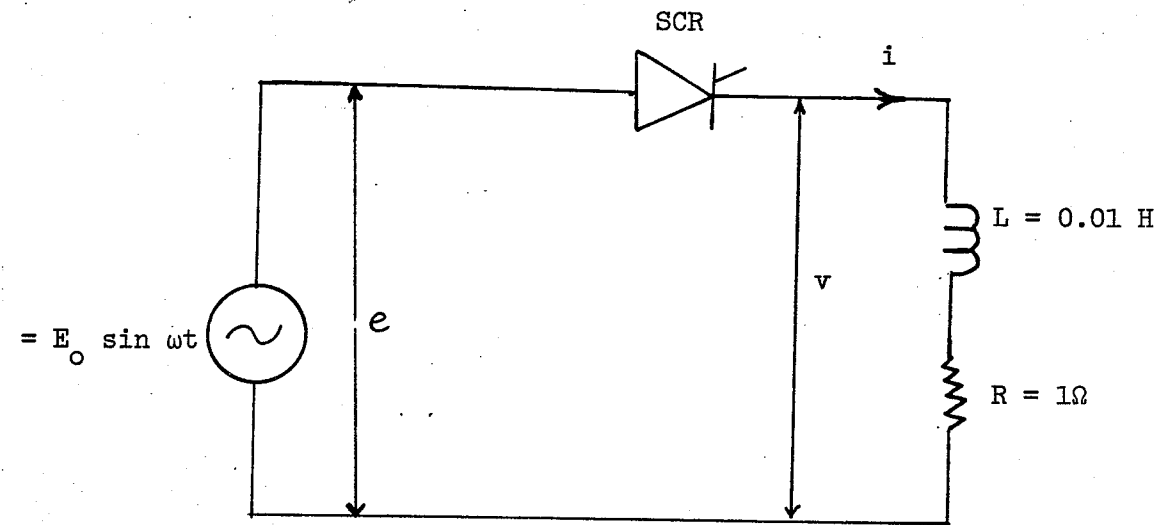


Fig. A2(a) Simplified half wave rectifier circuit

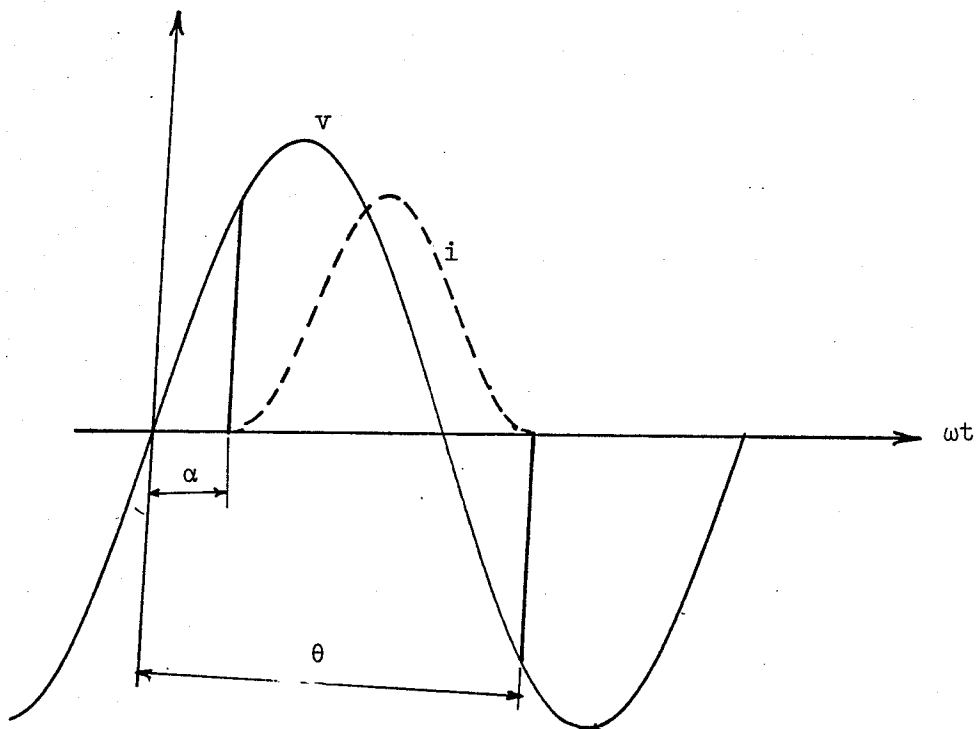


Fig. A2(b) Load voltage and current waveforms

Table A2(a)

$$E_o = 100,0 \text{ volts}$$

$$(R = 1,0\Omega, L = 0,01 \text{ H})$$

Harmonic order (K)	Harmonic content in (v) volts	Harmonic content in (i) amps	Ratio $\left(\frac{V_K}{I_K}\right) \Omega$	$Z_K = R + j k \omega L \Omega$
0	15.206	15.22	0.999	1.0
1	38.299	9.816	3.901	3.90
2	12.179	1.602	7.601	7.605
3	8.427	0.7422	11.354	11.353
4	4.229	0.279	15.129	15.112
5	2.328	0.123	18.858	18.87
6	3.208	0.141	22.619	22.64
7	2.882	0.109	26.426	26.40
8	1.619	0.053	30.233	30.17
9	1.618	0.047	33.86	33.94
10	2.039	0.057	37.86	37.71
11	1.531	0.036	41.576	41.48
12	0.98119	0.0217	45.205	45.25

N.B. The reason for the slight discrepancy between the ratio $\left(\frac{V_K}{I_K}\right)$ and (Z_K) is that the angle θ at which conduction stops was determined graphically.

(b) Computational program for d.c. side harmonic currents

The principle of superposition is adopted in calculating d.c. side harmonic currents.

The harmonic voltages are taken one at a time, and for each harmonic order the d.c. circuit impedance is calculated, and through a steady-state approach the harmonic current is obtained as a quotient of the harmonic voltage by the circuit harmonic impedance.

The harmonic currents through the transmission line and filter branches are obtained, as well as the voltage drop across filters.

The program is written in a most general form, the input data are the harmonic d.c. side voltages and circuit parameters, both as complex numbers.

There is a flexibility of omitting any parallel branch such as the situation of the 6th arm filter out of service.

The harmonic currents could be referred to any base value, similarly the input voltages.

In the following, copy of the harmonic currents program is included.

```

1 COMPLEX CMPLX
2 COMPLEX CTOT(14),CF(14),CF6(14),CF12(14),CTL(14),VF(14)
3 COMPLEX V(14),PU(14)
4 COMPLEX ZPI(14),YPI(14),YPI1(14),ZPI1(14)
5 COMPLEX Z6(14),Y6(14),Y12(14),Z12(14),YPIL(14),ZPIL(14)
6 COMPLEX YPIL12(14)
7 COMPLEX ZL(14),YL(14)
8 COMPLEX YF(14),ZF(14)
9 COMPLEX YFL(14),ZFL(14)
10 COMPLEX ZPILF(14),YPILF(14),ZTOT(14),YTOT(14)
11 COMPLEX ZPIO(14),YPIO(14)
12 REAL R6,C6,R12,C12,L6,L12
13 REAL NLL
14 REAL REASE
15 REAL XL(14)
16 REAL MCTOT(14),MCTL(14)
17 REAL LD
18 REAL MZFL(14)
19 REAL MCF(14)
20 REAL MV(14),MZTOT(14),MCF6(14),MCF12(14),MVF(14)
21 REAL W,WL(14),X6(14),X12(14)
C V IS HARM. VOLTAGES ON D.C. SIDE
C CTOT,CF6,CF12 ARE CURRENTS IN SYSTEM, 6TH FILTER, 12TH FILTER
C NLL IS THE RATIO OF VDO TO E-LL...REASE IS THE BASE IMPED
C VDCN...IDN ARE BASE VOLTAGE...AND CURRENT ON D.C. SIDE
C PU(K) IS JARMONICS CALCULATED WITH E-LL EO.1.0P.U.
C ZPI,YPI ARE LINE PI-SECTION IMPEDANCE, ADMITTANCE AT DIFF.
C FREQUENCIES
C LD IS LINE DAMPING REACTOR...VF(K) IS VOLTAGE DROP ACROSS
C FILTERING BRANCHES
22 READ,NLL
23 READ,REASE
24 READ,(PU(K),K=1,12)
25 READ,(ZPIO(K),K=1,12)
26 READ,(YPIO(K),K=1,12)
27 READ,R6,L6,C6
28 READ,R12,L12,C12
29 READ,LD
30 READ,W
31 DO 1 K=1,12
32 V(K)=NLL*PU(K)
33 ZPI(K)=ZPIO(K)*(1.0/REASE)
34 YPI(K)=YPIO(K)*(REASE)
35 WL(K)=W*K*LD
36 ZL(K)=CMPLX(0.0,WL(K))*(1.0/REASE)
37 YL(K)=1.0/ZL(K)
38 X6(K)=K*W*LD-1.0/(K*W*C6)
39 Z6(K)=CMPLX(R6,X6(K))*(1.0/REASE)
40 Y6(K)=1.0/Z6(K)
41 X12(K)=K*W*LD-1.0/(K*W*C12)
42 Z12(K)=CMPLX(R12,X12(K))*(1.0/REASE)
43 Y12(K)=1.0/Z12(K)
44 YPI1(K)=YPI(K)+1.0/ZPI(K)
45 ZPI1(K)=1.0/YPI1(K)
46 ZPIL(K)=ZPI1(K)+ZL(K)
47 YPIL(K)=1.0/ZPIL(K)
48 YPIL12(K)=YPIL(K)+Y12(K)
49 YPILF(K)=YPIL12(K)+Y6(K)
50 YF(K)=Y6(K)+Y12(K)
51 ZF(K)=1.0/YF(K)
52 ZFL(K)=ZF(K)+ZL(K)
53 ZPILF(K)=1.0/YPILF(K)
54 ZTOT(K)=ZPILF(K)+ZL(K)
55 YTOT(K)=1.0/ZTOT(K)
56 CTOT(K)=V(K)/ZTOT(K)

```

Program (4)

Calculation of d.c. harmonic currents on
account of asymeteries

```

58 CF6(K)=CF(K)*((Y6(K)/YF(K)+YFIL(K)))
59 CF12(K)=CF(K)*((Y12(K)/YF(K)))
60 VF(K)=CF(K)*YF(K)
61 CTL(K)=CTOT(K)-CF(K)
62 MCTOT(K)=CABS(CTOT(K))
63 MCF6(K)=CABS(CF6(K))
64 MCF12(K)=CABS(CF12(K))
65 MVF(K)=CABS(VF(K))
66 MV(K)=CABS(V(K))
67 MZTOT(K)=CABS(ZTOT(K))
68 MCTL(K)=CABS(CTL(K))
69 MCF(K)=CABS(CF(K))
70 MZFL(K)=CABS(ZFL(K))
71 CONTINUE
72 PRINT 100
73 100 FORMAT(' ','CURRENT IN 6TH ARM FILTER')
74 DO 101 K=1,12
75 PRINT102,K,MCF6(K),CF6(K)
76 102 FORMAT(' ','8X,I3,'6TH -CURRENT='',F12.7,8X,'6-REAL='',F12.6,6X,
77 X'6-IMAG='',F12.6)
78 101 CONTINUE
79 PRINT 200
80 200 FORMAT(' ','12X,' CURRENT IN 12TH FILTER')
81 DO 201 K=1,12
82 PRINT 202,K,MCF12(K),CF12(K)
83 202 FORMAT(' ','8X,I3,'12 TH-CURRENT='',F12.7,5X,'12 -REAL='',F12.6,
84 X'12-IMAG='',F12.6)
85 201 CONTINUE
86 PRINT 300
87 DO 301 K=1,12
88 301 FORMAT(' ','VOLTAGE DRCP ACROSS FILTERING BRANCHES')
89 302 K,MVF(K),VF(K)
90 302 FORMAT(' ','8X,I3,'HARM.V.D.='',F12.7,6X,'VF-REAL='',F12.6,5X,
91 X'V-IMAG='',F12.6)
92 301 CONTINUE
93 PRINT 400
94 400 FORMAT(' ','3X,' SYSTEM IMPEDANCE')
95 DO 401 K=1,12
96 PRINT 402,K,MZTOT(K),ZTOT(K)
97 402 FORMAT(' ','8X,I3,'ZSYS='',F12.7,5X,'ZS-REAL='',F12.6,3X,
98 X'ZS-IMAG='',F12.6)
99 401 CONTINUE
100 PRINT 600
101 600 FORMAT(' ','12X,' HARMONIC VOLTAGE GENERATOR AND HARMONIC CURRENTS')
102 DO 601 K=1,12
103 PRINT 602,K,MV(K),MCTOT(K),MCF(K),MCTL(K)
104 602 FORMAT(' ','5X,I3,'VN='',F10.7,3X,'IN='',F10.7,3X,'IF='',F10.7,
105 X'3X,'I-LINE='',F10.7)
106 601 CONTINUE
107 PRINT 700
108 700 FORMAT(' ','7-LOOP FORMED BY LD+ FILTERING')
109 DO 701 K=1,12
110 PRINT702,K,MZFL(K),ZFL(K)
111 702 FORMAT(' ','8X,I3,'Z-LOOP='',F12.6,6X,'ZL-REAL='',F12.6,6X,
112 X'ZL-IMAG='',F12.6)
113 701 CONTINUE
114 STOP
115 END

```

APPENDIX III

a) Effect of unequal transformer phase inductances on the level of unbalance in commutation angle (u)

Fig. A3(a) illustrates commutation between valves (1), (3).

During commutation between valves 1, 3 the current in valve (1) decays and that of valve (3) starts building up.

The differential equation governing commutation can be written as:

$$v_b - v_a = L_{C_2} \frac{di_3}{dt} - L_{C_1} \frac{di_1}{dt} \quad (A3-6)$$

$$\text{where } v_b - v_a = \sqrt{3} \hat{V} \sin \omega t \quad (A3-7)$$

$$\text{and the initial condition } i_1 = I_d - i_3 \quad (A3-8)$$

$$\text{So, } \frac{di_1}{dt} = 0 - \frac{di_3}{dt}$$

Equ. (A3-6) could be written as

$$\sqrt{3} \hat{V} \sin \omega t = (L_{C_1} + L_{C_2}) \frac{di_3}{dt} \quad (A3-9)$$

$$\text{i.e., } \frac{di_3}{dt} = \frac{\sqrt{3} \cdot V}{(L_{C_1} + L_{C_2})} \sin \omega t \quad (A3-10)$$

Integrating Equ. (A3-10),

$$i_3 = \frac{\sqrt{3} \cdot V}{\omega(L_{C_1} + L_{C_2})} (\cos \alpha - \cos \omega t) \quad (A3-11)$$

$$\text{in the range } \alpha \leq \omega t \leq \alpha + u$$

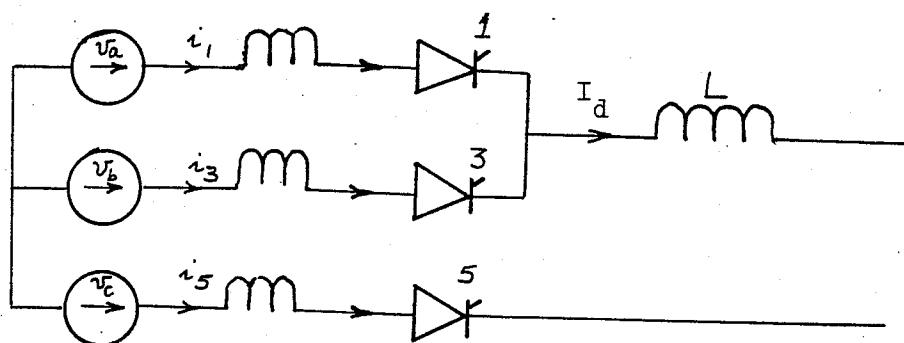


Fig. A3(a) Circuit diagram illustrating commutation between valves (1), (3).

When $\omega t = \alpha + u$, $i_3 = I_d = \text{constant}$ for a given value of α and u ,

Starting from equ. (A2-11),

$$\frac{\cos \alpha - \cos(\alpha + u)}{\omega(L_{C_1} + L_{C_2})} = \text{constant}, \quad (\text{A3-12})$$

and if $L_{C_1} = L_C$ and $L_{C_2} = L_C + \Delta L_C$, the value of

$u^* = (u + \Delta u)$ could be determined from the

following equality:

$$\frac{\cos \alpha - \cos(\alpha + u)}{2\omega L_C} = \frac{\cos \alpha - \cos(\alpha + u^*)}{\omega(L_C + L_C + \Delta L_C)} \quad (\text{A3-13})$$

The following table represents the level of unbalance in commutation angle (u), due to unequal transformer phase inductances L_C , from 1% up to 10% for different nominal operating values for α , u .

TABLE A3(a)

Unbalance in commutation angle u versus unbalance in converter trans-
former phase inductances

% ΔL	(Δu) in degrees		
	$\alpha = 15^\circ, u = 24^\circ$	$\alpha = 18^\circ, u = 24^\circ$	$\alpha = 18^\circ, u = 20$
1	0.0858	0.0889	0.0757
2	0.1715	0.177	0.151
3	0.257	0.266	0.227
4	0.342	0.354	0.302
5	0.427	0.443	0.377
6	0.512	0.531	0.452
7	0.597	0.619	0.527
8	0.682	0.707	0.602
9	0.767	0.795	0.677
10	0.851	0.882	0.752

b) Transmission line PI equivalent for different harmonic orders

Table T.A3(b) represent the PI-section parameters for different harmonic orders

Table T.A3(b)

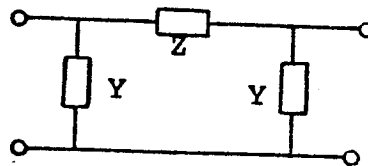
Harmonic	RPI	XPI	GPI	BPI	ZGPI	ZBPI
1	28.751	458.13	.0000836	.00222	16.919	-449.48
2	-77.895	5.5965	.025734	.00184	38.66	-2.768
3	-29.807	-458.63	.00068	-.00225	122.86	406.26
4	137.56	-70.058	.00036	-.000131	2431.7	878.95
5	67.082	453.67	.000604	.001702	185.25	-521.64
6	-183.03	197.46	.005623	.00503	98.738	-88.376
7	-134.77	-426.60	.0020706	-.0029666	158.20	226.67
8	205.00	-296.75	.0007496	-.000622	789.88	655.58
9	212.26	383.78	.00081257	.0009817	500.32	-604.49
10	-199.59	408.81	.002894	.003096	161.13	-172.38
11	-308.49	-303.00	.0041935	-.002571	173.32	106.26
12	152.29	-523.01	.0012456	-.001103	449.98	398.46
18	221.57	687.23	.0015935	.0011623	409.63	-298.78
24	-814.70	-337.83	.0036154	-.00051797	271.03	38.831
30	1039.7	-655.33	.0017750	-.00021667	555.12	67.765
36	-169.05	1712.5	.0023944	.00069255	385.40	-111.47

The PI is an exact equivalent for the total line for one conductor.

$$Z = RPI + jXPI$$

$$Y = GPI + jBPI$$

$$\frac{1}{Y} = ZGPI + jZBPI$$



APPENDIX IV

Calculation of mean equivalent a.c. system inductance

The harmonic voltages are regarded as sources on the d.c. side and the harmonic currents may be obtained as a quotient of the e.m.f. harmonics by the total impedance of the converter network. This impedance may be regarded as made up of the d.c. circuit impedance plus some equivalent inductance of the a.c. circuit which depend mainly on the converter circuit connection and the operating conditions.

In the d.c. side of the converter station, the mean equivalent a.c. system inductance is regarded as internal inductance for each voltage harmonic, reference [1].

In this appendix, the mean equivalent a.c. supply inductance is calculated as a driving point inductance for a 6-pulse and 12-pulse operations.

Within the bridge configuration, the valves which are not conducting are omitted and only those branches carrying currents are considered.

1. 6-pulse operation

The normal conduction in a 6-pulse bridge takes place in 2 valves, followed by a commutation period in which 3 valves are conducting.

In fig. 25(a), valves 1,2 are considered conducting and the rest of the valves are blocked. The transformer leakage inductance for the Δ/Δ transformer is replaced by equivalent electrical inductance (L_T)

Applying Kirchoff's laws on the loop shown in fig. A4(a) the ratio $\frac{V}{I}$ is denoted as $(j \omega L_2)$ where the suffix 2 represent the case of 2-valves are conducting simultaneously.

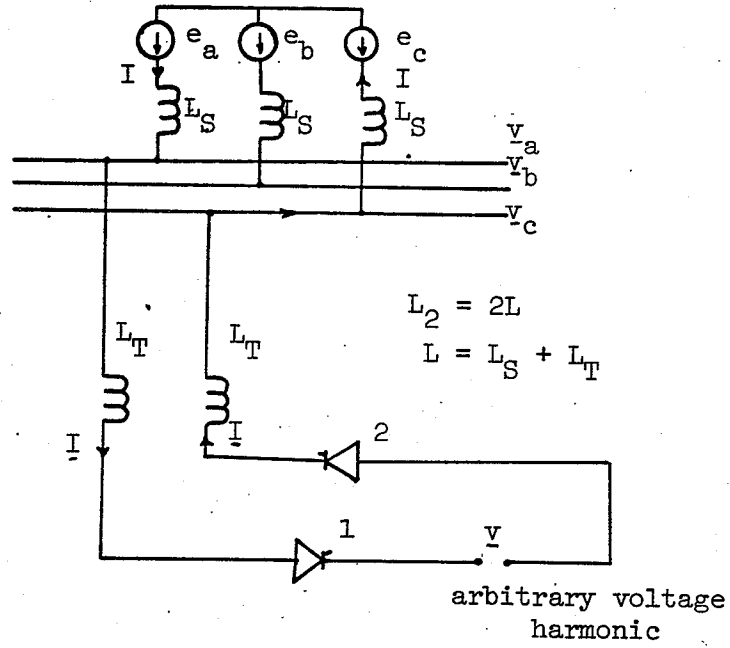


Fig. A4(a) Circuit configuration during conduction (6-pulse)

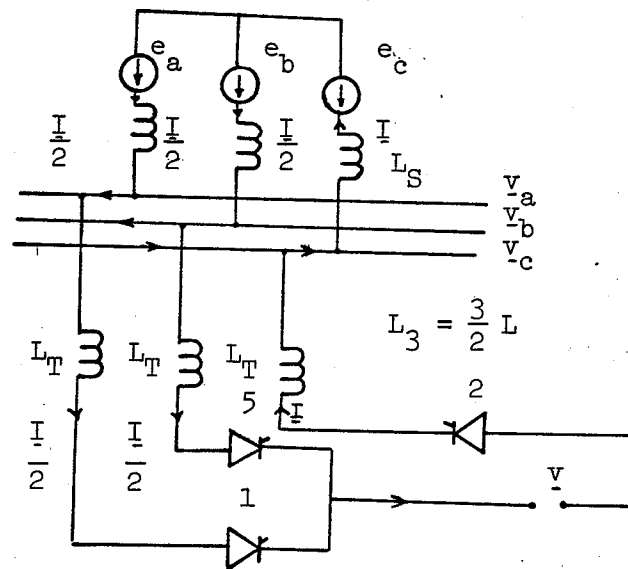


Fig. A4(b) Circuit configuration during commutation (6-pulse)

Assumptions

The procedure adopted in obtaining equivalent averaged inductance is based on the following assumptions:

- (a) Ideal sinusoidal a.c. sources.
- (b) The valves are regarded as ideal switches.
- (c) The valve damping reactors are added to the transformers leakage inductances.
- (d) Phasors are used even when part of the cycle is considered, i.e., assumption of a sinusoidal current during both conduction and commutation of each valve is considered.

Limitations

It should be noted that assumption (d) is not strictly valid. During commutation the current is not sinusoidal, thus, weighting the current waveform as a pure sinusoidal which lags the voltage waveform is not quite correct, and a special treatment is needed to study the transient currents during commutation.

The following approach is only useful as a first approximation for the weighted a.c. system inductance which should be taken as internal impedance for the harmonic generator on the d.c. side. Moreover, with the existence of high damping reactor on the converter side of the d.c. line, any internal inductance which is usually small does not make any difference when added to the high inductance to calculate for the d.c. current, and a global assumption of zero internal inductance is practically accepted in the calculation of d.c. side harmonic currents.

1.1 Calculation of internal inductance in case of 6-pulse operation

a) 2-values conducting

$$\frac{V}{I} = j \omega L_2 = j \omega (2L_T + 2L_S) = j \omega (2L) \quad (A4-1)$$

$$\text{where } L = L_S + L_T \quad (A4-2)$$

$$\text{and } L_2 = 2L \quad (A4-3)$$

b) 3-values conducting

This case represents commutation period in 6-pulse operation, and the converter configuration is shown in fig. 25(b).

$$\begin{aligned} \frac{V}{I} &= j \omega L_3 = j \omega (L_T \frac{I}{2} + L_S \frac{I}{2} + L_S \frac{I}{2} + L_T \frac{I}{2}) \\ &= j \omega (L_T + L_S + \frac{L_S}{2} + \frac{L_T}{2}) \frac{I}{2} \\ &= j \omega (\frac{3}{2} L) \end{aligned} \quad (A4-4)$$

$$\text{So } L_3 = \frac{3}{2} L \quad (A4-5)$$

An approximate weighted average of the a.c. system inductance in case of 6-pulse operation could be defined as:

$$\begin{aligned} L_{av} &= \frac{L_2 (\frac{2\pi}{3} - u) + L_3 u}{\frac{2\pi}{3}} \\ L_{av} &= \frac{3L}{\pi} [\frac{2\pi}{3} - \frac{1}{4} u] \end{aligned} \quad (A4,6)$$

2. 12-pulse operation

In 12-pulse operation, normal conduction takes place in four valves followed by a commutation period in which five valves are conducting (provided that $u \neq 60^\circ$).

For simplicity, the magnetic coupling of the Δ/Δ transformer is replaced by an equivalent electrical inductance (L_T). Also, the Δ/Δ transformer is assumed having an inductance equal to (L_T).

Fig. A4(d) represents the case when 4 valves are conducting (1, 1', 2, 2') and the branches containing non-conducting valves are omitted.

2.1 Calculation of internal inductance in case of 12-pulse operation

a) Four-values are conducting

In fig. 4A(d) the loop equations are written as follows:

$$\text{loop (1): } \underline{v} = j\omega(L_T \underline{I} + (\underline{I} + \frac{2\underline{I}}{\sqrt{3}}) L_S + (\underline{I} + \frac{\underline{I}}{\sqrt{3}}) L_S + L_T \underline{I} + 2 \underline{L}_2 \underline{I}) + (\underline{v}_a - \underline{v}_c)$$

$$\underline{v} = j\omega(2L + \sqrt{3} L_S + 2 \underline{L}_2) \underline{I} + (\underline{v}_a - \underline{v}_c) \quad (\text{A4-7})$$

$$\begin{aligned} \text{loop (2): } \sqrt{3} \underline{v}_a &= j\omega(\frac{\underline{I}}{\sqrt{3}} L_1 + (\underline{I} + \frac{2\underline{I}}{\sqrt{3}}) L_S + (\underline{I} + \frac{\underline{I}}{\sqrt{3}}) L_S) \\ 3 \underline{v}_a &= j\omega(\frac{\underline{L}_1}{3} + L_S + \frac{2}{\sqrt{3}} L_S) \underline{I} \end{aligned} \quad (\text{A4-8})$$

$$\begin{aligned} \text{loop (3): } -\sqrt{3} \underline{v}_c &= j\omega(\underline{L}_1 \frac{\underline{I}}{\sqrt{3}} + \frac{\underline{I}}{\sqrt{3}} L_S + (\underline{I} + \frac{2\underline{I}}{\sqrt{3}}) L_S) \\ -\sqrt{3} \underline{v}_c &= j\omega(\frac{\underline{L}_1}{\sqrt{3}} + \frac{L_S}{\sqrt{3}} + L_S + 2 \frac{L_S}{\sqrt{3}}) \underline{I} \\ -\underline{v}_c &= j\omega(\frac{\underline{L}_1}{3} + L_S + \frac{L_S}{\sqrt{3}}) \underline{I} \end{aligned} \quad (\text{A4-9})$$

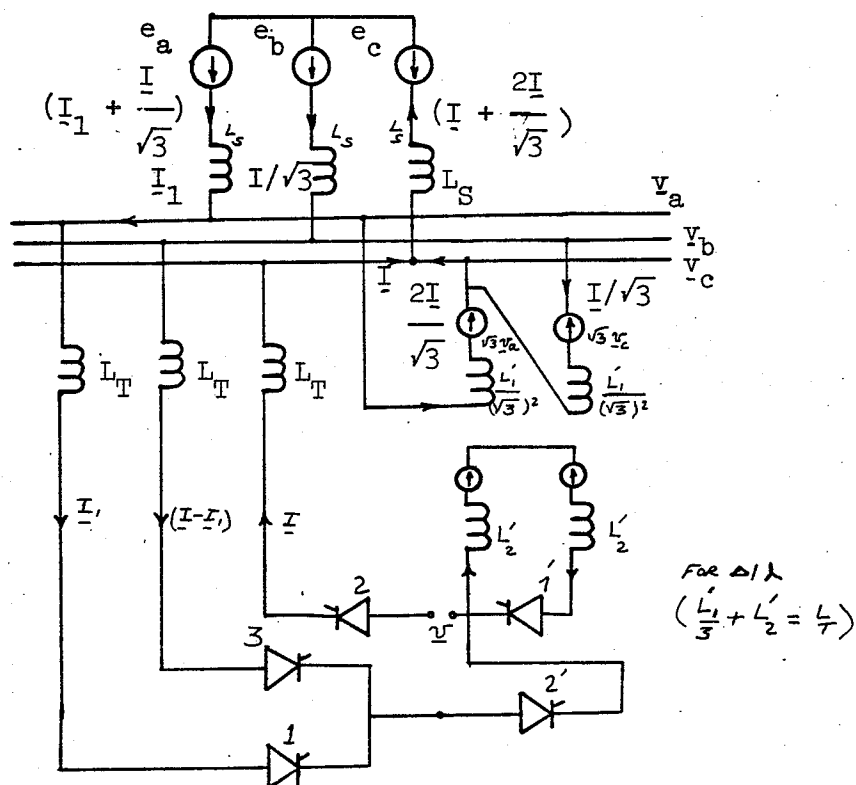


Fig. A4(c) Circuit configuration during commutation (12-pulse operation)

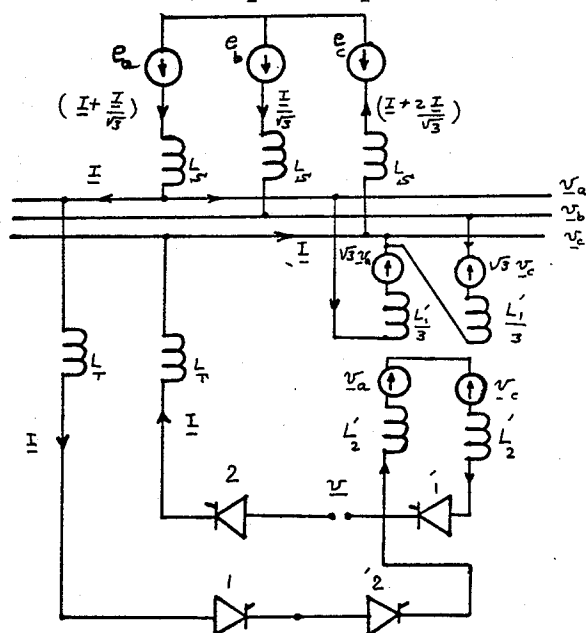


Fig. A4(d) Circuit configuration during conduction (12-pulse operation)

substitute for $\underline{v}_a, \underline{v}_c$ into (A4-7) where $(\frac{\hat{L}_1}{3} + \hat{L}_2) = L_T$.

$$\text{So } \underline{v} = j\omega \cdot 2 \cdot L [2 + \sqrt{3} \frac{L_S}{L_S + L_T}] \underline{I}$$

$$\underline{v} = j\omega L_u = j\omega \cdot 2 \cdot L [2 + \sqrt{3} \frac{L_S}{L_S + L_T}] \underline{I} \quad (\text{A4-10})$$

$$\underline{v} = j\omega L_u = j\omega 2L [2 + \sqrt{3} S] \underline{I} \quad (\text{A4-11})$$

$$\text{where } S = \frac{L_S}{L_S + L_T} = \frac{L_S}{L} \quad (\text{A4-12})$$

b) Five values are conducting

Fig. A4(c) illustrates the converter circuit configuration during commutation period in case of 12-pulse operation.

Writing Kirchoff's laws for the 3 loops:

loop (1):

$$\underline{v} = j\omega [L_T \underline{I} + (\underline{I} + \frac{2\underline{I}}{\sqrt{3}}) L_S + (\frac{\underline{I}}{2} + \frac{\underline{I}}{\sqrt{3}}) L_S + \frac{\underline{I}}{2} L_T + 2 \underline{I} \hat{L}_2] + (v_a - v_c)$$

$$\underline{v} + j\omega [\frac{3}{2} L + 2\hat{L}_2 + \sqrt{3} L_S] \underline{I} + v_a - v_c \quad (\text{A4-13})$$

loop (2):

$$\sqrt{3} \underline{v}_a = j\omega [(\frac{\underline{I}}{2} + \frac{\underline{I}}{\sqrt{3}}) L_S + \frac{\underline{I}}{\sqrt{3}} \hat{L}_1 + (\underline{I} + \frac{2\underline{I}}{\sqrt{3}}) L_S]$$

$$\underline{v}_a = j\omega [L_S + \frac{\hat{L}_1}{3} + \frac{\sqrt{3}}{2} L_S] \underline{I} \quad (\text{A4-14})$$

loop (3):

$$-\sqrt{3} \underline{v}_c = j\omega [\hat{L}_1 \frac{\underline{I}}{\sqrt{3}} + (\frac{\underline{I}}{\sqrt{3}} + \frac{\underline{I}}{2}) L_S + (\underline{I} + \frac{2\underline{I}}{\sqrt{3}}) L_S]$$

$$-\sqrt{3} \underline{v}_c = j\omega [\frac{\hat{L}_1}{\sqrt{3}} + \sqrt{3} L_S + \frac{3}{2} L_S] \underline{I} \quad (\text{A4-15})$$

substituting for \underline{v}_a , \underline{v}_c in equ. (A4-13);

$$\underline{v} = j\omega L_5 = \left[\frac{3}{2} L + 2 \dot{L}_2 + \sqrt{3} L_S + L_S + \frac{\dot{L}_1}{3} + \frac{\sqrt{3}}{2} L_S + \frac{\dot{L}_1}{3} + L_S + \frac{\sqrt{3}}{2} L_S \right] \underline{I}$$

$$L_5 = \left[\frac{3}{2} L + (2L_T + 2L_S) + 2\sqrt{3} L_S \right]$$

$$L_5 = 2L[1.75 + \sqrt{3}S] \quad (A4-16)$$

(notice that L_S is less than L_4)

An average weighted a.c. system inductance could be defined in the same manner as:

$$L_{av} = \frac{\left(\frac{\pi}{6} - u\right) L_4 + L_5(u)}{\frac{\pi}{6}} \quad (A4-17)$$

where L_{av} , is the reflected a.c. system inductance on the d.c. side of converter station, and is regarded as internal inductance for the harmonic voltages on the d.c. side.